Electrochemical Energy Reviews (2024) 7:2
https://doi.org/10.1007/s41918-023-00204-7

REVIEW ARTICLE

Polyethylene Oxide-Based Composite Solid Electrolytes for Lithium Batteries: Current Progress, Low-Temperature and High-Voltage Limitations, and Prospects

Xin Su[1] · Xiao-Pei Xu[2] · Zhao-Qi Ji[3] · Ji Wu[5] · Fei Ma[4] · Li-Zhen Fan[6]

Received: 25 December 2022 / Revised: 10 August 2023 / Accepted: 22 November 2023

Abstract

Lithium-ion batteries (LIBs) are considered to be one of the most promising power sources for mobile electronic products, portable power devices and vehicles due to their superior environmental friendliness, excellent energy density, negligible memory effect, good charge/discharge rates, stable cycling life, and efficient electrochemical energy conversion, which distinguish it from other power devices. However, the flammable and volatile organic solvents in carbonate-containing liquid electrolytes can leach, resulting in thermal runaway and interface reactions, thus significantly limiting its application. The use of polymer solid electrolytes is an effective way to solve this safety issues, among which poly (ethylene oxide) (PEO)-based solid polymer electrolytes (SPEs) have attracted much attention because of their stable mechanical properties, ease of fabrication, excellent electrochemical and thermal stability. Unfortunately, PEO-SPEs with their low room-temperature ionic conductivity, narrow electrochemical windows, poor interface stability, and uncontrollable growth of lithium dendrites cannot meet the demand for high energy density in future LIBs. Therefore, this review firstly describes the ion transport mechanisms and challenges that are crucial for PEO-SPEs, and then provides a comprehensive review of current approaches to address the challenges, including novel and efficient lithium salts, additives, composite electrolytes, stable solid electrolyte interfaces, 3-D lithium metals and alloys, cathode protection layers and multi-layer electrolytes. Finally, future research directions are proposed for the stable operation of PEO-SPEs at room temperature and high voltage, which is imperative for the commercialization of safe and high energy density LIBs.

Keywords Solid polymer electrolytes · Polyethylene oxide · Ionic conductivity · Electrochemical window · Lithium-ions batteries · Additives

✉ Xin Su
sux@hit.edu.cn

✉ Ji Wu
jwu@georgiasouthern.edu

✉ Li-Zhen Fan
fanlizhen@ustb.edu.cn

Xiao-Pei Xu
21S030032@stu.hit.edu.cn

Zhao-Qi Ji
zhaoqi.ji@hit.edu.cn

Fei Ma
ma.fei@shanshan.com

[1] Advanced Battery Technology Center, School of New Energy, Harbin Institute of Technology, Weihai 264209, Shandong, China

[2] Advanced Battery Technology Center, School of Marine Science and Technology, Harbin Institute of Technology, Weihai 264209, Shandong, China

[3] Advanced Battery Technology Center, School of Automotive Engineering, Harbin Institute of Technology, Weihai 264209, Shandong, China

[4] R&D Center, Shanghai Shanshan Technology Co., Ltd., Shanghai 201209, China

[5] Department of Chemistry and Biochemistry, Georgia Southern University, Statesboro GA30460, USA

[6] Beijing Advanced Innovation Center for Materials Genome Engineering, University of Science and Technology Beijing, Beijing 100083, China

Published online: 15 January 2024

1 Introduction

Lithium metal has become one of the most attractive anodes for rechargeable batteries due to its enormous theoretical capacity of up to 3 860 mAh g^{-1} and extremely low reduction potential (− 3.04 V) [1–5]. Since the commercialization of LIBs in the 1990s, their applications have expanded from mobile electronic devices to electric vehicles and stationary power grids [3, 6–8]. The demand for LIBs with higher energy density has forced researchers to develop advanced electrode materials with larger capacities and electrolytes with broader voltage windows [9–15]. Although liquid organic electrolytes are widely used in commercial LIBs, they remain potentially risky in emergency situations due to their low boiling point and high flammability [16–20]. In contrast, solid-state electrolytes can overcome these issues to produce safer LIBs. Thus, it has attracted extensive research interests in the last decade [10, 21–23].

Solid electrolytes can be divided into inorganic and organic solid electrolytes. Inorganic solid electrolytes include oxides, sulfides, nitrides, and phosphates, while organic solid electrolytes consist of a mixture of lithium salts and polymers. Despite the relatively high ionic conductivity (IC) of inorganic solid electrolytes, they do suffer from poor mechanical strength and interface issues, which still prohibited their practical applications [24–27]. Solid polymer electrolytes (SPEs) provide chain channels for Li^+ transport with excellent interface compatibility and enhanced safety [25, 28]. SPEs mainly include polyvinylidene fluoride-hexafluoropropylene copolymer (PVDF-HFP), polymethyl methacrylate (PMMA), polyethylene oxide (PEO), etc. Among these, PEO stands out due to its high flexibility of chains, high dielectric constant and strong solubility for Li^+ [29–32]. PEO-based SPEs have the following advantages: (1) Easy deformability, which can be adapted to a variety of battery structures; (2) Great flexibility, which is able to reduce the effect on the changes of electrode volume during the battery charging and discharging; (3) Excellent processability, which is consistent with the preparation process of current LIBs. Therefore, it has a better development prospect for the safety of LIBs.

However, the main obstacles limiting the development of PEO are the relatively low IC at room temperature [33, 34] and the high interface impedance between the electrolyte and the electrodes [35–37]. Furthermore, the low oxidation potential of PEO may cause its oxidative decomposition when the voltage is higher than 3.6 V as shown in Fig. 1a [22, 38]. Therefore, this work provides an overview of recent advances in the fabrication of PEO-based SPEs for LIBs. The review begins with a brief introduction of the problems with PEO-based polymer electrolytes, including lower IC at low temperatures, poor electrochemical stability at high voltages, terrible mechanical properties and stability at the electrolyte–electrode interface. Then, IC improvement strategies, mechanical property and electrochemical window enhancement methods are summarized in detail. Among these, the combination of PEO and fillers that are organic or inorganic has been tried, and the effect of fillers in types, contents, spatial distributions, and binding modes on the performance of PEO has been studied. This will be the key to improving IC,

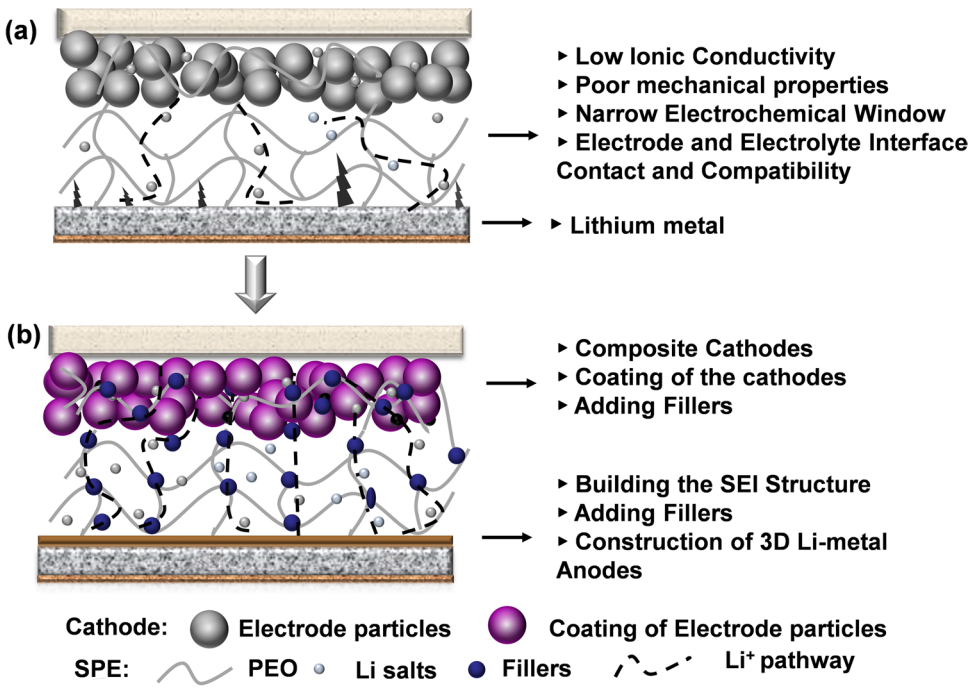

Fig. 1 **a** The challenges of lithium batteries with PEO-based electrolytes. **b** Schematic diagram on the improvement of PEO-based polymer electrolytes and their interfacial improvements

addressing the electrochemical stability of PEO-based SPEs and the interfacial compatibility between electrolytes and electrodes. However, a single solution is not good enough to significantly enhance the comprehensive performance of PEO-based SPEs. Therefore, this paper supplied multiple design strategies, such as adjusting electrolyte composition as well as modifying electrode coating and interfaces (Fig. 1b). Finally, the existing challenges and future research directions are summarized and prospected.

2 Deficiencies of PEO-Based Solid Electrolytes

2.1 Low Ionic Conductivity

Generally, the IC values of PEO at room temperature (RT) are between 10^{-8} and 10^{-6} S cm^{-1} [24, 25]. Pure PEO is not suitable as an electrolyte for LIBs without modification at structure. With the formation and breaking of Li–O chemical bonds, Li^+ migrates through PEO polymer chains or molecules. The biggest problem with PEO-based SPEs, their low IC at low temperatures, was caused by two factors. Firstly, the high crystallinity of PEO at low temperatures limits the segmental movement of PEO chains due to its glass transition temperature (T_g) of 60 °C. Secondly, the interaction between EO and Li^+ in the PEO electrolyte prevents the transport of Li^+ [39, 40].

2.2 Migration Mechanism of Li^+ in PEO-Based SPEs

As shown in Table 1, PEO with a relative molecular mass between 1×10^5 and 1×10^6 is a water-soluble and thermoplastic crystalline resin in the form of a white flowable powder with a repeating unit of (CH_2CH_2O)–. This resin has a low concentration of reactive end groups. The IC of

Table 1 The IC, EW, and TS of PEO electrolytes at different temperatures after the introduction of some optimal ratios of fillers

Li salt	PEO/Mw	EO/Li^+	Fillers	IC/(S cm^{-1})	EW/V	TS/MPa	T/°C	References
$LiClO_4$	6×10^5	8:1	10 wt% SiO_2	4.4×10^{-5}	5.5		30	[95]
LiTFSI	6×10^5	8:1	67.3 wt% LATP 4 wt% BMP-TFSI	2.42×10^{-4}	5		30	[77]
LiTFSI	6×10^5	8:1	64.6 wt% PEG 1.94 wt% LGPS	9.83×10^{-4}	5.1		25	[96]
LiTFSI	6×10^5	8:1	10 wt% PAN 15 wt% LLZTO	1.76×10^{-4}	5.2	9.47	30	[97]
LiTFSI	6×10^5	8:1	15 wt% SN 14 wt% LAGP	1.26×10^{-4}	4.9	9.1	30	[98]
LiTFSI	6×10^5	8:1	15 wt% PVDF-HFP 10 wt% LLZTO	1.05×10^{-4}	5.2		35	[99]
LiTFSI	6×10^5	10:1	1 wt% GO	1.54×10^{-5}	5	1.31	24	[100]
LiTFSI	6×10^5	10:1	6 wt% GDC	1.9×10^{-4}	4		30	[101]
LiTFSI	6×10^5	10:1	25 wt% LSGM	1.3×10^{-4}			30	[101]
LiTFSI	6×10^5	10:1	1 wt% HPMA	1.13×10^{-4}	5.1	2.0	35	[102]
LiI	4×10^5	12:1	0.1 wt% CdO	3×10^{-4}				[86]
LiTFSI	6×10^5	14:1	5 wt% LLTO1-D	2.4×10^{-4}	5.0		25	[103]
LiTFSI	6×10^5	15:1	15 wt% β-CD	1.02×10^{-5}	4.5	1.69	30	[104]
LiTFSI	6×10^5	18:1	1 wt% LGPS	1.18×10^{-5}	5.7		25	[63]
LiTFSI	6×10^5	18:1	15 wt% MB-LLZTO	3.11×10^{-4}	4.5		45	[105]
LiTFSI	6×10^5	18:1	3 wt% LLTO 3-D	2.04×10^{-4}	4.5	16.18	25	[106]
LiTFSI	6×10^5	18:1	12.14 wt% LLZTO	1.76×10^{-4}	5.2		25	[97]
LiTFSI	6×10^5	20:1	5 wt% g-C_3N_4	2.3×10^{-6}	4.7	1.8	30	[107]
LiTFSI	6×10^5	20:1	7 wt% vermiculite	1.22×10^{-5}	4.6	4.2		[108]
LiTFSI	3×10^5	20:1	6 wt% h-BN	7.7×10^{-6}	5.16	0.98		[109]
$LiClO_4$	4×10^5	20:1	3 wt% NS-CD	2.1×10^{-4}	5	2.51		[110]
LiTFSI	6×10^5	20:1	10 wt% HACC	5.01×10^{-4}	5.26	1.01	60	[90]
LiTFSI	6×10^5	20:1	5 wt% LATP	5.24×10^{-4}	5.0		55	[56]
LiTFSI	6×10^5	32:1	27 wt% SN	1.9×10^{-4}	4.7		25	[111]

Data come from different resources, and thus are with different significant digits; Mw means the relative molecular mass. The expression wt% means the weight percentage

PEO is quite low at RT, but it can be increased by raising the temperature. PEO-based SPEs have two main migration mechanisms of Li^+ followed by the relationship between temperature and ionic conductivity: Arrhenius or the Vogel-Tammany-Fulcher (VTF) model. Equation (1) is the Arrhenius model.

$$\sigma = \sigma_0 \exp\left(-E_a/k_B T\right) \tag{1}$$

where σ_0 is the exponential factor, E_a is the activation energy and k_B is the Boltzmann constant. The Arrhenius formula explains that the cation motion is not caused by the molecular motion of the polymer, but the cation migration mechanism is similar to that in ionic crystals, i.e., ions jump to the nearest vacancy. The molecular motion of polymers is strongly influenced by temperature. This relationship can be expressed by the Vogel-Tammany-Fulcher model in Eq. (2).

$$\sigma = \sigma_0 T^{-1/2} \exp\left[-E_a/(T - T_0)\right] \tag{2}$$

where T_0 is the equilibrium glass transition temperature, which is close to the T_g of SPEs, and T_g is the temperature at which the polymer backbone begins to move in segments. When the temperature is lower than T_g, the segmental motion of the polymer almost stops. And only when the temperature is higher than T_g, the segmental motion is gradually carried out. In general, the IC of the polymer electrolyte increases with decreasing T_g and improves with increasing amorphous proportion. When the temperature is higher than T_g, amorphous PEO starts to form, which is beneficial to improving the IC of PEO [30, 38, 41]. PEO polymers have the ability to dissolve lithium salts and form complexes of lithium ions. The relationship between σ and the concentration of charge carriers is shown in Eq. (3).

$$\sigma = \sum n q_i u_i \tag{3}$$

where q_i is the ionic charge, u_i is the mobility of each charge carrier, and n is the number of freely charged species or dissolved ions. The IC of PEO polymer electrolytes can be improved by increasing the dissociation capacity and carrier density of lithium salts, or by decreasing the crystallinity of the PEO polymer matrix. Lithium salts are an important component of electrolytes and can affect the IC of electrolytes. The choice of an appropriate lithium salt is crucial since most lithium salts can only be partially dissociated in polymers as shown in Fig. 2d. Figure 2 shows a schematic diagram of the Li^+ transfer process in the composite electrolyte from "ceramic-polymer", "intermediate" to "polymer-ceramic". There are three different transport paths for lithium ions in PEO-based SPEs, as shown in Fig. 2(a–c) [42]:

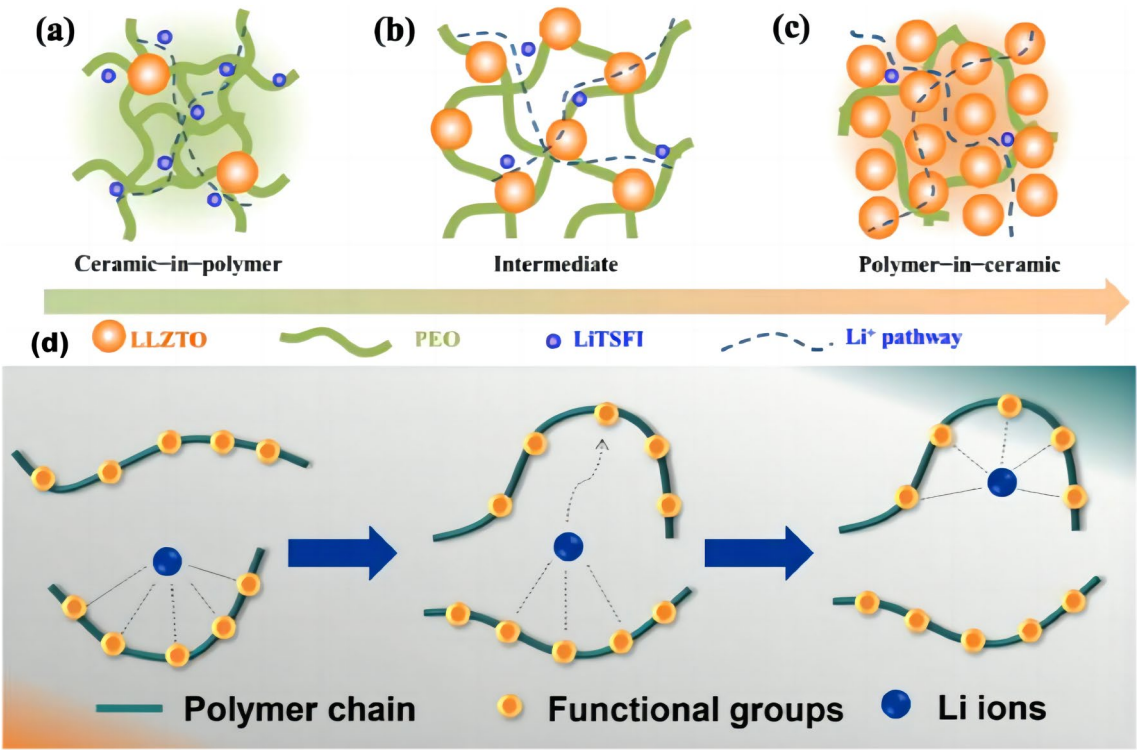

Fig. 2 **a-c** Different lithium-ion transport paths in different systems. Reprinted with permission from Ref. [42]. Copyright © 2018, Elsevier Ltd. **d** Schematic of Li^+ transport in PEO-based solid polymer electrolytes. Reprinted with permission from Ref. [43]. Copyright © 2021, Elsevier Ltd

(1) PEO phases; (2) PEO-LLZTO ceramic interface phases; and (3) LLZTO ceramic phases. The introduction of certain LLZTO particles into PEO polymers not only improves the motion of the PEO chain segment, but also enhances the ionic conductivity of PEO, providing a new pathway for Li^+ transportation.

2.3 Poor Mechanical Properties

Solid polymer electrolytes should have high mechanical strength and some elasticity. As predicted by Newman and Newman Monroe, when the shear modulus of the polymer is large enough, the growth of lithium metal dendrites can be effectively inhibited. In addition, the polymer electrolyte should have a certain elasticity to accommodate the volume expansion of the electrode. The shear modulus (G) is defined as the ratio of shear stress to shear strain, which imparts elastic properties to the polymer. The Young's modulus of most solid polymer electrolytes is less than 5 GPa, while dendritic polymers have a critical shear modulus of about 9 GPa. The modulus of elasticity of PEO is as low as 10^6 Pa at RT, and the PEO-based SPEs are too soft and have poor mechanical properties to inhibit the growth of lithium dendrites.

2.4 Narrow Electrochemical Window

There is a limit to the most positive and most negative potentials for an electrolyte, beyond which the electrolyte will decompose by the electrochemical reaction. Then, there is an interval between this most positive and most negative potentials, in which the electrolyte is stable, normally called EW. The oxidation potential of PEO polymer is low with a general decomposition voltage of 3.7 V. Therefore, it is commonly used with the low-voltage $LiFeO_4$ cathode. EW is an important indicator of electrolyte stability. The wide EW could ensure that the electrolyte remains electrochemically and chemically stable when in contact with the cathode and anode. SPEs should have an EW of 4 V or wider for proper charging and discharging of LIBs, which can match the high-voltage cathode material. Improving the EW of solid electrolytes not only broadens the application range of electrolytes, but also enables the preparation of high-voltage LIBs. Thus, the energy density of LIBs would be increased.

2.5 Poor Electrode and Electrolyte Interface Contact and Compatibility

The interface between electrolytes and electrodes in ASSLBs is quite different from liquid LIBs, in which the liquid electrolyte can wet the electrode and the transfer rate of ions between electrolytes and electrodes is fast. In contrast, PEO-based SPEs are in rigid contact with electrodes, and the impedance of the interface is quite high, which affects the transfer rate of charges at the interface of electrodes and electrolytes. During charging and discharging, the volume change of the electrode decreases the interface contact between the electrode and PEO-based SPEs, which increases polarization and results in LIBs failure.

Figure 1a shows the problems of terrible interface contact of cathodes, poor mechanical and electrochemical stability in PEO-based SPEs in ASSLBs. Figure 1b shows a series of improvement to the interface, including improving the composition of the PEO-based electrolyte and adjusting the structure of cathodes and cathodes to create a stable solid-state interface layer.

3 Improving Ionic Conductivity of PEO at Low Temperatures

3.1 Li Salts with Larger Anions

Lithium salts with larger anions have been reported to have relatively higher IC. In 1973, Fenton et al. [29] developed a PEO-LiX electrolyte material with high IC for alkali metals. Subsequently, $LiCF_3SO_3$ [44–47], $LiBF_4$, $LiClO_4$, $LiPF_6$ and $LiAsF_6$ [38], LiBOB [48], as well as LiN $(CF_3SO_2)_2$(LiTFSI) [49] have been reported. Among them, LiTFSI is the most widely used because of its strong electron-withdrawing groups (SO_2CF_3), flexible groups (–SO_2–N–SO_2–), better thermal, chemical, and electrochemical stabilization properties [50, 51].

It has been found that increasing the concentration of lithium salts can promote the migration of Li^+. However, the high concentration of lithium salts is detrimental to the thermal movement of the PEO molecular chains, the migration of ions, the formation of films, and mechanical properties of the SPEs, resulting in a rise in T_g of the polymer and an increase in salt-ion complexation. Therefore, the molar ratio of EO to Li^+ in the electrolyte must be in a suitable range [52–54]. According to Table 1, the optimal ratio of EO/Li lies between 8 and 20. Lukas Stolz et al. experimentally demonstrated that PEO-LiX has similar performance and specific charge capacity at 60 °C when the ratio of EO/Li is lower than 20, but an obstructive polarization occurs when the ratio is above 20 [55]. The experiments were conducted at 40 °C as well to investigate the effect of temperature on the performance of different salt concentrations. The results showed that the overvoltage, specific capacity, and polarization in Fig. 3a and b became dispersed compared to that at 60 °C. When EO/Li is higher than 20, the voltage rises nearly vertically with time, indicating the presence of obstructive polarization in the LIBs. The transition time (τ) and current density of this polarization mathematically coincide with the Sander's equation, from which the Li^+ diffusion constant (D_{Li^+}) can be calculated. In turn, the maximum

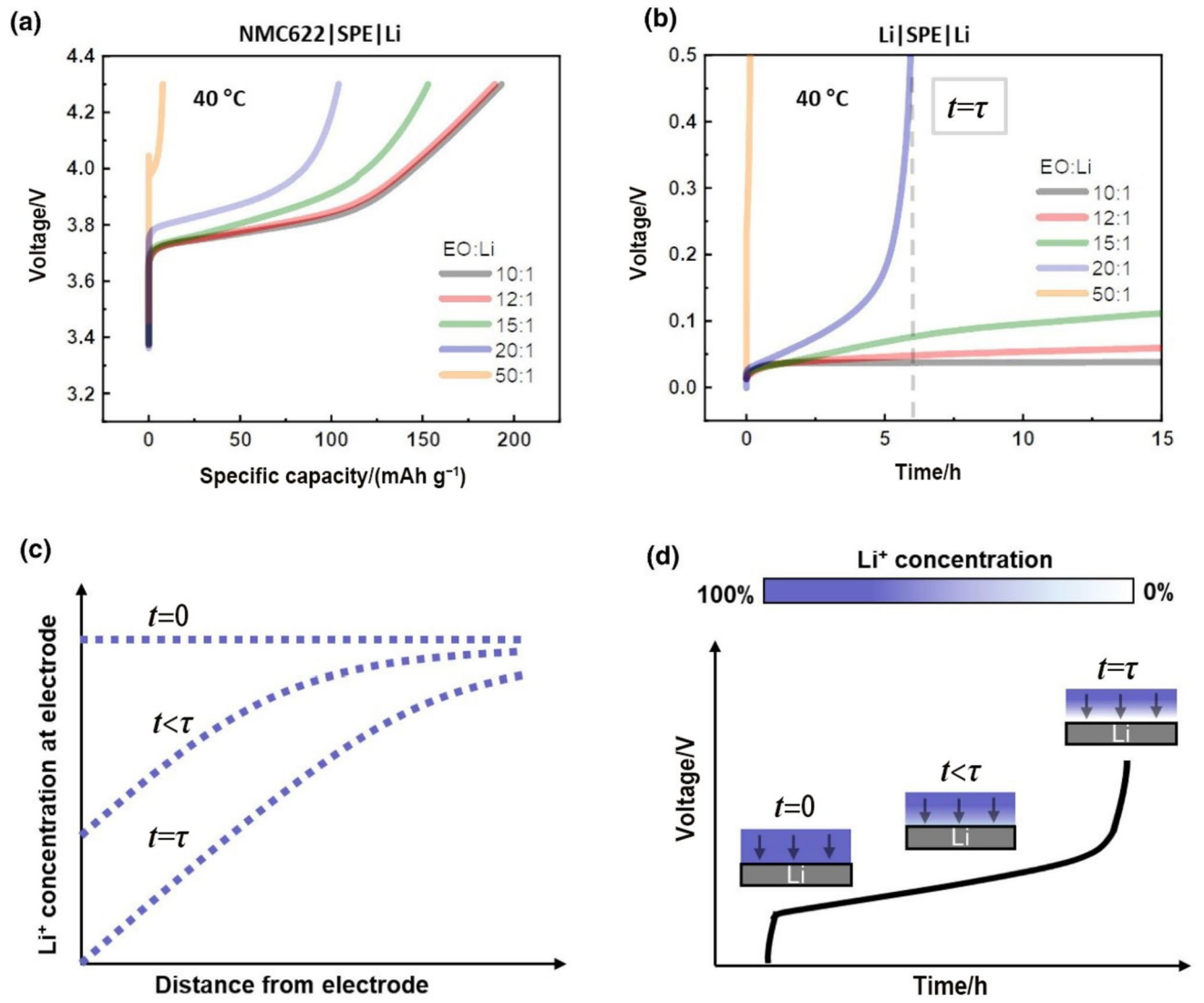

Fig. 3 **a** Voltage profile and specific capacity of NMC622 ‖ SPE ‖ Li cell at 40 °C. **b** Voltage curve of Li ‖ SPE ‖ Li batteries at 40 °C. The transition time and current density are mathematically consistent with the Sand equation schematic. **c** When $t=\tau$, blocking polarization appears in the diagram voltage profile and specific capacity of NMC622 ‖ SPE ‖ Li cells at 60 °C. **d** The transition time (τ) for the electrolyte on the electrode surface with a Li^+ concentration of 0. Reprinted with permission from Ref. [55]. Copyright © 2021, Elsevier Ltd

current density of SPEs can be calculated and predicted as well under a certain salt concentration and temperature. This polarization stems from the lack of Li^+ in the electrolyte at the surface of electrodes and is limited by the kinetics of ion transport as verified in Fig. 3d. The obstructive polarization occurs when Li^+ is completely depleted at the surface, because the consumption rate of reactants is faster than that of the Li^+ transport rate through the SPEs, as shown in Fig. 3c. Therefore, it is preferable to use a low concentration of salts, which not only saves costs [31, 56] but also improves mechanical properties of the enhancer [57–60].

However, the inhomogeneity of the PEO-LiX composite electrolyte is a major problem, which can lead to high current density regions at the interface between the anodes, the PEO and internal short circuits (> 0.2 mA cm^{-2}) in LIBs. In addition, it can reduce the mechanical strength and prevent PEO-LiX films from inhibiting the growth of lithium dendrites when the temperature is higher than 50 °C [61]. Different mixing technologies [58, 62], addition of fillers [63–65] and various salts [66–70] can promote a more homogeneous mixture of PEO and LiX, and further improve the physical and chemical properties of the composite electrolytes.

3.2 Filler Doping

Adding fillers to PEO-based electrolytes to form composite polymer electrolytes (CPEs) is a popular research direction for ASSLBs. The fillers not only promote the IC and migration of Li^+, but also improve the mechanical properties of solid electrolytes and the stability of the interface between the electrolyte and the electrode. Fillers are mainly classified into inorganic and organic materials. Inorganic fillers are mainly nano-sized and can be subdivided into active and inert fillers. Among them, inert fillers were studied at the beginning and they generally do not have Li^+ components and transport capacity. However, they can disrupt the crystalline morphology of PEO to improve the mechanical properties and the thermal stability of the electrolyte. In recent years, research has focused on active fillers that contain Li^+ components and are capable of Li^+ transportation. The conductivity of the electrolyte is improved by providing an additional amount of Li^+ and broadening the EW. Several improvements have been proposed to achieve homogeneous dispersion of fillers in the polymer, such as enhancing the binding of fillers to polymers [71–74], increasing the size of fillers [75–77], and improving mixing technologies [76, 78].

3.3 Passive Fillers

Since Weston and Steele [79] first added α-Al_2O_3 to the PEO_8-$LiClO_4$ system in 1982 and significantly enhanced the IC of the electrolyte, many metal oxides, including TiO_2 [80], Al_2O_3 [79–82], ZrO_2 [83], Fe_2O_3 [84], CuO [85], CdO [86], CeO_2 [87, 88], CaO [89], MnO_2 [90], and ZnO [64, 91], have been further studied. Currently, there are two theories on the role of inorganic fillers in improving the IC. Firstly, Wzorek et al. [92, 93] considered that the cations of inorganic fillers can bind to anions in the electrolyte through Lewis acid–base interactions and increase the amount of free Li^+ in the system by promoting the dissociation of Li^+ salts. Secondly, Croce et al. [94] suggested that inorganic fillers can promote local reorganization of chain segments in the polymer and reduce the crystallinity of the polymer, thus promoting chain movement. Table 1 shows the IC, EW and tensile strength (TS) of PEO-based SPEs at different temperatures after the introduction of optimal ratios of fillers.

The composite polymer electrolyte was prepared by using a PEO-based polymer. However, many crystalline regions formed by the agglomeration of the incorporated nanoparticle fillers limit the enhancement of IC. Therefore, the dimensionality of the filler was increased from nanoparticles to nanosheets as is desirable to further improve the dispersion of the nano-filler and enhance the interaction between the filler and the polymer [107, 112].

The crystallinity of the polymer is related to the size of the inorganic filler, incorporation, own properties, and dispersion in the polymer [113]. The solution casting method is commonly used to prepare polymer nanocomposites that are filled with different concentrations of metal oxide particles [114–118]. In 1998, F. Croce et al. added nano-sized TiO_2 and Al_2O_3 ceramic powders to a PEO-based electrolyte via a casting method [80]. They demonstrated that the conductivity of the composite electrolyte (PEO-$LiClO_4$) containing 10% by weight (wt%) TiO_2 with 13 nm and 10 wt% Al_2O_3 with 5.8 nm in diameter was approximately 10^{-4} S cm^{-1} at 50 °C and 10^{-5} S cm^{-1} at 30 °C. Kamaka. A. Ghosh observed that 0.10 wt% CdO nanoparticles with an average size of 2.5 nm dispersed in a PEO matrix by using a casting method can improve IC to 3×10^{-4} S cm^{-1} at 30 °C. The decreasing T_g of the PEO-LiI electrolyte was observed with the introduction of CdO nanoparticles into the polymer. Results characterized by X-ray diffractometry, electron microscopy and differential scanning calorimetry indicated that the amorphous phase of PEO increased with the introduction of CdO nanoparticles. At a 0.1 wt% CdO doping amount, the conductivity of direct current was significantly enhanced by three orders of magnitude over that of the PEO-LiI electrolyte. However, the conductivity decreases when CdO is added more than this concentration because the nanoparticle aggregation blocks ion transport. Meanwhile, the PEO-LiI electrolytes incorporated with CdO nanoparticles showed a VTF behavior. The conductivity is inversely proportional to the temperature, suggesting a strong coupling between the ionic motion and the polymer chain segment motion. When the amount of CdO is above this concentration, the conductivity decreases as a result of the hindering effect of the nanoparticle aggregation on the ion transport [86]. Some complex metallic oxides materials can also be used as fillers such as $MgAl_2O_4$ [119], $Gd_{0.1}Ce_{0.9}O_{1.959}$ (GDC), $La_{0.8}Sr_{0.2}Ga_{0.8}Mg_{0.2}O_{2.55}$ (LSGM) and zirconium 1,4-hydroxyphenyl metal–organic framework (UIO) [120]. Among them, Nan Wu et al. presented two oxides $Gd_{0.1}Ce_{0.9}O_{1.95}$ and perovskite $La_{0.8}Sr_{0.2}Ga_{0.8}Mg_{0.2}O_{2.55}$ in oxide/polymer. Lithium solid-state nuclear magnetic resonance (NMR) measurements confirmed the presence of two different localized Li^+ landscapes in the composite polymer electrolyte, namely A1 and A2. The distribution of Li^+ at the A1 and A2 sites is changed with the introduction of GDC or LSGM. While Li^+ at the A2 is weakly coordinated to the ether oxygen, Li^+ at the A1 is tightly coordinated. Density functional calculations (DFT) were performed to reveal that bonds formed on the surface of the $TFSI^-$ anion and the introduced filler. Oxygen vacancies on the surface of GDC/LSGM combine with the $TFSI^-$ anion in the PEO-LiTFSI composite electrolyte to enhance the number of freely moving Li^+ in the electrolyte. The maximum ionic conductivities are 1.9×10^{-4} and 1.3×10^{-4} S cm^{-1} at 30 °C for CPE-5 wt% GDC and CPE-25 wt% LSGM CPES, respectively[101].

Compared with other spherical particles, carbon materials like carbon nanotubes and graphene have a very high specific surface area, which keeps PEO-based polymers in a disordered state for a long time and inhibits crystallization. When lithium salts are doped into the carbonaceous material system, Li/Li^+ will adsorb on the carbon nanotubes or graphene, facilitating the migration of Li^+ and increasing electrical conductivity. Chemical modifications are commonly required for carbon materials because carbonaceous materials are highly metallic and cannot be used directly as fillers. Carbon nanotubes modified with a clay layer can effectively reduce the risk of short circuits in LIBs. At the same time, the conductivity of electrolytes can be improved by almost two orders of magnitude [121]. Xu et al. [110] studied the PEO-$LiClO_4^-$ nitrogen and sulfur co-doped carbon dots (NS-CD) and found that the maximum conductivity can reach 2.1×10^{-4} S cm^{-1} at 25 °C when the concentration of the filler is about 3 wt%. It is a result of the interaction between the marginal nitrogen/sulfur and Li^+ in NS-CD. Solid-state NMR shows that more freely mobile Li^+ ions are generated in the electrolyte. Metal–organic frameworks (MOFs) are materials with organic–inorganic hybrid properties, high specific surface area and ordered microporous structure [122]. Liu's group [123] first reported the addition of MOF-5 (Zn_4O $(BDC)_3$) as a filler in PEO-based SPEs, which resulted in an increase in IC to 3.16×10^{-5} S cm^{-1} at 25 °C. The reasons for the increase in IC are speculated as follows: (1) The Lewis acid sites on the surface of MOF-5 and the EO groups on PEO interacted with the lithium salts; (2) The reduced crystallinity of PEO increases the movement of chain segments in the polymer and the dissociation of lithium salts; and (3) The pores of MOF-5 adsorb impurities in the polymer electrolyte and reduce interface reactions. Later, the addition of MIL-53(Al) [124], Cu-BDC MOF [125], Mg-TPA MOF [126], HKUST-1 MOF [127] and $EACe_2$ MOF [128] as fillers into PEO-based electrolytes has been reported. However, the research on MOFs is still booming and the ion migration mechanism needs to be further clarified.

Some ideas for the simple mixing of nanoparticles into polymer electrolytes have been proposed in recent years, including electrostatic spinning, in situ synthesis, in situ hydrolysis, and other synthetic methods. Cui's group [95] reported a new method for preparing ceramic polymer

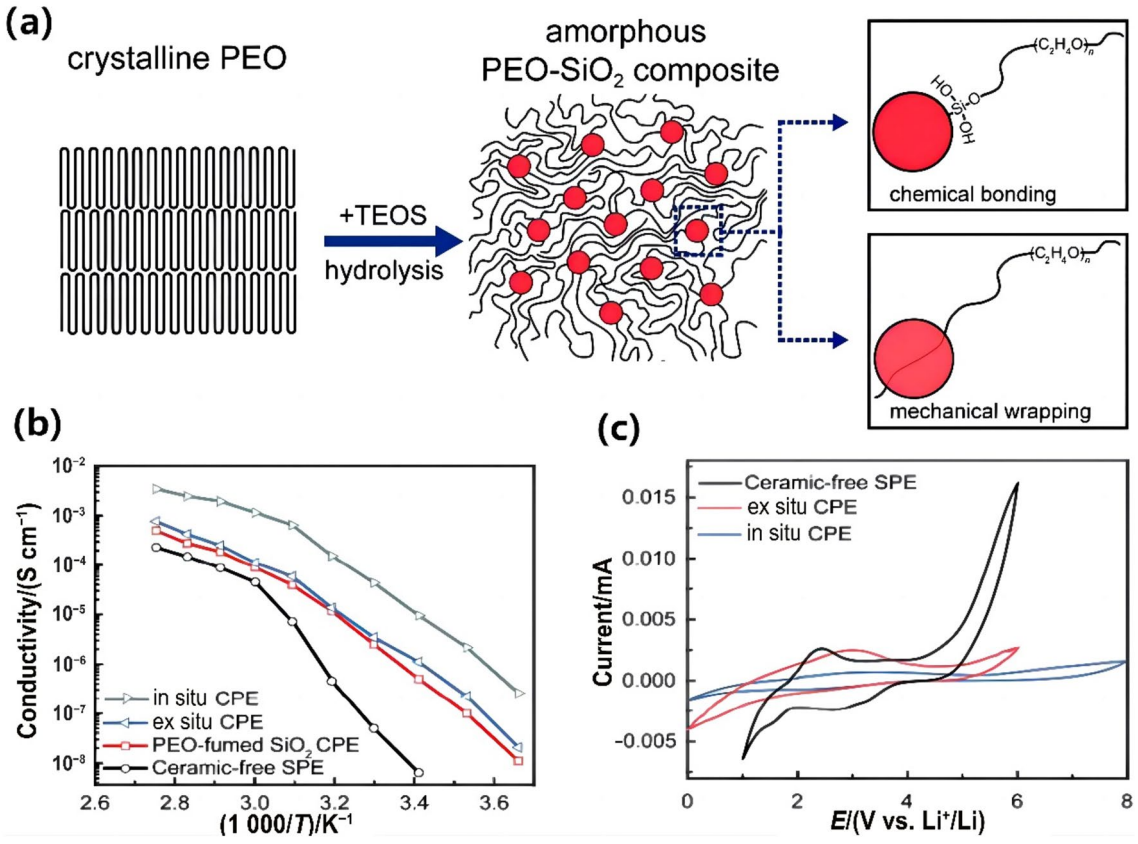

Fig.4 **a** Schematic diagram showing the process of in situ hydrolysis and the mechanism of interaction between PEO chains and $MUSiO_2$. **b** Arrhenius curves for different electrolytes at different temperatures. **c** Electrochemical windows for different electrolytes. Reprinted with permission from Ref. [95]. Copyright © 2016, American Chemical Society

electrolytes by in situ synthesis of ceramic particles in polymer electrolytes (Fig. 4a). The incorporation of monodisperse ultrafine silica ($MUSiO_2$) not only reduces the crystallinity of PEO, but also increases the dissociation of $LiClO_4$, which increased the IC of the electrolyte to 1.2×10^{-3} S cm^{-1} at 60 °C as shown in Fig. 4b and expanded the EW to 5.5 V in Fig. 4c. Moreover, Bao et al. [91] demonstrated that ZnO quantum dots can be chemically doped into PEO substrates by a special variant of atomic layer deposition (ALD) and vapor phase infiltration (VPI). ZnO quantum dots have a strong chemical interaction with PEO polymer chains, thus inhibiting PEO crystallization and enhancing the transportation of Li^+. The strong interaction also contributes to the uniform distribution of ZnO quantum dots in the PEO-based solid electrolyte matrix as well as at the surface, which leads to a significant reduction of the interface resistance to the transportation of Li^+. The PEO-LiTFSI-VPI ZnO composite polymer electrolyte can be compatible with the high-voltage NCM811 cathodes and exhibits excellent cycling performance.

3.4 Active Fillers

In recent years, polymer electrolytes have been intensively studied and more inorganic solid electrolytes have been fabricated. However, their fabrication processes are complex, costly and result in various side reactions at the interface between the positive/negative electrodes and electrolytes and further cause fractures. The addition of active fillers increases the IC by providing new pathways for the transportation of Li^+ [97, 129, 130]. When PEO and electrodes come into contact, the presence of O and OH in PEO reacts chemically with the lithium metal to produce an unstable layer of lithium oxide [42]. The addition of active filler can reduce the physical contact between PEO and Li^+ and the interfacial resistance to improve the electrochemical stability [56, 131, 132]. The active fillers include $Li_{10}GeP_2S_{12}$ (LGPS) [63, 96], $Li_{1.5}Al_{0.5}Ge_{1.5}(PO_4)_3$ (LAGP) [133], LLZO [134, 135], $Li_{1.3}Al_{0.3}Ti_{1.7}P(O_4)_3$ (LATP) [56, 136–139], $Li_{0.3}La_{0.557}TiO_3$ (LLTO) [103, 106, 140], $Li_{6.4}La_3Zr_{1.4}Ta_{0.6}0_{12}$ (LLZTO) [105], $LiZr_2(PO_4)_3$ (LZP) [129], Li_2OHBr [141], $Li_{6.25}La_3Zr_2Al_{0.25}O_{12}$ (LLZAO) [142], etc.

The size (nano and micron) and morphology of inorganic fillers and their homogeneity significantly affect the crystallization kinetics of ion pathways in polymers [143]. Huo et al. [144] suggested that the particle size of LLZTO is a key factor, with smaller LLZTO particles improving IC and larger LLZTO particles improving the mechanical strength. The reason is that small active filler particles have a large specific surface area and are more prone to agglomeration, resulting in rapid migration of ions in the vicinity of the active filler particles. Large active filler particles have a small specific surface area, which might reduce the contact area between the activated filler particles and the polymer, leading to a decrease in the migration pathway of Li^+ [56]. Skaarup et al. [47] first added the active Li_3N to the PEO-$LiCF_3SO_3$ system in 1988 and it significantly enhanced the IC by a factor of 1 000. However, Li_3N is extremely unstable and sensitive to heat and moisture. Additionally, Li_3N has a narrow electrochemical stability window (2.5 V compared to Li^+/Li).

The electrolytes can be prepared by solvent casting or dry mixing of PEO-LiTFSI substrates with LATP nanofiller particles. The solvent-free mixing improves the conductivity of the electrolyte [145]. The maximum of the PEO-LiTFSI-10 vol% (vol% means the volumetric percentage) LATP electrolyte is 2.5×10^{-3} S cm^{-1} at 80 °C, which is almost two times more compared to the electrolyte containing SiO_2 filler [65]. Because of the absence of solvents and the fact that contact between the sample and air is greatly avoided during the production process, the mechanical strength and thermal stability of the films produced by the dry-blending process are higher [146]. Prof. Goodenough [42] investigated a new idea for composite electrolytes from "ceramic-in-polymer" to "polymer-in-ceramic". LLZTO particles increase the proportion of amorphous phases in the PEO matrix and decrease the crystallinity, which not only improve the chain segment motion but also provide more Li^+ pathways to enhance the IC of PEO. When the amount of LLZTO is less than the percolation threshold, the conductivity of the composite electrolyte is mainly determined by the movement of PEO polymer chains. In the case of percolation, the conductivity is determined by both PEO and LLZTO. When the particle concentration is higher than the percolation threshold, LLZTO provides new pathways for Li^+ transport. Therefore, the conductivity of LLZTO ceramic dominates the property of polymer-ceramic composites. The electrolyte has good electrochemical properties with IC above 10^{-4} S cm^{-1} at 55 °C and a 5.0 V vs. the Li/Li^+ electrochemical stability window. PEO-LLZTO composite electrolytes prepared by hot pressing have excellent cycle stability and a high discharge capacity of 139.1 mAh g^{-1} in Li ‖ $LiFePO_4$ cells with a capacity retention rate of 93.6% after 100 cycles.

The population of lithium ions in the composite electrolyte determines the Li salt concentration and the amount of active fillers [129]. Previous studies have shown that IC usually has a peak value when the volume fraction of active fillers is less than 15%. Good mechanical properties can be achieved when the volume fraction is greater than 40% [42, 147–149]. There is a percolation flow threshold for the amount of active fillers added. Both the polymer and active particles can provide the lithium-ion transfer pathway below the threshold. Once it is greater than this value, the primary lithium-ion conduction pathway is provided by the active filler [42].

LLZTO was used in the PEO polymer matrix to produce flexible self-supporting composite electrolyte membranes in which no additional lithium salts were added, but rather the lithium ions on the surface of LLZTO were leached out and conducted by using the percolation effect [149]. In all composite polymers, there are two different Li^+ sites. The distribution of Li^+ in the composites depends on the active filler and the concentration of lithium salts. Wu et al. [129] proposed to investigate the Li^+ distribution and Li^+ conduction mechanism of composite polymer electrolytes by using ^7Li relaxation time and $^6Li \rightarrow {}^7Li$ trace exchange nuclear magnetic resonance (NMR) measurements to test three different PEO-LiTFSI composite electrolytes: PEO-LiTFSI, PEO-LiTFSI-Al_2O_3 and PEO-LiTFSI-NASICON-$LiZr_2(PO_4)_3$ (LZP) electrolytes. The reaction product of LZP and lithium metal is Li_3P, which increases the contact between the solid electrolyte and lithium metal anode, thus decreasing the interfacial resistance between lithium metal anodes and polymer electrolytes and improving the cycle stability of symmetric Li || Li batteries at low temperature. PEO-LiTFSI-25 wt% LZP has the highest conductivity of 1.2×10^{-4} S cm^{-1} at 30 °C. Zhang et al. [150] proposed a new synthetic route to prepare a composite electrolyte (CE, LAGP || SPE) for all-solid-state $LiFePO_4$ || Li cells by coating a PEO-based solid polymer electrolyte (SPE) of PEO-1%-75% Li_2S-24%-P_2S_5-1% P_2O_5 (LPOS) onto LAGP particles. The all-solid-state lithium batteries (ASSLBs) of $LiFePO_4$ || Li with this advanced structural strategy have good interface compatibility, an extremely long cycle life, a high capacity, and a reversible discharge capacity retention of 127.8 mAh g^{-1} at 1 C for the 1 000th cycle with a retention rate of 96.6%. However, nanoparticles tend to agglomerate easily due to their high surface energy [28, 129, 151]. As a result, they are not homogeneously mixed with PEO polymers [152, 153]. Several improvements are used to make the filler uniformly dispersed into the polymer as follows.

(1) Modify the active particles with other substances to increase their contact area with PEO [105, 151, 154].
(2) Improve the compatibility of the filler and the polymer by adding cross-linking agents to chemically bond the filler and the polymer [96, 148, 155].
(3) Prepare fillers with different dimensions like one-dimension (1-D), two-dimension (2-D), and three-dimension (3-D) fillers, which not only reduce the agglomeration of the filler, but also provide continuous channels for the transportation of Li^+ [103, 106, 142, 156].

Wenwen Li et al. [105] proposed grafting molecular brushes (MB) onto the LLZTO surface to increase the wettability between PEO and LLZTO, so MB-LLZTO nanoparticles can be uniformly distributed in organic matter. The irregular structure of MB-LLZTO particles reduces the crystallinity of PEO and provides fast transfer channels for lithium ions, thus increasing the IC of the polymer electrolyte. The PEO-based SPEs of PEO-LiTFSI-15 wt% MB-LLZTO have an IC of 3.11×10^{-4} S cm^{-1} at 45 °C. A high-resolution solid-state lithium NMR indicates the transport mechanism of Li^+ in the composite electrolyte, i.e., Li^+ favors conduction in the region introduced by brushes on the surface of MB-LLZTO. To make LLZTO uniformly dispersed in PEO, a 4–5 nm dopamine (PDA) coating with good wettability was applied to the LLZTO surface. The IC of the composite electrolyte increased from 6.3×10^{-5} S cm^{-1} to 1.1×10^{-4} S cm^{-1} at 30 °C by dopamine modification and the interfacial resistance from 308 to 65 Ω cm^2 between the composite electrolyte and the lithium metal anode at 50 °C. [151]. This PDA coating improves the binding between PEO and LLZTO and reduces their interface resistance. The thermal and electrochemical stability of the composite electrolyte was enhanced. A PEO-PEG-LGPS flexible composite electrolyte was prepared by an in situ coupling reaction. The LGPS was chemically bonded to PEO, and the LGPS was highly dispersed in PEO at RT. PEO-PEG-3LGPS has a conductivity of up to 9.83×10^{-4} S cm^{-1} and the lowest activation energy (0.26 eV) and a high t_{Li^+} (0.68). Additives were introduced to inhibit the growth of lithium dendrites, and the symmetrical lithium battery was reported by Kecheng Pan et al. [96].

The introduction of a composite electrolyte with more than zero-dimension active fillers can improve IC to 10^{-4} S cm^{-1} at RT [103, 106, 137, 140, 156, 157]. The 1-D LLTO increases the Li^+ conductivity of the polymer electrolyte to 2.4×10^{-4} S cm^{-1} at RT by increasing the concentration and disorder of more mobile Li^+ ions [103]. After adding LLZO nanowires to PEO-LiTFSI, the electrical conductivity is an order of magnitude higher than that of adding nanoparticles [156]. The active fillers are randomly distributed in the polymer, and the lithium ions are not evenly distributed at the interface between the cathode and the electrolyte. This leads to the growth of lithium dendrites, potentially rapid battery degradation, and even short-circuiting [158, 159]. Cui's group [160] investigated the effect of directionally aligned LLTO nanowires on the conductivity of the composite electrolyte. These nanowires without cross-parallel structures are able to provide a fast ionic conduction pathway, and the IC of composite electrolytes is ten times higher than that of the randomly dispersed LLTO nanowire composite electrolytes. The development of composite polymer electrolytes with aligned nanowires provides a good way to improve the IC of solid electrolytes through new nanostructure designs. Then, Zhai et al. [139] fabricated vertically aligned structured LATP fillers by using an ice template method. Its conductivity approaches 5.2×10^{-5} S cm^{-1}, which is 3.6 times higher than that of the composite electrolyte with

randomly dispersed LATP NPs. The composite electrolyte has improved geometric stability at 180 °C and enhanced electrochemical stability of the PEO polymer electrolyte.

The configuration of the active filler was further improved by preparing a vertically aligned porous framework. A bi-layer composite electrolyte with an asymmetric bi-layer LATP vertically arranged porous layer framework was reported by Yanke Lin et al. [137]. PEO-LLTO framework solid electrolytes with a vertical bi-continuous phase have a higher ionic conductivity than PEO-LiTFSI (PL) electrolytes and PEO-LiTFSI-LLTO nanoparticles (PLLN) electrolytes at the same salt concentration, as shown in Fig. 5g. Scanning electron microscopy images revealed that PLLF electrolytes effectively suppressed lithium dendrites (Fig. 5a–f). This PLLN electrolyte can have an IC of up to 12.04×10^{-4} S cm^{-1} at RT, which is 72 times higher than that of the PL electrolyte (Fig. 5h). It has excellent cycling stability and interfacial compatibility, and the $LiFePO_4$ ‖ Li cell, after 150 cycles at 1 C, has a discharge capacity of 154.7 mAh g^{-1}. In short, this vertical bi-continuous structure greatly improves the ion transport capacity of the active filler, LATP, and the stability of the polymer, and provides an effective way to

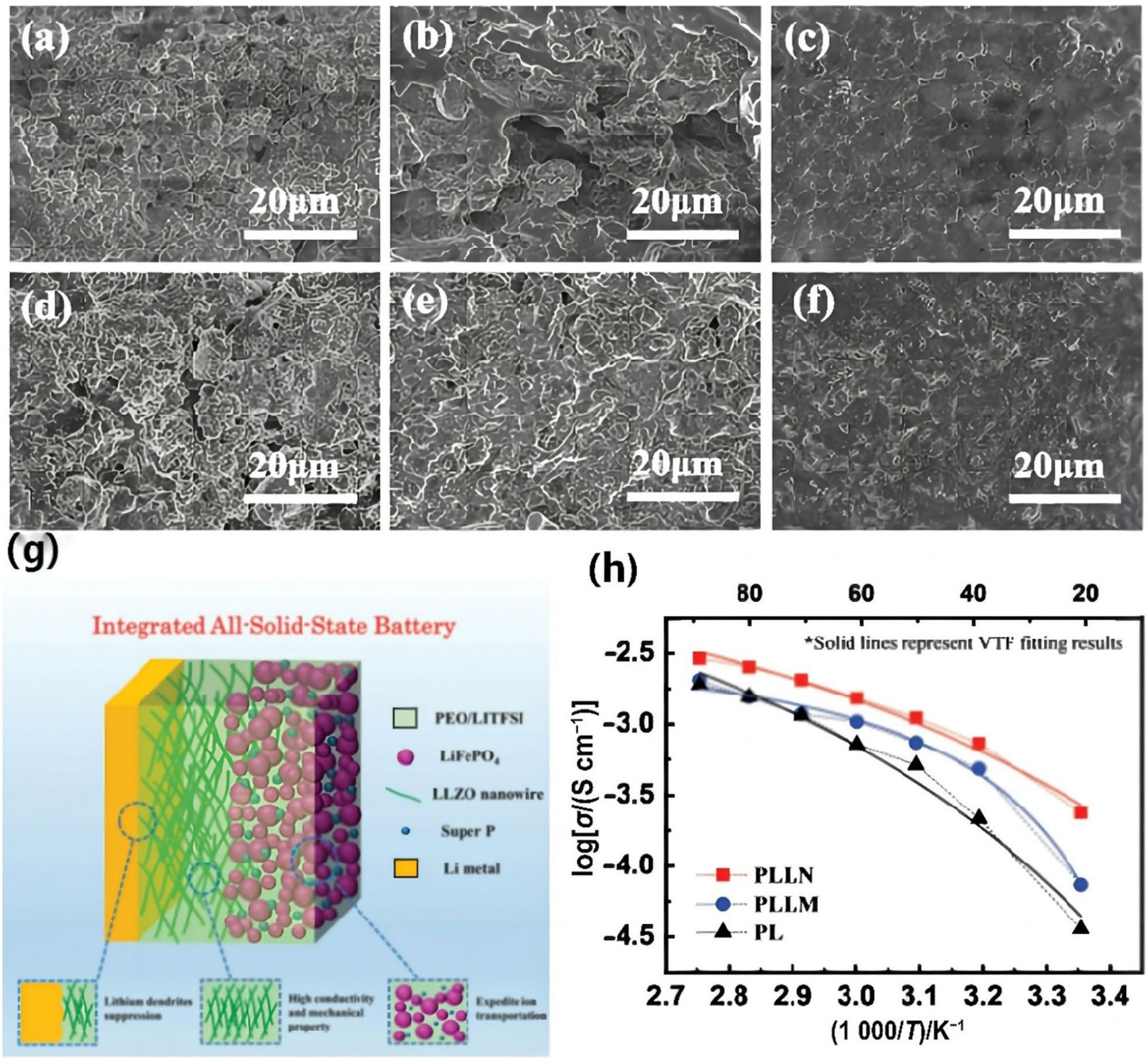

Fig. 5 Surface morphology of lithium anodes after cycling with different electrolytes: **a** Li ‖ PL ‖ Li cell and **b** Li ‖ PLLM ‖ Li cell with stable cycling of about 750 h. **c** Li ‖ PLLN ‖ Li cell with the cycling of about 1 075 h. **d** Surface morphology of lithium anodes of the $LiFePO_4$ ‖ PL ‖ Li cell. **e** $LiFePO_4$ ‖ PLLM ‖ Li cells and **f** $LiFePO_4$ ‖ PLLN ‖ Li battery surface morphology of lithium anodes after 70 cycles at 0.5 C and 60 °C. **g** The schematic representation of an all-solid-state $LiFePO_4$ ‖ PLLN ‖ Li cell. **h** Conductivity of different electrolytes. Reprinted with permission from Ref. [156]. Copyright © 2018, John Wiley & Sons, Inc

improve the IC at low temperatures for all-solid-state batteries and interfacial stability at low temperatures [140].

Vertically aligned electrolytes have good IC and electrochemical properties, and the alignment of the filler in the polymer is especially important. For example, Guo et al. [134] prepared homogeneous and anisotropic CPEs by the coaxial electrostatic spinning of LLZO particles highly dispersed in PEO. This electrospun composite solid electrolyte (ES-CSE) has a unique vertically and horizontally oriented structure that improves the IC and inhibits the formation of lithium dendrites (Fig. 6a–c). LLZO particles were uniformly distributed in the PEO-LiTFSI system, enhancing the interaction between PEO and LLZO to form a continuous channel of lithium-ions transport. This continuous transport path enabled the vertical/horizontal anisotropic transport of lithium ions in CSEs, delayed the side reactions at the interface, inhibited the formation of lithium dendrites, and strengthened the resistance to deformation. It shows a conductivity of 1.5×10^{-4} S cm^{-1} (Fig. 6a) and a tensile strength of 7.46 MPa at 35 °C (Fig. 6c). In Li ‖ ES-CSE ‖ Li symmetric cells it can suppress lithium dendrites at 0.1 mA cm^{-2} for more than 1 570 h (Fig. 6e). Research on 2-D fillers is limited compared to the fillers of other dimensions due to the difficulty of methods for physical problems such as stripping [142]. Some 2-D fillers, such as vermiculite nanosheets and LLZAO nanosheets, have been successfully prepared in recent years, but more in-depth exploration is needed in the future.

3.5 Organic Additives

The addition of organic substances with excellent thermal stability can enhance the IC of the composite polymer electrolyte [33]. In 1983, Tsuchida et al. [161] first incorporated PMMA to improve the IC of PEO-based SPEs. The IC of the PEO-PMMA composite electrolyte at 60 °C was 1.3×10^{-5} S cm^{-1}. Jinisha et al. [162] reported that the IC of the mixture (PEO, PVP and $LiNO_3$) was 1.13×10^{-3} S cm^{-1} at RT. Subsequently, a large number of organics have been added to the PEO-based polymers, of which the main polymers incorporated include polyimide (PI) [163], poly-(propylene oxide) (PPO) [164], poly(vinylpyrrolidone) (PVP) [162], waterborne polyurethane (WPU) [165], etc.

Adding small organic molecules to the polymer electrolyte not only reduces the crystallinity of the polymer but also promotes the decomposition of the lithium salt in the polymer electrolyte [166]. Generally, there are three types of organics. The first group is small non-conductive molecules, such as low molecular weight polyethylene oxide (PEO), ethylene carbonate (EC), propylene carbonate (PC) and succinyl cyanide (SN). The second group is small molecules with conductive ionic liquids, such as

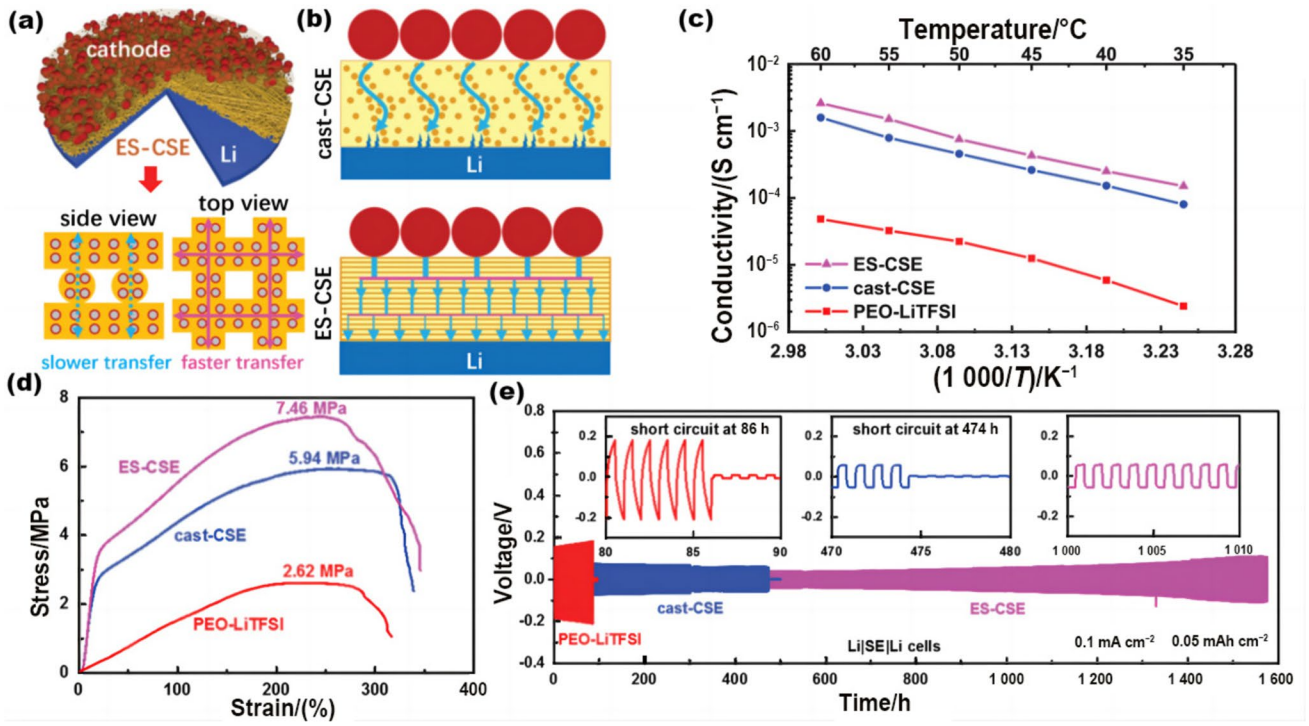

Fig. 6 ES-CSE schematic in a solid-state battery **b** Cast-CSE diagram of the lithium-ion transfer pathway. **c** ES-CSE diagram of the lithium-ion transfer pathway. **d** The IC at different temperatures. **e** Schematic diagram of the long cycle. Reprinted with permission Ref. [134]. Copyright © 2021, John Wiley & Sons, Inc

hydroxypropyl trimethylammonium bis(trifluoromethane) sulfonimide chitosan salt (HACC-TFSI) [167] and *N*-methyl-*N*-propylpyrrolidinium bis(trifluoromethane)-sulfonimide (PYR13TFSI) [168]. The third category is non-conductive polymers like polypropylene (PAN) [54, 169], polyvinylidene fluoride (PVDF) [169], etc. Different organics bind to PEO in different ways as shown in Fig. 7.

3.5.1 Small Molecule Organics

Adding small molecules of organic matter increases the proportion of the amorphous phase of PEO and improves the IC of the electrolyte. PEG and PEO have the same molecular structure, but PEG has no phase separation issue and can provide more hydroxyl (-OH) groups and yield a faster lithium-ion transport rate over a range of molecules [96].

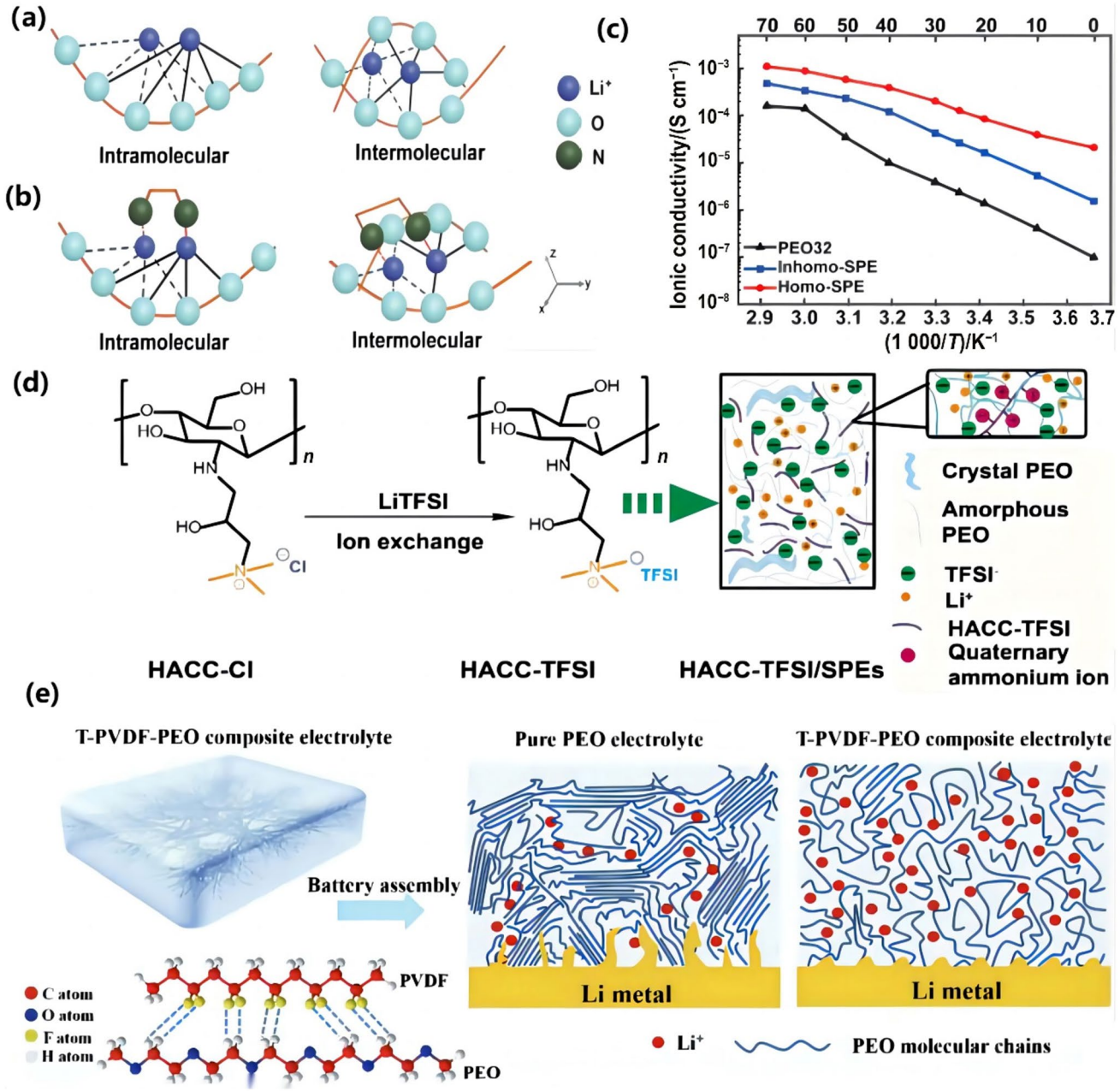

Fig.7 **a** Li^+ transport mechanism in PEO32. **b** Li^+ transport mechanism in Homo-SPE. **c** Diagram of ionic conductivity of different electrolytes. Reprinted with permission from Ref. [111]. Copyright © 2020, John Wiley & Sons, Inc. **d** Synthesis method of HACC-TFSI SPEs. Reprinted with permission from Ref. [90]. Copyright © 2020, Elsevier Ltd. **e** Schematic diagram of lithium-ion conduction paths in all-solid-state batteries assembled with PEO and T-PVDF-PEO electrolytes, respectively. Reprinted with permission from Ref. [75]. Copyright © 2020, Elsevier Ltd

The introduction of PEG into PEO systems can reduce the crystallinity of PEO and increase the lithium-ion transport rate. Dioctyl phthalate (DOP) can also inhibit PEO crystallization and increase the proportion of amorphous phases. Klongkan et al. [170] analyzed the effect of three different materials on the performance of the PEO-$LiCF_3SO_3$ electrolyte. PEG and DOP improved the lithium-ion conductivity of the electrolyte by one order of magnitude with 15 wt% PEG additive and by two orders of magnitude with 20 wt% of DOP additives. However, the –OH end of PEG will chemically react with lithium metal, which limits its use [38]. Organic solvents, such as EC and PC, can not only inhibit PEO crystallization but also promote the dissociation of lithium salts. Wang et al. [171] investigated the effect of EC and PC additives on the conductivity of the PEO-$LiClO_4$-LATP electrolyte system. It was found that T_g was decreased with increasing EC and PC content in polymeric electrolyte films.

Although the addition of liquid small molecule organics can improve the electrical conductivity, the mechanical properties of the electrolyte will also be comprised, which can cause serious problems in terms of the cycle and safety performance of the battery [38]. SN, a solid small molecule non-ionic organic compound, is widely used as an additive to promote the disassociation of lithium salts [172–174]. The organic filler and PEO-based electrolyte are generally mixed by a simple solvent casting method. PEO, LiTFSI, and SN were mixed by solvent casting to produce a hybrid electrolyte with a 100 times increase in maximum IC (Fig. 7c) and an EW of up to 4.7 V (Li/Li^+). PEO-based SPEs with the addition of SN have good cycling performance at RT or even 0 °C [111]. Figure 7a shows the lithium-ion transport path for PEO32 and Fig. 10b shows the Li^+ transport path with the addition of SN. The results confirm that SN weakens the forces between EO and Li^+, resulting in a continuous and fast transportation pathway of Li^+ in the PEO-based SPEs. It is important to note that SN molecules are toxic. Thus, serious protective gear is required during operation.

3.5.2 Large Molecule Organics

Polymer electrolytes prepared by adding macromolecular organic substances have the advantage of simple preparation and easy control of physical properties through compositional changes. Yang et al. [175] reported a PEO-$LiAsF_6$-α-cyclodextrin (α-CD) polymer electrolyte by the supramolecular self-assembly method. The IC of this electrolyte at RT is 30 times higher than that of an electrolyte with relative PEO-LiTFSI. The nanochannels formed by α-CDs provide channels for the directional movement of Li^+ ions. It prevents the entry of anions through size exclusion as well. Thus, it can achieve a good separation of Li^+ and anions. Organic molecules (β-CD) present at the nanoscale can also increase the IC of the composite electrolyte. The β-CD molecule not only forms hydrogen bonds with the EO unit of PEO to form uniform and continuous lithium-ion conduction channels and networks but also increases its Lewis basicity and promotes the dissociation of lithium salts, thus improving the conductivity of the electrolyte [104].

Organic molecules with a nanofibrous structure will provide the transport channels of Li^+ [76, 175, 176]. The alignment of the polymer chains facilitates the diffusion of ions in the direction of alignment [177]. The nanochannels formed by α-CDs provide chances for the directional movement of Li^+ ions while preventing the entry of anions through size repulsion, thus achieving a good separation of Li^+ ions and anions [175]. Additives made of large organic molecules containing the elements of N, O, and F were introduced into PEO. The polar groups containing the above elements not only form hydrogen bonds with a large number of terminal hydroxyl-OH in PEO (Fig. 7e) but also bond with $TFSI^-$ by electrostatic interaction to promote the dissociation of lithium salts. Under their synergistic effect, the additive can be uniformly dispersed in the electrolyte to enhance the migration and diffusion of lithium ions [75, 78, 177, 178]. For example, Lehao Liu et al. [179] developed ANFs as nano-additives in PEO-based solid polymer electrolytes by using a casting method. The IC of the hybrid electrolyte containing PEO-LiTFSI-5 wt% ANFs is 6 times higher than that of the PEO-LiTFSI system at 30 °C. Furthermore, the PI membrane of porous nanoporous polyimide provided a vertical transport channel for lithium ions. SPEs with PEO-LiTFSI-PI containing vertical ion channels have an IC four times higher at 30 °C than the PEO-LiTFSI system. Furthermore, Li || PEO-LiTFSI-5 wt% ANFs || $LiFeO_4$ batteries exhibited good rate performance and cycle stability [176].

Cellulose, a natural polymer widely found in nature, can be extracted in large quantities from plants and is non-toxic and environmentally friendly. The addition of cellulose to PEO-based polymer electrolytes deliberately improves their mechanical properties while promoting lithium salt dissociation. For example, Ali Asghar et al. [178] reported the addition of NC to the PEG-$LiClO_4$ system. It has high thermal stability at 150 °C and an EW of 4.7 V. Furthermore, Zhangqin Shi et al. [180] reported a kind of 3-D tubular structure of the loofah sponge anion exchange fiber (LS-AEF) as an additive for PEO-based SPEs. LS-AEF forms hydrogen bonds with PEO to build an interconnected mesh structure. Its surface charge can also interact electrostatically with $TFSI^-$ to promote the dissociation of PEO. The SPEs have high IC and good mechanical properties, excellent thermal stability, and a wide EW. The $LiFePO_4$ || 5% (weight percentage ratio) LS-AEF SPEs || Li full cell showed a capacity retention rate of 96.7% after 150 cycles. The cell still exhibited excellent cycling performance at an ultra-high rate of 10 C. The soft pack battery assembled with the

5% (weight percent ratio) LS-AEF SPE achieved capacity retention of 98.9% after 1 000 cycles at a current density of 0.2 mA g^{-1}.

3.5.3 Ionic Liquids

Ionic liquids (ILs) are composed entirely of ions, usually large anions and smaller cations, which have high IC, and good thermal and electrochemical stability [25, 181]. Ionic liquids are often used as an excellent additive to improve the IC of PEO-based polymer electrolytes. The IC of the polymer electrolyte is enhanced by the addition of substances that can bind to the $TFSI^-$ anion and facilitate the decomposition of the lithium salt [168, 180, 182]. Diddo Diddens et al. [168] proposed to introduce PYR13TFSI into PEO-LiTFSI electrolytes to study the effect of different concentration series by lithium volume concentration. LiTFSI-*x*PYR13TFSI can enhance the segmental mobility of PEO chains, and improve the lithium diffusion rate and the IC. The fast movement of PEO improves the lithium ions coordinating with PEO chains. It is concluded that the transport mechanisms of lithium ions are different at various salt concentrations. Lithium-ion transportation is on specific PEO chains with progressive coordination of $TFSI^-$ ions at high salt concentrations. In contrast, it is mainly on PEO chains at low salt concentrations, being consistent with the transport mechanism of the PEO-LiTFSI system. However, this ionic liquid additive hinders Li^+ transport and leads to the lower mobility of lithium ions.

Atik et al. [183] proposed the preparation of different ionic liquid additives using oligomeric (ethylene oxide) substituents with seven repeating units to prepare pyrrolizidine cations. Despite the similar physical properties, the IC of the improved PEO-based polymeric membranes performs 3 times higher than that in Pyr14TFSI analogs. Moreover, Li et al. [184] have designed a poly(ionic liquid)-poly(ethylene oxide) semi-interpenetrating polymer network CSE for use in safe lithium-ion batteries. Differential scanning calorimetry data indicate the crystallinity of the composite solid electrolyte is 15.5 wt% lower than that of the ILs solid electrolyte due to the limitations of the ILs interpenetrating network. The conductivity is 6.12×10^{-4} S cm^{-1} at 55 °C. The excellent electrochemical performance of this electrolyte is 147 mAh g^{-1} at a 0.2 C rate at 55 °C in $LiFePO_4$ || Li of LIBs.

4 Improve Mechanical Properties of PEO-Based SPEs

The mechanical properties of the material are determined by the strength of chemical bonds as well as the crystal structure. Therefore, there are two ways to improve the mechanical strength of PEO-based electrolytes. One is to change the chemical bonds of PEO itself to polymerize with other organic substances. The other is to introduce substances with high mechanical strength, such as high-strength polymers and hard ceramic fillers.

4.1 Superior Mechanical Strength Organics

The introduction of other units in the main chain of PEO through co-polymerization, cross-linking, and different types of bonding can not only reduce the crystallinity of PEO, but also improve the mechanical strength of the electrolyte. Generally, crosslinking refers to the use of UV [185], thermal radiation [186], photo-polymerization [187], and electron beam radiation polymerization [188] to crosslink two or more linear polymers. Moderate cross-linking of linear polymers can enhance mechanical strength, elasticity and dimensional stability. Cross-linked PEO polymers, such as polyacrylonitrile-polyoxyethylene (PAN-PEO) [189], poly(ethylene oxide)-g-poly(ethylene glycol) (PEO-g-PEG) [190], poly(ethylene oxide-co-propylene oxide) (PEO-co-PPO) [191] and PPG-PEG-PPG [192], have already been studied. A multi-technical study of the structural and transport properties of novel 3-D interconnected networks doped by UV-induced PEO and tetra(ethylene glycol) dimethyl ether (g4) with bis(trifluoromethyl) was reported by Marisa Falco et al. [185]. The crosslinking reaction can significantly reduce PEO crystallinity and thus enhance its IC at RT. Guang Yang et al. [193] reported a very simple single-step synthetic strategy based on the in situ cross-linking of poly (ethylene oxide) (*x*PEO) in the presence of woven glass fibers (GF). This simple method can produce CPEs with an exceptionally high elastic modulus being up to 2.5 GPa over a wide temperature range (20–245 °C), which has never been documented before. Rigorous constant current cycling tests show that this CPE can be cycled stably for > 3 000 h at moderate temperatures (near 1 500 C cm^{-2} Li equivalent) in lithium metal symmetric cells. Layer-by-layer (LbL) self-assembly can form polymer nanocomposites with good mechanical strength and excellent ion mobility through the formation of ordered structures, which cannot be achieved by simple polymer blending. For instance, Zhen Wang et al. [73] prepared PEO-PAA composite thin films via LbL self-assembly in an aqueous solution (Fig. 8a). LbL technology can achieve self-assembly with nanoscale precision. A PEO-based composite polymer electrolyte with excellent homogeneity was obtained by the above method (Fig. 8b–f). The IC of PEO-PAA 240 K at 30 °C is as high as $(2.3\pm0.8)\times10^{-4}$ S cm^{-1}, and the mechanical strength can be enhanced in terms of a tensile strength of (3.7 ± 0.2) MPa. This confers good stability to PEO-PAA240k films in cyclic plating/peeling tests at a constant current of 0.05 mA cm^{-2} for at least 1 000 cycles.

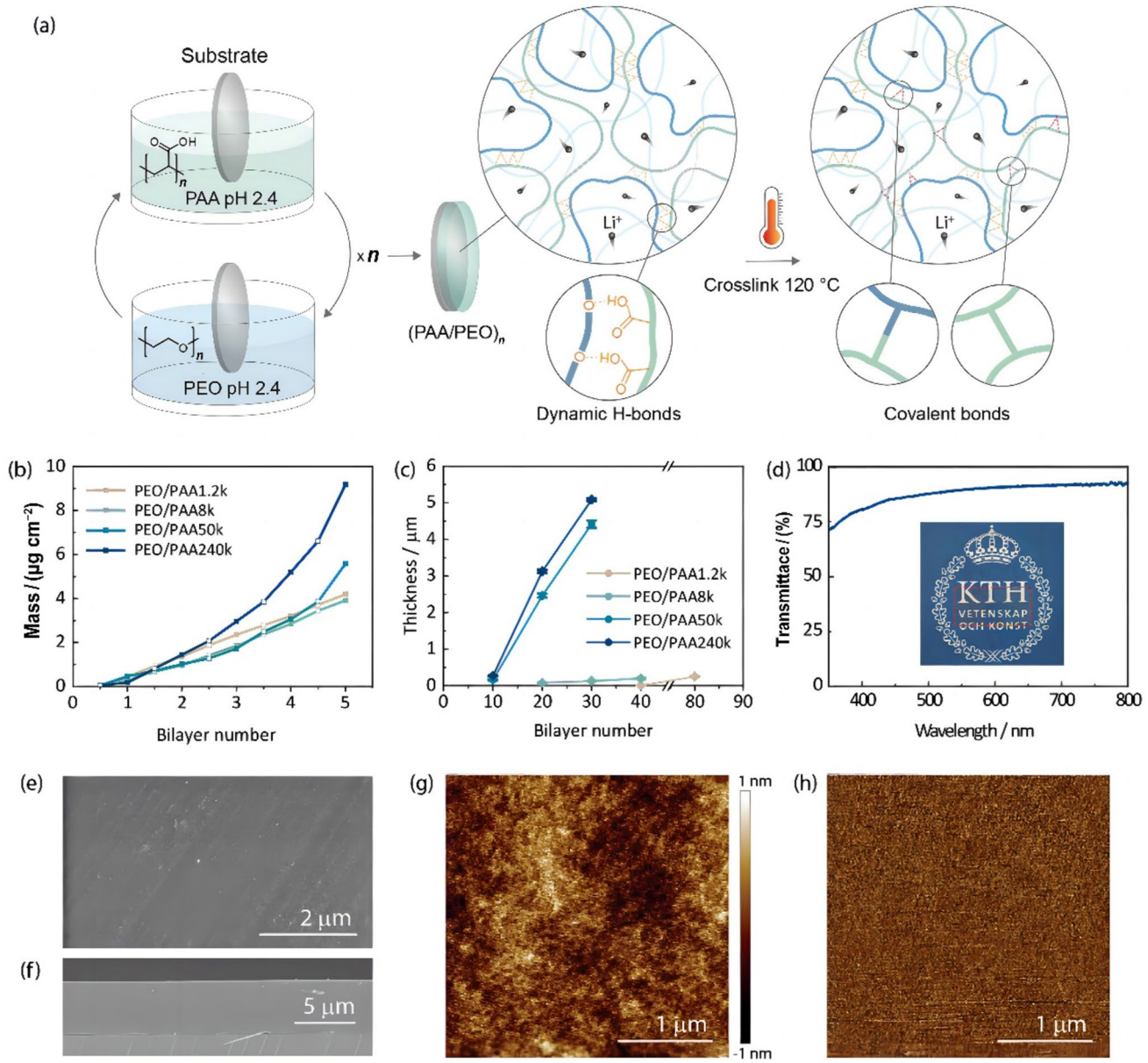

Fig. 8 **a** Schematic illustration of the process of LbL self-assembly and heat-induced crosslinking. **b** Mass growth calculated from the QCM data of the first five bilayers of PEO and PAA with various molecular weights. **c** The thickness of the PEO/PAA films assembled with PAA of different molecular weights. **d** Transmittance spectrum of the (PEO/PAA240k)100. The inset is a photo of the corresponding sample with the shape indicated by the red dashed line. Representative **e** top-view SEM image, **f** cross-sectional SEM images, **g** height image from AFM, **h** peak force error image from AFM of the (PEO/PAA240)30 composite thin film. Reprinted with permission from Ref. [73]. Copyright © 2021, John Wiley & Sons, Inc

4.2 Improvement of Mechanical Properties of PEO Polymers by Introducing Fillers

PEO polymer electrolytes have low mechanical strength and good ductility, while high-hardness ceramic electrolytes have high mechanical strength and poor ductility. A composite polymer electrolyte with suitable mechanical strength and ductility can be prepared by combining the advantages of both materials. The addition of active fillers increases mechanical strength through its strong mechanical robustness [42, 63, 134]. The introduced filler can range from 0 to 1, 2, and 3-D structure of small particles, which increases the contact area with polymer PEO and strengthens the interaction between PEO and filler. Therefore, it improves the mechanical strength of the composite electrolyte, inhibits the formation of lithium dendrites and boosts the electrochemical performance of LIBs.

For example, Tan et al. [90] proposed chitosan ionic liquid HACC-TFSI as a filler. 10 wt% HACC-TFSI-SPEs showed a tensile strength of 1.01 MPa, which was 3.6 times higher than that of blank SPEs. The combination of PEO chains and HACC-TFS increased the interaction between PEO polymers and improved the mechanical properties of the complex electrolytes (Fig. 7d). In addition, g-C_3N_4 nanosheets with 2-D structure were introduced into the PEO-based electrolyte, due to the large area of interaction between the g-C_3N_4 nanosheets and the polymer. The polymer chains are less prone to relative sliding under external forces due to the large area of interaction between the g-C_3N_4 nanosheets and the polymer. Thus, it improves the mechanical properties of the electrolyte. The tensile strength of PEO-LiTFSI-5 wt% g-C_3N_4 reached 1.8 MPa, which is much higher than that without g-C_3N_4 (0.86 MPa). The tensile modulus of this composite electrolyte is as high as 65.7 MPa at EO/Li = 30 and effectively inhibits lithium dendrite nucleation. The LLTO network of 3-D as a nano-skeleton in the PEO matrix showed significantly enhanced mechanical properties with a tensile strength of 16.18 MPa and Young's modulus of 0.98 GPa [106]. It could inhibit the formation of lithium dendrites and thus improve the electrochemical stability in Li-Li symmetric cells at 0.1 mA cm^{-2} for 800-h Li^+ stripping and plating.

Gel polymer electrolytes based on polyvinylidene fluoride (PVDF, –[CH_2–CF_2]–) has been introduced into GPEs as a matrix material due to its excellent mechanical strength. PVDF has a high dielectric constant, high mechanical strength and a multilayered structure that could overlap each other, which can help reduce the crystallinity of PEO, enhance the mechanical strength and inhibit the formation of lithium dendrites. Raghavan Prasanth et al. [78] prepared fibrous membranes with good mechanical strength and porosity from a blend of PEO and PVDF by using electrostatic weaving. This composite electrolyte has a conductivity of 4.9×10^{-3} S cm^{-1} at RT. PVDF nanofibers membranes with different diameters were prepared by the electrostatic spinning method and blended with PEO [75] (Fig. 10e). Generally, the polymer is infiltrated into the 3-D skeleton by filtration, which prevents the polymer from being uniformly dispersed in the framework due to the capillary tension of the nanopores [76].

The high crystallinity of PVDF makes it unsuitable for use as an electrolyte alone [38]. In most cases, PVDF is copolymerized with HFP, which decreases the crystallinity of PVDF, maintains good mechanical strength and plays an important role in the structure of the composite polymer [194, 195]. For instance, Gao et al. [196] proposed to introduce gadolinium-doped CeO_2 (GDC) ceramic nanowires with oxygen vacancies into PVDF-PEO composite nanofiber membrane polymer electrolytes with core-shell structure and lower cost via a casting method. The mechanical strength of the composite electrolyte is 10.8 MPa. The core layer of PVDF can improve the mechanical strength, and the shell layer of PEO in the composite nanofibers can provide 3-D ordered transport channels for lithium ions. Polyvinylidene fluoride-hexafluoropropylene (PVDF-HFP) copolymer was added to the PEO-based polymer, and then, plasticizers [197], LLZTO [198] and LLZO [68] were added to the PEO-PVDF-HFP system. Yu et al. [68] reported a free LLZO nanoparticle consisting of a Li_2CO_3 CSSE with a vertically aligned structure (labeled PLLZO$_V$) in a PVDF-HFP-PEO-LiTFSI (PPL) matrix by plasma treatment. In most studies, the filler was randomly dispersed and connected in a solid composite electrolyte. The removal of the Li_2CO_3 layer significantly improved the IC of the LLZO, which gives PLLZO$_V$/PPL fast Li^+ transport capability together with a vertically aligned array. The NCM622 ‖ PPL ‖ Li cell has a high capacity of 102.1 mAh g^{-1} at 1 C compared to 60.0 mAh g^{-1} for the blank cell without filler. After 200 cycles at 0.5 C, as much as 77.4% capacity retention was achieved for the NCM622 ‖ PPL ‖ Li cell, much higher than the 52.0% capacity retention of the blank control.

Liying Tian et al. [76] reported a novel hot-pressing method to load PEO onto organic nanofiber membranes and form a homogeneous structure. This work combines the advantages of a superior 3-D structure for lithium IC and the good mechanical properties of the nanofiber-reinforced network. The addition of lithiated organic nanofiber membrane (LOF) not only reduces the crystallinity of PEO and accelerates the segmental motion of PEO, but also constructs a high-speed conduction channel of Li^+. As a result, the prepared LOF-CPE has an excellent IC of 7.41×10^{-5} S cm^{-1} at 30 °C. The good bonding between PEO and LOF results in a homogeneous structure of the composite electrolyte and enhanced mechanical properties, i.e., the tensile strength increases to 8.9 MPa. The $LiFePO_4$ ‖ Li cell exhibits good cycling performance and capacity after 500 cycles at 0.5 C with a retention rate of 82%. This work provides a very promising approach for solid polymer electrolytes to achieve high IC and superior mechanical properties at the same time.

5 Improve the Electrochemical Window

LIBs with PEO-based SPEs usually use cathodes with a low charge/discharge plateau, such as $LiFePO_4$, because the electrolytes do not have a wide enough EW to be used for high-voltage cathode materials and may have some side reactions at the cathode. To broaden the EW, lithium salts, polymers and fillers have been introduced into PEO-based SPEs. The addition of some lithium salts has been identified to be effective in improving the EW of PEO-based electrolytes. A dry ball milling process was developed for the preparation of polymer electrolytes based on LiTFSI

and PEO systems without the use of any solvents [62]. Not only does it increase the IC, but it also improves the oxidative stability of PEO-based polymer electrolytes above 4 V. Guo et al. [74] created an elastic polymer network through in situ synthesis of PEO and lithium salts. For another instance, the resultant ternary salt polymer electrolytes prepared from three salts, $LiNO_3$, LiTFSI, and LiBOB, exhibited oxidative stability up to 4.6 V [69].

Some organic can improve the EW of PEO-based SPEs to be higher than 5 V. For example, Rolland et al. [71] also designed a mechanically clamped liquid PEO electrolyte that combines the high IC of low molecular weight PEO through block copolymer engineering. Oligo (ethylene glycol) with 9 units (OEG9) exhibited a high IC of 10^{-3} S cm^{-1}. PS-bPOEG9MA side chain length was designed to allow an IC of more than 10^{-5} S cm^{-1} and an electrochemically stable window higher than 5 V. Furthermore, Jiewen Tan et al. [90] reported the use of HACC-TFSI as an additive in PEO-based SPEs (Fig. 10d). The electrochemical stability, mechanical strength, and thermal stability of PEO-LiTFSI-10 wt% HACC-TFSI SPEs are superior to that of PEO-LiTFSI electrolytes. The stable EW is as high as 5.26 V vs. Li/Li^+. The $LiFePO_4$ || 10 wt% HACC-TFSI-SPEs || Li battery can run when the temperature is above 150 °C.

Inorganic fillers can also broaden the EW and improve the electrochemical stability of LIBs. A simple solvothermal method has been developed for the synthesis of Nacikon-structured LATP nanomaterials, which are then embedded in PEO polymers to form PEO polymer electrolytes [56]. Due to the potentially wide EW of the LGPS, the PEO-LiTFSI-LGPS composite electrolyte has EW stability of 5.7 V vs. Li/Li^+ [96]. In the PEO-LiTFSI-1 wt% Graphene Oxide (GO) system, the IC is 7 times better compared with the electrolyte without GO, and the EW is 5 V vs. Li/Li^+. GO not only reduces the crystallinity of PEO but also improves the ability of PEO chain segments to transfer ions [100]. For example, Li et al. [109] proposed the addition of hexagonal boron nitride (h-BN) to the PEO-LiTFSI system. h-BN additives can improve the chain-segment mobility and mechanical properties of PEO polymers and further increase the EW of PEO SPEs. The electrochemical stability window of PEO-LiTFSI-6 wt% h-BN SPEs is 5.16 V as compared to 4.43 V of PEO-LiTFSI. PEO-based SPEs have good cycling performance, with a long cycle time of 430 h at 0.2 mA cm^{-2} in Li || Li symmetric batteries. 140 cycles for $LiFeO_4$ || PEO-LiTFSI-h-BN || Li full cells are in stark contrast to merely 39 cycles for $LiFeO_4$ || PEO-LiTFSI || Li full cells. Due to the reaction of BN with the SO_2 group in $TFSI^-$, the movement of the $TFSI^-$ anion was inhibited, and the decomposition of LiTFSI was promoted, thereby synergistically promoting the dissociation of lithium ions.

6 Improve the Overall Performance

The application of PEO-based SPEs in ASSLBs is limited due to the low IC and poor electrochemical stability of PEO-based SPEs, especially at high voltages. In order to produce high-performance ASSLBs, PEO-based SPEs need to be prepared for use at both low temperatures and high voltage. For example, Tan et al. [199] demonstrated a cryogenic engineering technique that improves the PEO-based SPE of ASSLBs operating at RT. At 0.5 C, the cryogenic PEO electrolyte could achieve an initial discharge capacity of 88 mAh g^{-1}, which is quite higher than that of 4.4 mAh g^{-1} in the blank PEO LIBs. The rapid in situ cooling process can lead to the formation of homogeneous PEO nuclei, which will limit the growth of large PEO crystals in the SPE. The new crystalline structure further improves the IC of SPEs as evidenced by an excellent IC of 2.17×10^{-5} S cm^{-1}, which is 6 times higher than that in blank PEO (3.53×10^{-6} S cm^{-1}). In addition, the PEO polymer electrolyte prepared by cryogenic engineering has high electrochemical stability and can match the NCM622 high-voltage cathode.

Considering the complex system of batteries, composite fillers are generally used to improve the overall performance with higher IC at low temperatures, wider EW to match the high-voltage cathode, and more excellent mechanical strength to inhibit the formation of lithium dendrites. A mixture of organic or inorganic substances is added to PEO-based SPEs. For example, Fang et al. [200] evaluated Li_2S_6 as an additive to PEO-TiO_2-LiTFSI CPEs by a conventional casting method. The introduction of Li_2S_6 additive can not only combine with PEO and reduce the crystallinity of PEO to improve the overall IC of the electrolyte but also form a thin layer of Li_2S/Li_2S_2 to enhance the ion transport at the interface and inhibit the growth of lithium dendrites, thus improving the stability of the lithium metal and electrolyte interface (Fig. 9a). CPEs-3 wt% Li_2S_6 films showed the highest Li^+ conductivity of 1.7×10^{-4} S cm^{-1} at 40 °C (Fig. 9b). The Li || CPEs-1% Li_2S_6 || $LiFePO_4$ battery achieved a capacity retention of 89.2% after 700 cycles at 50 °C (Fig. 9c). Zhang et al. [201] suggested the introduction of short-chain organic tetramethylene glycol dimethacrylate (TEGDMA), and tetramethylene glycol dimethyl ether (TEGDME) to simultaneously increase IC and mechanical strength. The IC is as high as 2.7×10^{-4} S cm^{-1} at 24 °C and the electrochemical window is increased to 5.38 V. As the SPEs were prepared in situ on the electrode surface, the reduction of the interface resistance resulted in excellent long-cycling performance. The enhanced mechanical strength of PEO-based SPEs effectively inhibits the formation of lithium dendrites. The capacity of the $LiFePO_4$ || SPEs || Li cell

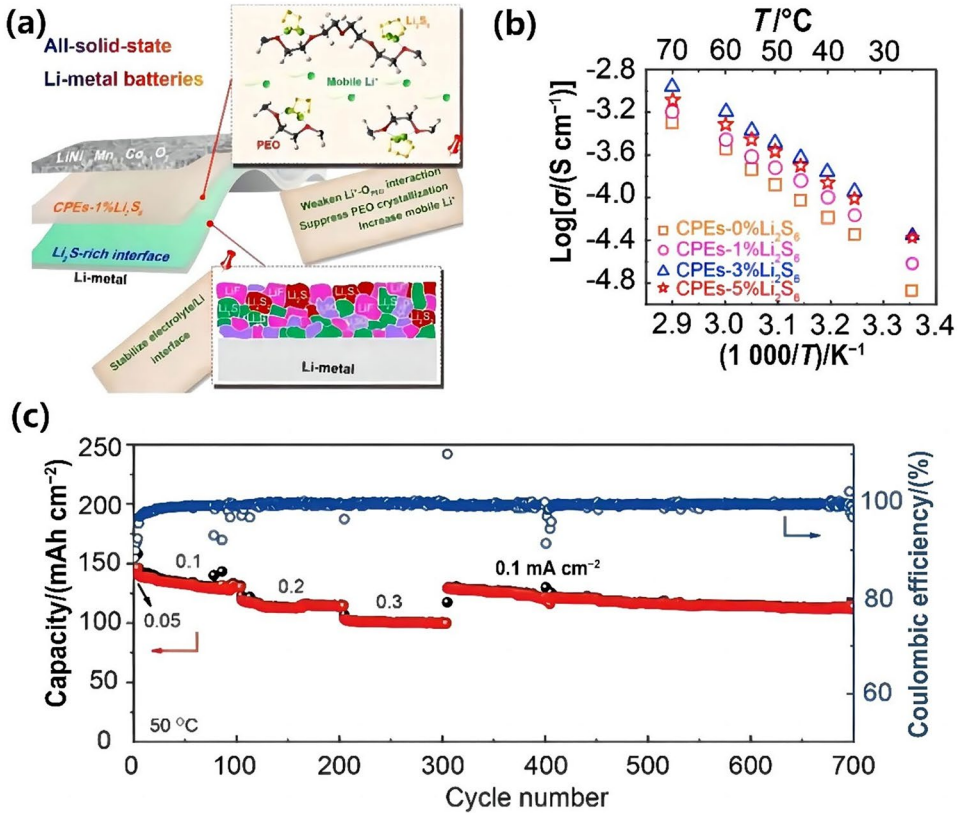

Fig. 9 Is **a** Schematic diagram of the role of the introduction of Li_2S_6 additive. **b** The IC of PEO-based SPEs with different quantities of Li_2S_6 additives introduced at different temperatures. **c** Long cycling performance at 50 °C. Reprinted with permission from Ref. [200]. Copyright © 2021, John Wiley & Sons, Inc

is ~ 160 mAh g^{-1} at 0.05 C at RT after 100 stable cycles. The capacity can reach 60 mAh g^{-1} at a 1 C rate after 100 cycles or more. SEM analysis of SPE-based cells shows that there is no dendrite on the surface of the lithium metal anode after 100 charge/discharge cycles at 0.1 C.

Organic or inorganic substances are added to the lithium salt system of PEO either by simple physical mixing [56, 80, 100, 104] or chemical bonding [72, 74, 102]. One filler can only improve electrical conductivity, mechanical properties, or electrochemical stability. However, the overall performance of PEO polymer composite electrolytes is normally improved by the synergistic effect between fillers and PEO-lithium salts [173, 197, 202].

Copolymerization is a reaction in which two or more compounds are polymerized under certain conditions to form a single substance. PEO copolymers are classified as dimer (such as polystyrene-block-poly(ethylene oxide) (PS-PEO) [203], poly(ethylene oxide)-poly(propylene oxide) (PEO-PPO) [204], poly(ethylene oxide carbonates) (PEO-PCs) [205]) and trimer (poly(isoprene-*b*-ethylene oxide) (PI-B-PEO) [206]) in terms of the type of monomer. The copolymerization of PEO and monomers or short-chain organics with functional groups (these monomers and short chains are functional units) can improve the comprehensive properties of PEO-based SPEs. Thus, they can also be divided into block copolymerization and graft copolymerization. Gomez et al. [203] proposed utilizing a mixture of a lithium bis(trifluoromethane) sulfonyl imide salt and a symmetrical PS-PEO as the electrolyte. In contrast to the current solid and liquid electrolytes, the conductivity of the PS-PEO/salt mixture is improved with an increase in the molecular weight of the copolymer. Furthermore, Leire Meabe et al. [205] proposed PEO-PCs consisting of PEO and PCs functional units. By adjusting the ratio of PEO and PCs, the IC was increased up to 3.7×10^{-5} S cm^{-1} at 25 °C. In addition, Zhang et al. [207] designed a new ultra-thin polymer electrolyte (UTPE) made of a single helix structured agarose (AG) with PEO. This unique single-helix structure can provide high mechanical strength and fast ion transport channels (Fig. 10a–b). Therefore, the PEO-AG-30 wt% LiTFSI system exhibited excellent performance with an IC of 1.2×10^{-4} S cm^{-1} (Fig. 10c) and a tensile strength of 5.5 MPa at RT. The specific capacity of the $LiFePO_4$ || SPE || Li full cell reached 131 mAh g^{-1} at 1 C for 600 stable cycles at RT with a capacity retention of 92.9% (Fig. 10d).

PAN has good mechanical and electrochemical properties. The presence of electron-rich polar nitrile (C≡N) groups helps to form hydrogen bonds between PAN and PEO. For example, Cui's group [202] prepared a composite electrolyte consisting of LLTO-PAN-$LiClO_4$ by electrostatic spinning (Fig. 11a), and the IC of the composite electrolyte was increased by three orders of magnitude to 2.4×10^{-4} S

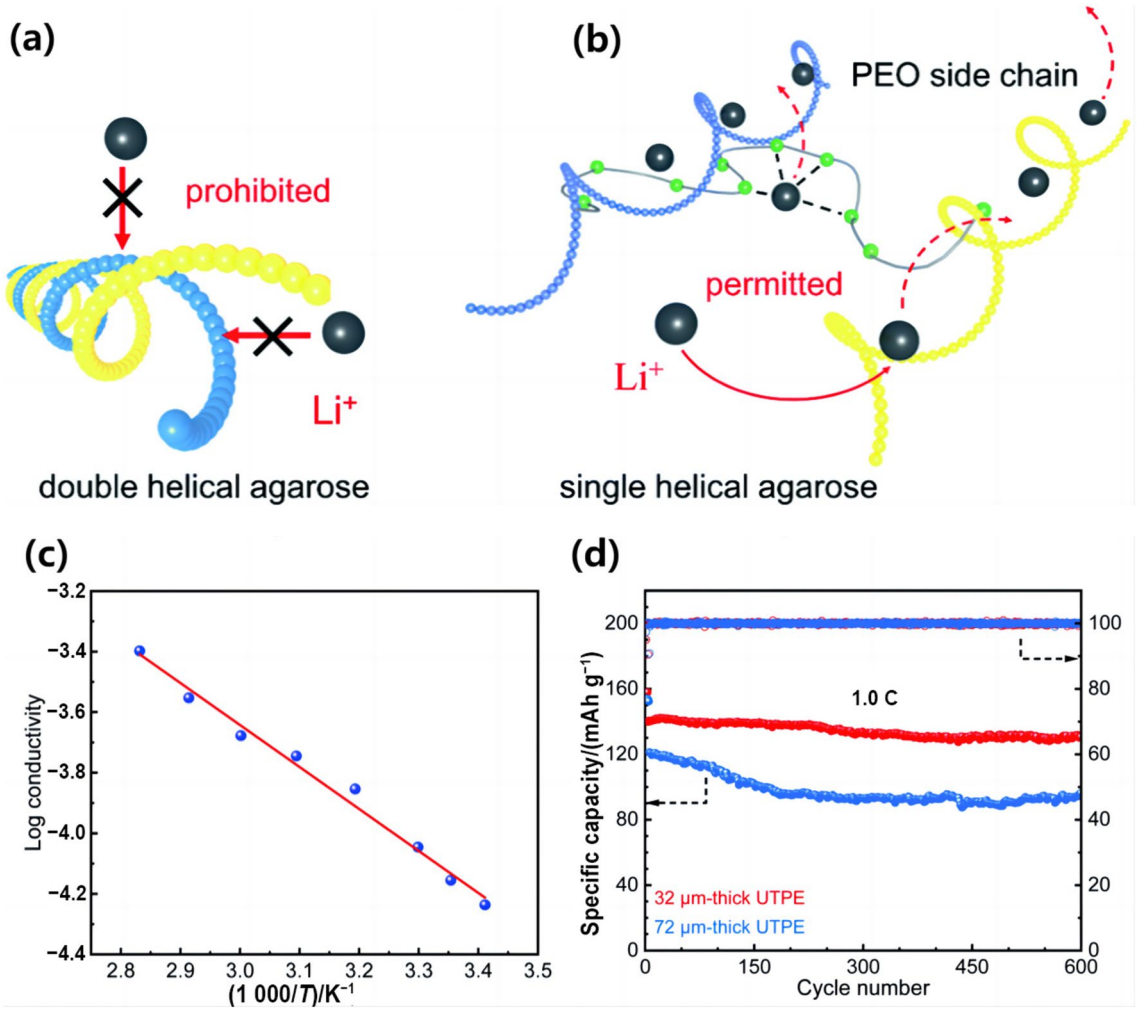

Fig. 10 **a** Schematic diagram of lithium-ion transport by double helix agarose. **b** Schematic diagram of lithium-ion transport by single helix agarose and PEO side chain. **c** The IC of ultra-thin polymer electrolytes at different temperatures. Reprinted with permission from Ref. [207]. Copyright © 2021, The Royal Society of Chemistry

cm^{-1} at a 15 wt% of PAN doping level (Fig. 11d–e). Due to the introduction of fillers as nanowires rather than nanoparticles, the transport pathway for lithium ions is provided as shown in Fig. 11b, which in turn leads to an increase in IC. Subsequently, electrochemical AC impedance tests were conducted with different fillers and various ratios of electrolytes to compare the differences in performance (Fig. 11c).

For example, Peng et al. [98] reported the addition of LAGP and SN fillers to a PEO system. The crystallinity of PEO decreased significantly with the addition of LAGP and SN. The PEO18-LiTFSI-14 wt% LAGP-15 wt% SN solid-state electrolyte has the highest IC with 1.26×10^{-4} S cm^{-1} at 30 °C. Li ‖ SPE ‖ $LiFePO_4$ in ASSLBs was cycled 200 times at 40 °C with a capacity retention of 91.2%. Wang et al. [59] proposed that the addition of SN and TEOS can undergo hydrolysis to form SiO_2 in the PEO-LiTFSI. The combination of SiO_2 with hydroxyl groups on the surface or PEO, SN and LiTFSI through hydrogen bonding can improve the mechanical strength. The synergistic effect of both fillers can reduce PEO crystallinity and enhance the IC. The $LiFePO_4$ ‖ Li cell delivered a high discharge capacity of 161.2 mAh g^{-1} at 0.5 C with a capacity retention of 88% after 400 cycles at 30 °C.

In addition to the above additives, many other types of fillers were employed to modify the electrolytes. The PMA-PEG-$LiClO_4$-3 wt% SiO_2 CPE exhibited an optimum IC of 2.6×10^{-4} S cm^{-1} at RT [208]. Siyal et al. [138] prepared a composite gel polymer electrolyte PEO-Bp-LATP film by ultraviolet (UV) irradiation with benzophenone (Bp) as the photoinitiator. PEO-Bp-15 wt% LATP has the highest IC of 3.3×10^{-3} S cm^{-1} at 30 °C. Pan et al. [96] used LGPS as a filler for CSEs by the in situ coupling reaction method. PEO-PEG-LiTFSI-3 wt% LGPS has the highest conductivity of 9.8×10^{-4} S cm^{-1} at RT and a high

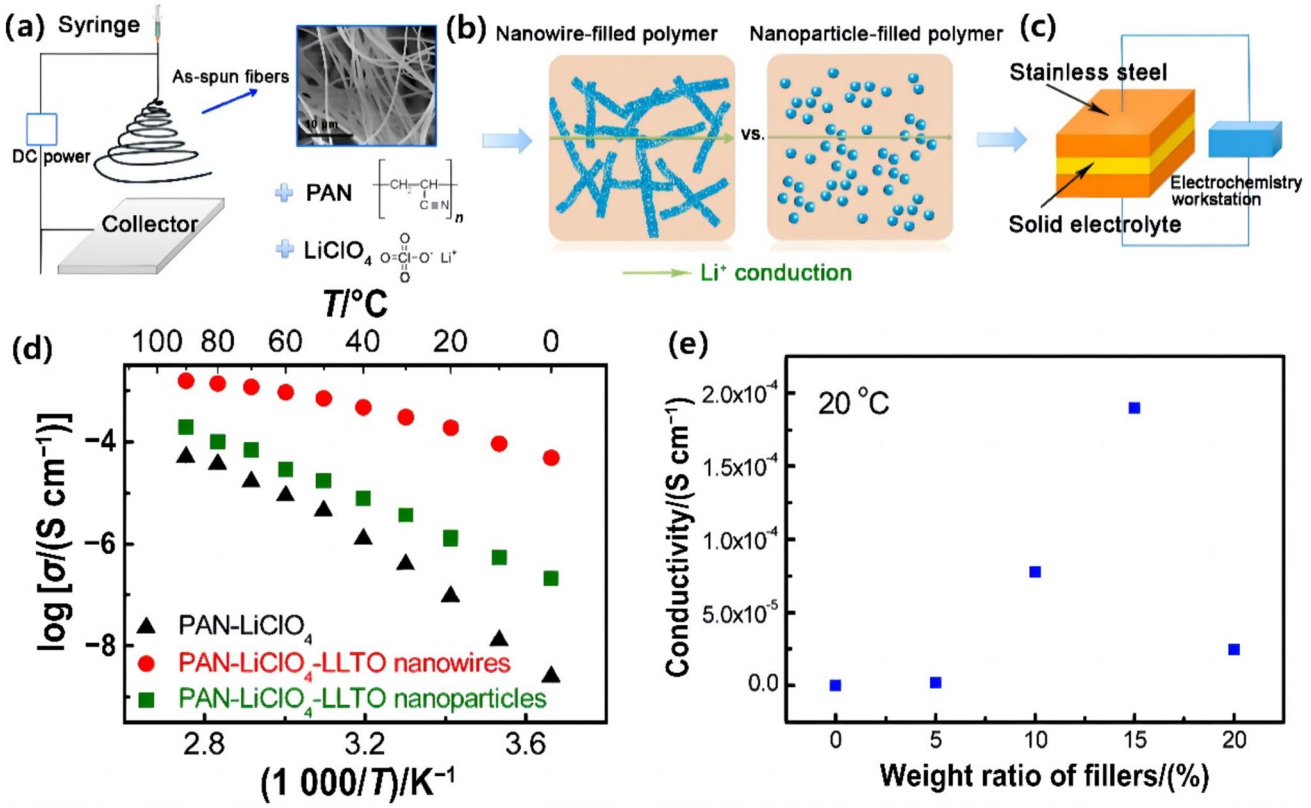

Fig. 11 **a** Schematic diagram of PEO-based SPE synthesis. **b** Illustration of the ion transport paths of different forms of fillers. **c** Electrode configuration diagram for AC impedance spectrometer measurements. **d** Arrhenius with different electrolytes. **e** Conductivity of the packed electrolyte with different mass fractions is introduced. Reprinted with permission from Ref. [202]. Copyright © 2015, American Chemical Society

Li^+ transfer rate of 0.68. The CSEs have a stable EW of 5.0 vs. Li/Li^+ and high-capacity retention compared to PEO polymer electrolytes without the addition of PEG and LGPS fillers. Furthermore, Zhang et al. [97] reported a PEO-PAN-LLZTO composite electrolyte consisting of a 3-D fibrous network formed by PAN-LLZTO homogeneously dispersed in a PEO polymer (PPL) matrix. The 3-D structure of PAN-LLZO is uniformly distributed in PEO to form continuous ion transfer channels, which not only facilitates the rapid transfer and uniform deposition of lithium ions, but also improves the mechanical strength of PEO polymer and effectively inhibits the growth of lithium dendrites. The PPL electrolyte has superior electrochemical properties, with IC up to 1.76×10^{-4} S cm^{-1} at 30 °C and a wide electrochemical stability window of 5.2 V. The Li || PPL || Li symmetric cell can operate stably for more than 4 000 h. In the $LiFePO_4$ || PPL || Li battery, the reversible capacity is 120.7 mAh g^{-1} after 1 000 cycles at 1 C. In addition, the PPL electrolyte exhibited superior cycling performance at high-voltage cathodes. This study suggests that this 3-D fiber network reinforced polymer electrolyte is the key to achieving solid-state high-energy density batteries.

7 Improvement in Interface Stability and Compatibility between Electrolyte and Electrode

As shown in Fig. 1, PEO-based SPEs, cathodes, and lithium metal anodes are the basic components of all-solid-state lithium metal batteries, in which PEO-based SPEs serve as the lithium-ion transport path. Figure 1a shows the problems of PEO-based SPEs all-solid-state lithium metal batteries, and Fig. 1b shows a series of improvement measures for the interface between the electrolyte and the electrode, including optimizing the composition of the PEO-based electrolyte and providing an efficient method to enhance the stability of interfaces.

7.1 Approaches to Improve the Interfacial Stability of PEO-Based SPEs and Lithium Metal Anodes

The use of lithium metal as the anode to enhance the energy density of the battery also brings about some solid–solid interface problems. This is related to the high interface impedance [22, 25], the non-uniform deposition behavior of lithium ions [23, 209], and the volume change of lithium anodes after cycling [25, 31, 210, 211]. These problems can cause the generation of lithium dendrites that could potentially poke through the solid electrolytes, resulting in short circuits in the battery. The root cause of lithium dendrite formation is the exposed crystalline surface, inhomogeneous surface composition, and roughness of the anode, which results in the inhomogeneous migration of lithium ions and inhomogeneous lithium plating and stripping rates. The deposition of Li^+ becomes inhomogeneous with significant increasing in local current density. The construction of an artificial solid electrolyte intermediate phase SEI has recently been proposed to protect lithium metal electrodes [212–215]. The uniform deposition of lithium ions by adding additives is a common strategy to suppress the growth of lithium dendrite [98, 216–218].

7.1.1 Formation of Solid Electrolyte Interface Layer Enhances Electrochemical Stability

The limited contact among the lithium anode and PEO-based SPEs and the poor wettability of the solid electrolyte compared to the liquid electrolyte [23] leads to a high interfacial impedance, which inhibits the transport of lithium ions at the interface between the SCE and the lithium anode. Increasing the interface contact between the solid electrolyte and the anode can reduce the interface impedance and local current density, which can help to slow down the dendrite growth. The addition of different substances to the PEO matrix can facilitate the formation of a stable inorganic or organic solid electrolyte phase interface (SEI) between the lithium anode and the electrolyte.

To gain a better understanding of the electrolyte–electrode interface chemistry in SPEs-based lithium metal batteries, more efforts have been devoted to SEI characterization in SPE batteries. Peled et al. [219] first proposed a model for the growth of SEIs at the polymer and lithium interface; although this technique was not sufficient to analyze its composition, the authors concluded that the growth of SEIs was related to the effective contact area between lithium metal and polymer. Ismail et al. [220] used X-ray photoelectron spectroscopy (XPS) to study the surface layer formed after the contact of lithium metal with lithium salt-doped SPEs. The formed layer was found to be composed of the salt decomposition product LiF and the natural thin film compounds Li_2CO_3, LiOH, and Li_2O present on the pristine lithium metal. Introducing an intermediate interface layer between the solid electrolyte and the lithium cathode is a common method. The ion-conductive and electron-insulating SEI layer slows down the growth of lithium dendrites and avoids the reaction between lithium metal and electrolytes, such as LiF, Li_3N and Li_2S [210].

PAN [221], $LiNO_3$ [222], PVDF-HFP [99], Li_2S_6 [200], PAM [223], and other additives can be introduced, which contain polar groups of N, F, S, and other elements to form LiF and Li_3N at the SEI. On the one hand, Li_3N promotes ion transport and inhibits undesirable interfacial reactions. On the other hand, LiF enables homogeneous deposition of Li^+ [210]. Li_3N and LiF synergize to improve interfacial stability. For example, Cui's group [167] prepared an SPE film composed of PAN-PEO-LiTFSI. The interface contact area between the electrolyte and lithium electrode was increased. The PAN fibers constructed an SPE and Li interface rich in Li_3N and LiF, which promoted the stable cycling of lithium batteries. The excellent thermal stability of PAN makes SPEs safer to use at high temperatures and can increase the battery operating temperature up to 150 °C. Zhao Zhang et al. [222] presented that the PEO-LiTFSI-LLZTO (PLLE) polymer electrolyte with $LiNO_3$ can induce the formation of a stable Li_3N-LiF enriched interface between the PEO-based solid electrolyte and the lithium anode in situ. The ICs of PLLE and 2 wt% $LiNO_3$ at 60 °C were 1.1×10^{-3} and 8.4×10^{-4} S cm^{-1}, respectively. The Li || PEO || NCM battery keeps 91.4% of the capacity retention at 0.2 C after 200 cycles. The formation of LiF SEIs is based on the slow decomposition of LiTFSI (Fig. 12d-e). The lithium salt in the PEO-LiTFSI-LLZTO composite electrolyte (PLLE), on the surface of Li, and the C–S or C–F bonds show a gradual increase from 0 to 20 ps as shown in Fig. 12a-b. PLLE and PLLE containing 2, 5, 8 wt% $LiNO_3$ have IC of 1.1×10^{-3}, 8.4×10^{-4}, 6.7×10^{-4} and 8.8×10^{-5} S cm^{-1} at 60 °C (Fig. 12c).

7.1.2 Fillers Suppresses Growth of Lithium Dendrites

In the process of lithium metal stripping, if the rate of lithium replenishment is slower than the rate of lithium stripping from the interface, holes will be created at the interface, even causing the solid electrolyte and lithium metal cathode from surface contact to point contact, resulting in a sharp increase in interface impedance [224]. The ideal lithium deposition is a planar homogeneous deposition; however, due to the properties of lithium itself and the inhomogeneity of the interface, the lithium-positive property is prone to inhomogeneous deposition [225].

Adding large amounts of Li^+ with ceramic to the PEO-based SPEs could increase its mechanical strength, and further inhibit the formation and the growth of lithium dendrites [22]. For example, $Mg(ClO_4)_2$ has been employed as

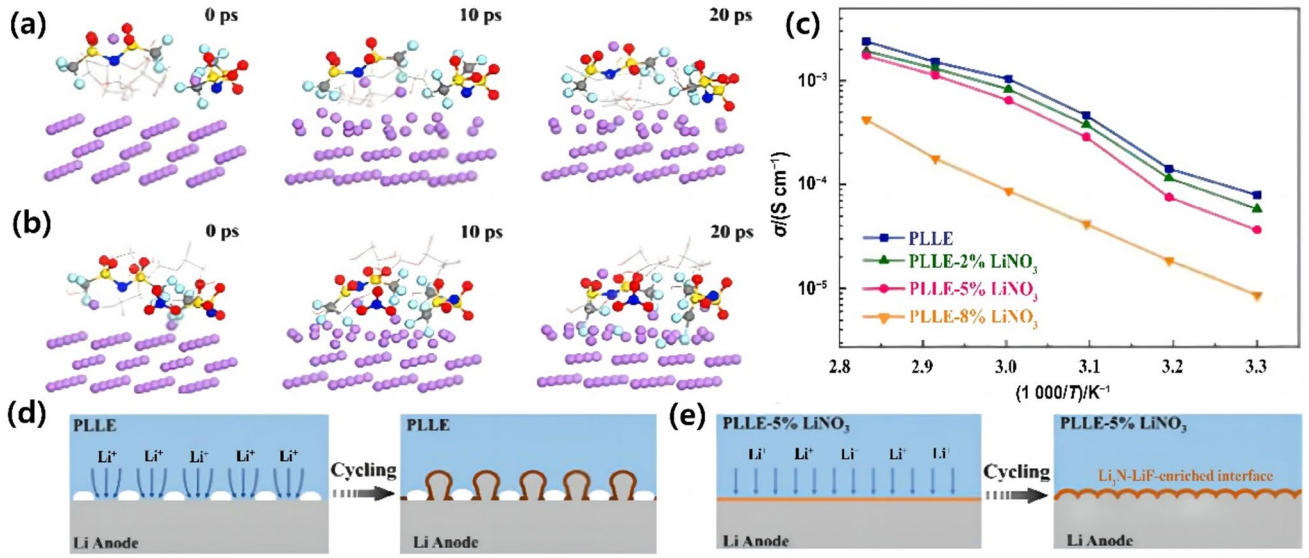

Fig. 12 **a** PLLE and **b** PLLE-5 wt% $LiNO_3$ solid electrolyte contiguous to the metal Li surface at 0, 10 and 20 ps. **c** Schematics of ionic conductivity of different electrolytes. **d** PLLE and **e** PLLE-5 wt% $LiNO_3$ as solid electrolytes. Reprinted with permission from Ref. [222]. Copyright © 2021, Elsevier Ltd

an additive to increase the IC of PEO electrolytes and assist in the construction of lithium-ion conducting SEI layers at the lithium and polymer interfaces. The combination of cation Mg^{2+} and anion $TFSI^-$ promotes the dissociation of lithium salts (LiTFSI) and increases the concentration of freely movable Li^+ in the electrolyte. The in situ formation of an interface layer with Li_2MgCl_4 and LiF between the lithium metal and electrolytes could reduce the interface resistance during Li^+ transport and inhibit the formation of lithium dendrites [226]. Wan et al. [156] prepared a composite electrolyte (PLLN) by adding LLZO nanowires synthesized by electrostatic spinning to PEO-LiTFSI and adding PEO-LiTFSI as a binder to the cathode. The cathodes and the PEO in the PLLN were fused at high temperatures to form an integrated structure of ASSLBs, which effectively enhances the interface compatibility and stability between the cathodes and PLLN. It ensures efficient ion transportation over long-term cycles. The solid electrolyte interface layer formed by the reaction of $LiZr_2(PO_4)_3$ with the lithium metal cathode in situ stabilizes the Li/composite electrolyte interface and reduces the interfacial resistance, thus providing symmetrical Li || Li cells and ASSLBs [129]. NASICON-type ionic conductors are covered with PEO-based polymers. The $LiFePO_4$ || PEO-1%-LPOS || Li full cell table maintained a reversible discharge capacity of 127.8 mAh g^{-1} after the 1 000th cycle at 1 C with a capacity retention rate of 96.6%, and an initially discharged capacity of 153.4 mAh g^{-1} after 200 cycles at 0.1 C with a capacity retention rate of 99.9%. The combination of inorganic and organic electrolytes exhibits superior electrochemical stability and good compatibility with lithium metal anodes, which is an advanced strategy for building high-density solid-state batteries [150].

7.1.3 Modification of Lithium Anode Surface Structure to Homogenize Lithium Deposition

Atsutaka Kato et al. [227] reported the intercalation of Au thin films at the electrode and electrolyte interface to better the cycling performance of lithium dissolution and deposition. The dissolution of the film into lithium metal is a possible reason for the enhanced electrochemical performance. Interface modification and optimized operating temperature are among the ways to achieve high energy density ASSBs. Yang et al. [228] prepared a self-healing electrostatic shield for the uniform deposition of lithium by introducing 0.05 M (1 M = 1 mol L^{-1}) Cs^+. In comparison with the reduction potential of Li^+, the reduction potential of Cs^+ is lower so that during lithium deposition, Cs^+ forms a positively charged electrostatic shield around the initial Li tip, which causes lithium to be deposited into the adjacent region of the anode and inhibits the formation of lithium dendrites. Li || Li symmetric cells can operate for longer periods of time, up to 10 times longer than Cs^+ free PEO electrolytes. Li || $LiFeO_4$ cells with Cs^+ maintain a capacity of around 90% after 100 cycles at 0.5 C. Furthermore, Han et al. [229] proposed the preparation of nanoscale lithium-aluminum alloys by lithium thermal reduction to promote uniform lithium deposition and suppress side reactions. With good chemical properties, the capacity retention was 72% after 490 cycles at 30 °C when combined with the NCM622 cathode.

To prepare the uniform deposition of lithium, the following measures can be taken to construct 3-D solid electrolytes [97, 196, 230] and 3-D lithium metal anodes [141, 212]. For example, Yang et al. [231] proposed a stencil printing method to divide the lithium anode into multiple recesses approximately 100 μm deep. The lithium in the grooves on the surface was deposited first, inhibiting the formation of lithium dendrites during the coating/exfoliation process. The construction of 3-D Li-Cu metal compound anodes in PEO-LiTFSI-Li_2OHBr SPEs was proposed by Ye et al. It has good cycling stability and excellent mechanical properties [141]. Lithium metal can be dissolved in PEO [232], and lithium dendrites make it unavoidable in the battery cycle [233]. Furthermore, Li et al. [234] incorporated gas–liquid Ga-Sn metal anodes. The fluidity of the liquid metal allows the self-healing of cracks formed by volume expansion. Gas–liquid metal anodes showed a better ability to maintain their mechanical integrity and were more capable of engaging with solid electrolytes. A potential strategy, liquid metal alloys containing polymeric solid electrolytes, was used to address the challenges in rechargeable LIBs.

7.2 Interface Problems of PEO-Based SPEs, Cathodes and Solutions

The interface between the cathode and the electrolyte is mainly caused by chemical instability and poor interface compatibility since the PEO-based electrolyte is susceptible to the oxidative decomposition under high voltages. Meanwhile, the electrochemistry and structure properties change as well. The interface problems would become more terrible over time, eventually leading to mechanical and structural instability of the electrode [10, 23, 25, 209]. The interface problem between the cathode and the polymer electrolyte can be improved from the following aspects. PEO-LiX can be used in the cathode to form a continuous transport channel of Li^+ with PEO-based SPEs to promote contact and compatibility between electrolytes and cathodes. Filler particles can be added to PEO-based SPEs to increase the oxidative stability of PEO-based SPEs [10, 95, 96] and facilitate the adsorption due to the high specific surface area of the filler and removal of impurities, such as H_2O from the electrolyte, to reduce the occurrence of side reactions [106, 149]. At the same time, the cathode surface can be coated and protected, so the battery can operate at higher voltages [159, 235–237]. Multi-salt additives simultaneously stabilize the cathode and anode interface. PEO and lithium salts can also be introduced into the cathode to maintain the stable transport of lithium ions [133, 150, 238, 239].

7.2.1 Composite Cathodes Improve Contact and Compatibility between PEO-Based SPEs and Cathodes

The cathode is a continuum of low ion–electron conduction, and it is difficult for SPEs to penetrate into the pores of cathodes. As a result, the interface between the electrolyte and the electrode is low, which influences a continuous pathway of Li^+. The addition of a corresponding polymer electrolyte to the cathode can form a composite cathode to improve interface contact and compatibility. For example, Wan et al. [156] suggested preparing a composite electrolyte (PLLN) by adding LLZO nanowires synthesized by electrostatic spinning to PEO-LiTFSI and adding PEO-LiTFSI as a binder to the cathode. The cathodes and the PEO in the PLLN were fused at high temperatures to form an integrated ASSLBs, which effectively enhanced the interface compatibility and stability between the cathodes and PLLN and ensured efficient ion transport over long cycles. The conductivity of Li^+ at the cathode layer was also optimized by adding PEO-$LiClO_4$ to the $LiFePO_4$ to prepare a composite cathode with a three-dimensional continuous ion and electron conducting network (PEO-$LiFePO_4$-$LiClO_4$) [150].

Recently, some new research programmes have emerged where other types of lithium salts and nanofibers with high IC are added to mitigate interface problems. For example, Li et al. [240] proposed the addition of PEO-LiTFSI and lithium borate (LiBOB) salts to the NCM811 cathode to improve interfacial stability, respectively. Firstly, PEO-LiBOB electrolytes have higher electrochemical stability than PEO-LiTFSI. Secondly, LiBOB can form a stable CEI film on the surface of the NCM811 cathode, which can prohibit the continuous oxidative decomposition of PEO-based SPEs. Thirdly, LiBOB can inhibit the corrosion of aluminum foil by $TFSI^-$ anions. Combining these advantages, the PEO-LiBOB electrolyte as a binder and ionic conductor in the NCM811 composite cathode greatly improved the electrochemical performance of the all-solid-state battery. Moreover, Ma et al. [238] constructed efficient "solid-polymer-solid" elastic lithium-ion transport channels with the cathode by using $La_2Zr_2O_7$ nanofibres (LZONs) and PEO at the cathode. Even with a low IC of 4.56×10^{-6} S cm^{-1} for PEO-based SPEs, $LiFePO_4$ || Li ASSLBs can be stable after 1 500 cycles under trial. In addition, PEO-LZONs-NCM811 || Polyvinylidene fluoride SPEs-Li cells can be stably cycled for 2 880 cycles. The abundant oxygen vacancies in the LZONs can significantly elevate the lithium-ion transport efficiency and achieve high ASSLB performance at RT with different cathodes and electrolytes because they not only provide an efficient lithium-ions transport path, but also immobilize the $TFSI^-$ anion to facilitate lithium salt dissociation and generate sufficient free lithium ions in the PEO binder. This work revealed that building an efficient ion

transport network inside the cathode can fully activate the RT performance of ASSLBs. This work provides a strong guide for the development of advanced ASSLBs.

7.2.2 Cathodes Coating Broadens the Electrochemical Window of PEO-Based ASSLB

The cathode material contains transition metals that are susceptible to catalytic decomposition. Adding a coating layer to the surface of the cathode could enhance the electrochemical stability of the electrode, and it allows stable operation of ASSLBs when the voltages is higher than 4 V [10, 23, 25]. Conventionally, a coating is added to the $LiCoO_2$ particles to reduce the interface reaction between the electrolyte and the cathode. The coating materials include Al_2O_3 [241], Li_3PO_4 [242], poly(ethyl cyanoacrylate) (PECA) [243], LATP [235], LAGP [244], etc. For example, Kaihui Nie et al. [235] proposed to apply LATP coating on $LiCoO_2$ particles. Due to the oxidative dehydration of PEO, HTFSI was generated on the cathode side and hydrogen H_2 is released on the lithium anode side. The introduction of stable LATP can mitigate this surface catalysis, thus extending the stable operating voltage to a voltage extension of > 4.5 V. For example, Zeyuan Li et al. [240] proposed synergies between the addition of LAGP coating on the surface of the cathode and the addition of LiBOB salt to the electrolyte, aiming to boost interface stability. Multiple characterization data showed that the active surface of $LiCoO_2$ caused rapid oxidation of PEO, which induced defects and destroyed the crystallinity of the cathode, which is the mechanism for the reduced ion diffusion rate. Coating a layer of LAGP on the cathode surface can inhibit the oxidation of PEO and maintain the crystallinity of $LiCoO_2$ to allow normal Li^+ transport and improve the interface stability of the electrolyte and cathode. With Li || PEO || $LiCoO_2$ charged to 4.25 V in a pure polyether electrolyte, the battery was stable after 400 cycles with a capacity retention of 81.9% at 60 °C and stable over 100 cycles in Li || PEO || NCM523 batteries with a capacity retention of 93.8% at RT.

The physical or chemical method does not guarantee a uniform distribution of the coating layer on the cathode. ALD is a unique method of protecting the cathode-SPEs interface by coating the electrode with particles of active material. This method of atomic deposition results not only in a more uniform coating thickness but also in a deposition process that takes place at low temperatures. For instance, Liang et al. [237] proposed to use lithium-niobium oxide (LNO) as a coating on NCM811 to stabilize the PEO-based electrolyte-cathode interface by ALD. The LNO coating on the NMC811 cathode can stabilize the cycling at high temperatures and high pressures. It can reduce the decomposition of PEO-based SPEs as well. Further research by these individuals reported a unique approach to improving the interface of the electrolyte and electrode by introducing lithium tantalate thin-coated sexual material particles on top of $LiCoO_2$ active material particles and conductive carbon using the ALD method, as shown in Fig. 14c. Under high voltage, PEO-based SPEs are severely degraded by oxidation, increasing the interface resistance (Fig. 13a). Although the $LiCoO_2$ coating protects the $LiCoO_2$/SPEs interface, the conductive carbon is still in direct contact with the SPEs (Fig. 13b). Conductive carbon can accelerate the oxidation of SPEs under high voltage; therefore, the protection of the carbon/SPEs interface is important to stabilizing high-voltage ASSLBs. The performance of ASSLBs with $LiCoO_2$ and carbon coatings is greatly enhanced compared to ASSLBs without coatings or with only $LCoO_2$ coatings (Fig. 13d-f) [236].

7.2.3 Fillers Increase Electrochemical Stability of Electrolytes

PEO has poor IC and lower oxidation potential. It is susceptible to oxidative decomposition from 3.6 V [22, 38]. In order to adapt PEO-based SPEs for high voltages, stable fillers are added to increase their electrochemical stability. The addition of different fillers, such as h-BN [109], GO [100], SiO_2 [95], LGPS [96], SN [111] and HACC-TFSI [90], can increase the electrochemical window of PEO-based SPEs to above 4.6 V and the cycling stability of the electrolyte [69]. For example, Alogen-free diethyl aluminum hypophosphite (ADP) flame retardant was proposed to be introduced into PEO-based polymer electrolytes by Han Longfei et al. [244]. It inhibited the crystallinity of PEO polymer and improved the IC of SPEs. The results also showed the enhancement of the electrochemical stability in SPEs. The electrochemical window of PEO-LiTFSI-15 wt% ADP SPEs is about 4.7 V compared with that of 3.9 V in PEO-LiTFSI SPEs. Achieving the stable operation of PEO-based SPEs all-solid-state batteries below 45 °C has been the goal in the world. A low molecular weight polymer, hydrolyzed polymaleic anhydride (HPMA), seems to be a promising organic filler since it can significantly reduce the crystallinity of PEO polymers. Gulian Wang et al. [102] used HPMA as a filler in $LiFeO_4$ with PEO-1%-HPMA, whose IC was improved to 1.13×10^{-4} S cm^{-1} at 35 °C. It can withstand deformation of up to 20%, improving the interface contact between the electrolyte and electrode. It also had a wide EW with a stable operating voltage of 5.1 V at 35 °C, which is much higher than that of pure PEO electrolytes (3.6 V). The significantly enhanced decomposition potential again indicates that a strong interaction between HPMA and PEO, which effectively modifies the internal microstructure of the PEO electrolyte and greatly improves the stability of the PEO at high voltage. Li || PEO-HPMA || $LiFeO_4$ batteries exhibit

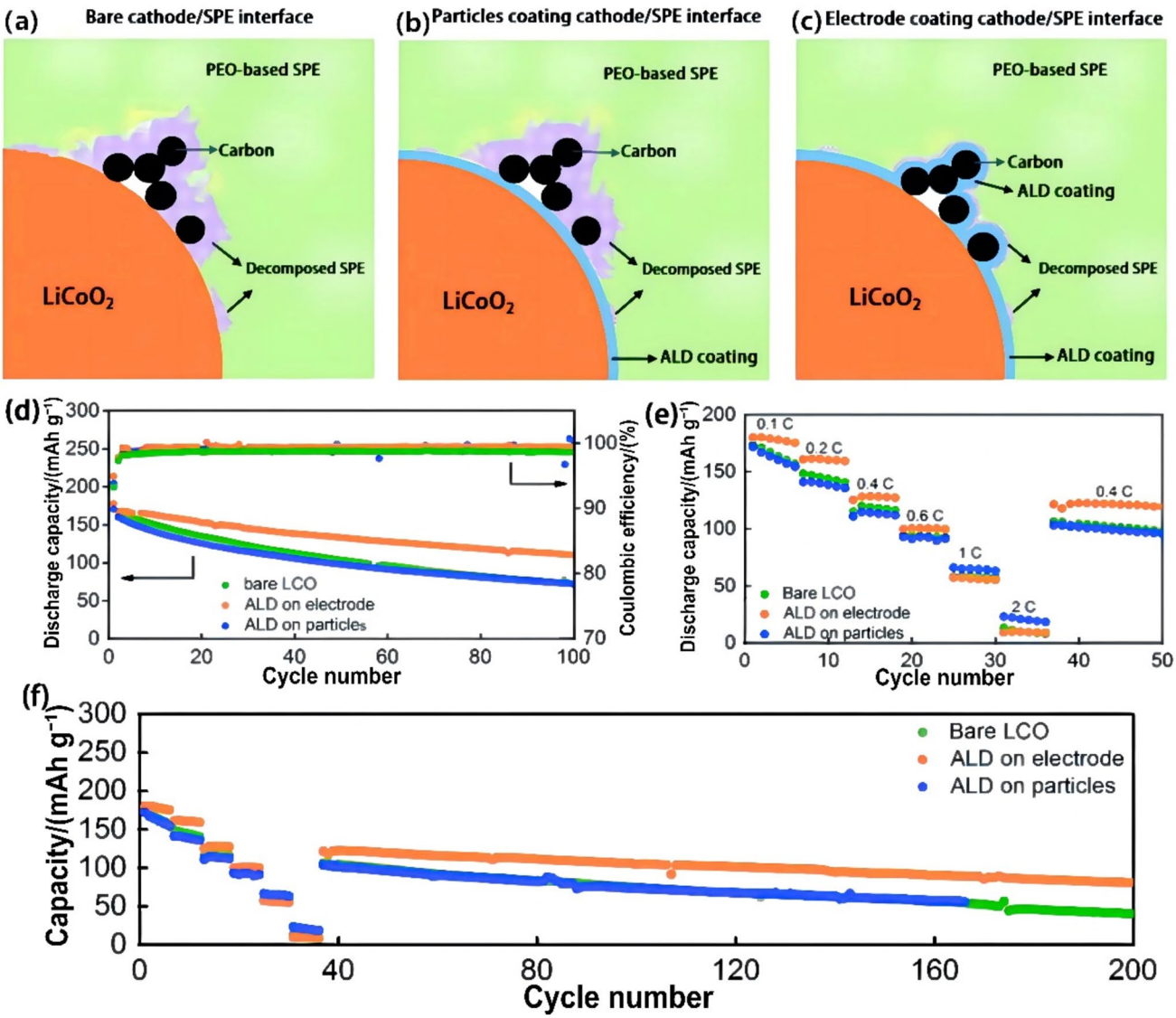

Fig. 13 **a-c** Diagram of an ALD coating used to stabilize interface contact. **d** Cycling performance. **e** Rate performance and **f** long-term cycling performance after rate performance testing for ASSLBs with different $LiCoO_2$ electrodes at 60 °C. Reprinted with permission from Ref. [236]. Copyright © 2020, The Royal Society of Chemistry

a superior cycling ability at 35 °C with a long lifetime of 1 250 cycles.

7.2.4 Multi-Salt Additives

A single lithium salt as an electrolyte-modifying additive can improve the interface stability of electrodes and PEO-based SPEs. However, it is difficult to rely on a single lithium salt to improve both the IC and electrochemical performance at the same time. Li et al. [68] suggested the addition of LiF and $LiNO_3$ as synergistic additives to PEO-PVDF-LLZTO for the development of composite solid-state electrolytes. The additive LiF improves the electrochemical stability of CSEs at high voltage and boosts the stability of the cathode and CSE interface. The addition of $LiNO_3$ increases Li^+ mobility and improves the IC of CSEs and the stability of the Li interface by forming an SEI on the surface of the anode and inhibiting the formation of lithium dendrites. Zhao et al. [69] proposed a stabler SPE in PEO-based electrolytes by redesigning the salt so that the SPE reaches the right balance between lithium-ion transport and stability properties. The PEO-HNC electrolyte was prepared by adding the tri-salt mixture $LiNO_3$ as an SEI-forming agent, LiTFSI as an easily dissociable charge carrier for bulk ion transport, and LiBOB as an effective CEI-forming agent to the composite electrolyte, which exhibited impressive electrochemical stability. The prepared ternary salt SPE exhibited sustained oxidative

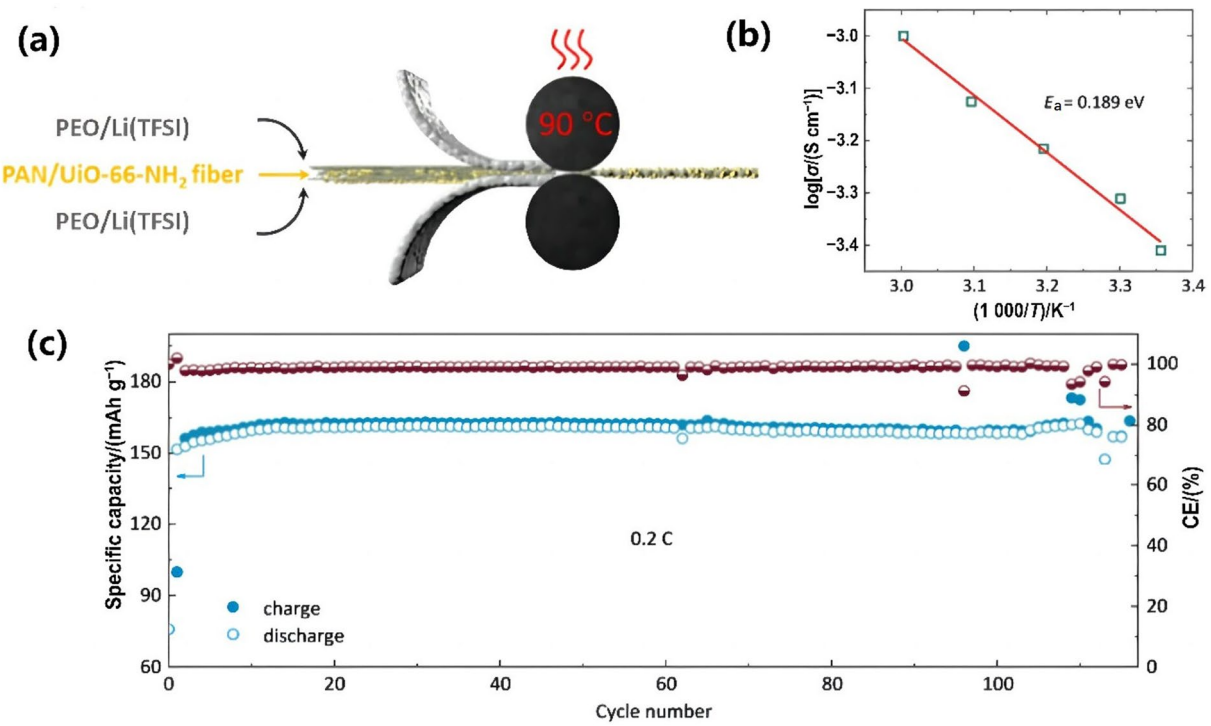

Fig. 14 **a** Diagram of sandwich structure multilayer solid polymer electrolyte preparation. b The IC of PEO-based SPEs at different temperatures. **c** Long cycling performance at 0.2 C. Reprinted with permission from Ref. [247]. Copyright © 2022, Elsevier Ltd

stability over 4.6 V in long-term electrochemical tests. This work provides a simple way to improving the electrochemical properties of SPEs. The salts species can not only change the T_g and crystallinity of PEO polymers, but also influence the IC and the mechanical properties of the polymers. Alexander Santiago et al. [245] also added the fluorine-free salt LiTCM and the fluorinated salt LiFSI into polymer electrolytes, aiming to extend the cycle life of solid-state lithium metal batteries. Accession of LiFSI salt will first reduce decomposition and form a stable solid electrolyte phase interface (SEI) layer on the surface of the lithium metal electrode. Therefore, the cycling stability of Li || Li stacked cells and Li || $LiFePO_4$ full cell batteries was improved after the addition of LiFSI.

7.3 Stabilizing Electrode and PEO-Based Electrolyte Interface Through Better Cell Design

The strategies described above for improving the cathode or anode are only for individual electrodes. For better ASSBL cycling performance, the whole cell should be designed with multi-layer electrolytes. Multilayer SPEs can protect both the anode and cathode at high and low voltages [23, 25, 209]. It can be divided into symmetrical sandwich structures [128, 246] and asymmetrical multilayer structures [66, 67].

7.3.1 Symmetrical Sandwich Structures

High IC interlayers are generally introduced into polymer electrolytes to increase IC and improve interface compatibility. Dan Cai et al. [128] designed a sandwich structure of PEO-PVDF-HFP-PEO solid electrolytes. The experimental results demonstrated that the ionic-liquid-containing poly(vinylidene fluoride-hexafluoropropylene) (IPL) interlayer can effectively suppress interfacial side reactions and improve interface stability between the PEO-based solid electrolyte and the $LiCoO_2$ cathode at high voltage. The researchers used density functional theory (DFT) to investigate the highest occupied molecular orbital (HOMO) and lowest unoccupied molecular orbital (LUMO) energy levels of PEO, LiTFSI, PVDF-HFP and PYR13TFSI. The HOMO energies reflect the antioxidant properties of the electrolyte and can be used to assess the stability of the electrolyte in the cathode. All HOMOs of the IPL intercalation were lower than that of the PEO-LLZTO (PLL) electrolyte, suggesting that the IPL is well stabilized against the cathode at high voltages. In addition, XPS were performed to gain insight into the reasons for the stabilization of anodes by IPL intercalation and confirm the composition of the lithium/electrolyte interface. It was observed from the F 1 s spectra that the surface of anodes cycled with the IPI electrolyte typically showed stronger LiF strength compared to anodes

cycled with PLL electrolytes, which is good for the reversible lithium stripping/plating process. The LiF-rich interface, which may originate from the decomposition of the high-concentration $TFSI^-$ in the IPL intercalation, is the main reason for the stabilization of the electrolyte/lithium interface during cycling. SEM images of anodes after 100 cycles reveal that the surface of anodes cycled with the IPI electrolyte at 4.3 and 4.5 V is flat, and that there are no lithium dendrites observed, which indicates that lithium deposition is uniform. The excellent electrochemical performance can be attributed to the stable electrolyte–electrode interface, as verified by DFT, SEM, and XPS. This multi-layer strategy can be applied to all PEO electrolytes, providing a new approach for the construction of high-voltage ASSBs using PEO-based SPEs.

Zr-based MOF, UiO-66-NH_2 fillers with stable structures and ultra-high porosity, can be introduced into PEO polymers to improve the overall performance of PEO-based SPEs. However, MOF and PEO composite polymers are easy to agglomerate after physically mixing. Thus, the spinning process of MOF nanoparticles with a polymer matrix can effectively solve this issue and achieve a uniform distribution of MOF particles. For example, Congyuan Li et al. [247] also reported the design of SPEs with a MOF-2-amino terephthalic acid (UiO-66-NH_2) sandwich structure accompanied by the design of operable heat-assisted processes (Fig. 14a) and multi-phase composites to reduce the crystallinity of PEO. The interlayer not only reduced the crystallinity of PEO, but also boosted the mechanical strength, the EW, and electrochemical stability (Fig. 14c). The IC of SPEs is up to 4.9×10^{-4} S cm^{-1} at 25 °C (Fig. 14b) with an EW of 5 V. The overall electrochemical performance of the PEO-based SPEs has been improved, and the prepared Li || CSPEs || $LiFeO_4$ batteries showed excellent and stable cycling performance with a specific capacity being up to 160 mAh g^{-1} at 0.2 C. Meanwhile, the plating and stripping time is more than 1 800 h.

7.3.2 Asymmetrical Multilayer Structures

Asymmetric multilayer electrolytes are constructed that: (1) The rigid electrolyte inhibits the formation of lithium dendrites and is therefore placed on the anode, and (2) The flexible electrolyte is placed on the cathode side for better contact [144, 239]. For example, Li et al. [67] reported a rational design of an inhomogeneous bilayer composite solid electrolyte through a synergistic strategy of an asymmetric polymer matrix and a functional additive. The composite solid electrolyte (CSE) consisting of a hybrid polymer matrix (PEO + PVDF) was used as the cathode-side CSE (CSC) due to its high electrochemical stability, while lithium peroxide hydrated fluorophosphate (LiBODFP) was added to the CSC due to its ability to be oxidized to form a layer of $LiP_xO_yF_z$-rich cathodic electrolyte interface (CEI) film to stabilize the cathode electrolyte interface. $LiFe_{0.5}Mn_{0.5}PO_4$-CSE(CSC/ASC)-Li batteries had an excellent capacity retention of 90.6% at 1 C. Wang et al. [66] presented a design consisting of differential salts and multi-layer PEO-based solid polymer electrolytes (DSM-SPE) to improve the stability of the electrolyte and cathode interface (Fig. 15a-g). The electrolyte on the anode side is PEO-LiTFSI-5 wt% LiTFPFB, and the electrolyte on the $LiCoO_2$ cathode side is PEO-SN-LiTFPFB. The LiTFPFB on the electrode side significantly improved the interfacial contact, and the PEO-SN-LiTFSI electrolyte in the middle layer maintained the overall high IC of the electrolyte. The addition of different lithium salts in different layers aims to increase the IC as well as the interfacial stability (Fig. 15h).

8 Summary and Outlook

This review article summarizes different solution strategies based on the challenges of PEO polymer electrolytes. The IC, EW, and mechanical properties of PEO-based SPEs can be improved by adding different types and ratios of lithium salts and fillers. In addition, the overall performance of LIBs is also determined by the interface stability between electrodes and electrolytes interfaces at both cathodes and anodes. To solve the interface problem between the lithium anode and SPEs, the following strategies have been utilized such as building a stable SEI, changing the shape and size of the lithium anode, and improving the composition of the SPEs. The interface between the active cathode and electrolyte can be improved by coating the cathode with inert materials and varying the composition of the SPEs. Interface problems can be significantly relieved by combining multiple strategies, e.g., introducing multiple lithium salts and multi-layer electrolytes simultaneously. Although recent research initiatives have led to notable scientific achievements, PEO-based polymeric electrolytes for LIBs are still in their burgeoning state, which is worth more extensive and in-depth investigation in the future. For instance, the IC of modified PEO at RT is still much lower than the required value for practical applications in most electrochemical energy storage devices since IC is critically important for the normal charging and discharging of LIBs. So far, the IC of PEO electrolytes at RT has been increased from 10^{-6} to 10^{-4} S cm^{-1} but is still way below that of liquid electrolytes. It is believed that the presence of amorphous regions in polymers hinders the transport of lithium ions. Additionally, the electrochemical performance of solid polymer batteries can be significantly improved by increasing the IC and the compatibility and stability of the electrolyte and electrodes.

We believe the following three aspects require special emphasis, including (1) Improving IC without reducing

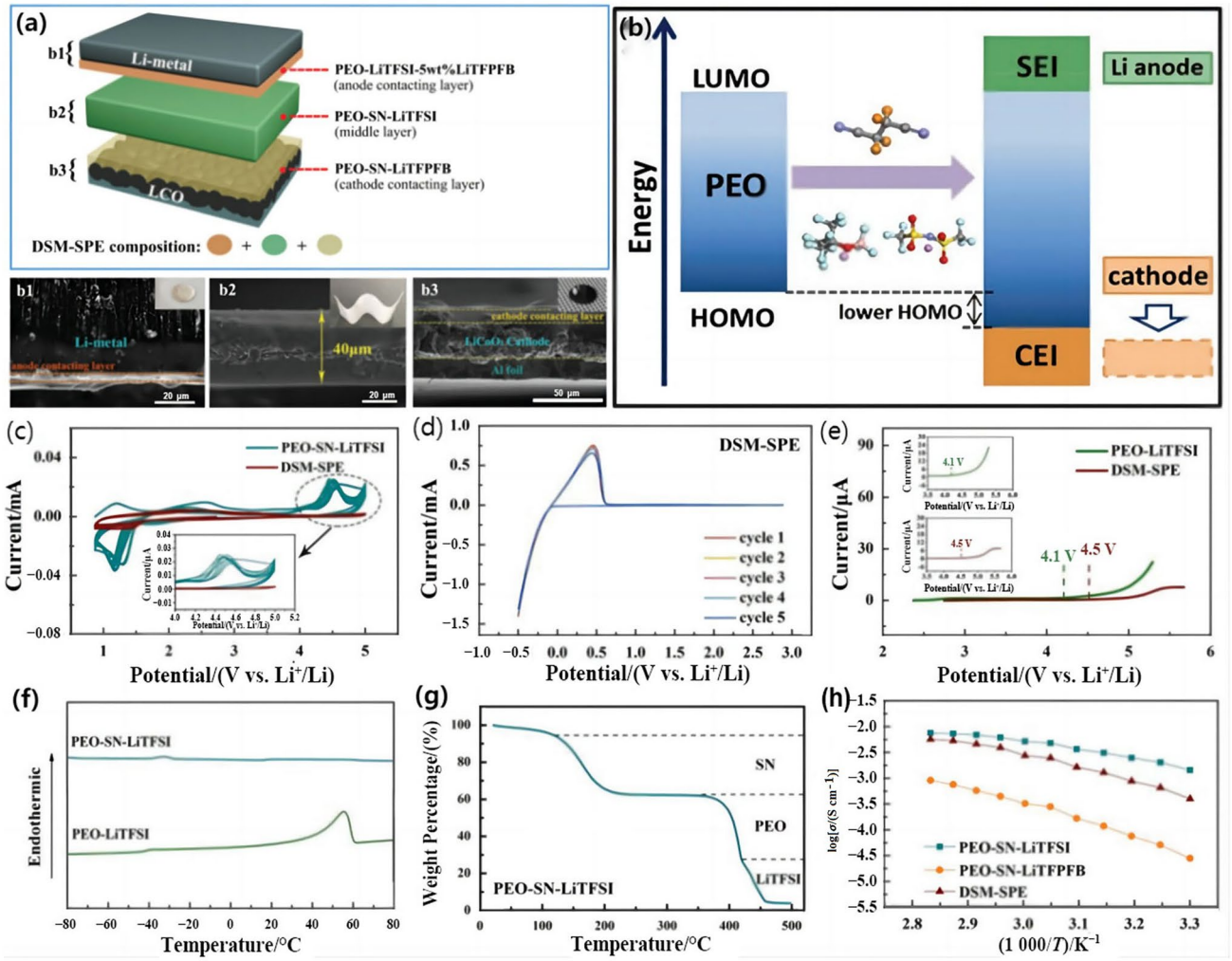

Fig. 15 **a** Schematic diagram of a differentiated salt-based multilayer solid polymer electrolyte (DSM-SPE). **b** Schematic representation of the interface stability of the cathode made possible by DSM-SPEs and the lower CEI of HOMO. **c** CV plots of the Li metal/stainless-steel batteries of PEO-SN-LiTFSI and the DSM-SPE at a scan rate of 0.5 mV s^{-1}, using stainless steel as the working electrode, and Li as the counter and reference electrode. **d** Stability and reversibility of Li stripping and plating of DSM-SPE. **e** LSV of PEO-LiTFSI and the DSM-SPE, the inset shows the magnification part. **f** DSC profiles of SN, PEO-LiTFSI, and PEO-SN-LiTFSI. **g** TGA thermogram of PEO-SN-LiTFSI. **h** Temperature-dependent IC of PEO-SN-LiTFSI, PEO-SN-LiTFPFB, and DSM-SPE. Reprinted with permission from Ref. [66]. Copyright © 2019, John Wiley & Sons, Inc

mechanical strength, (2) Improving the thermodynamic and kinetic stability of PEO-based SPEs under high-voltage use, and (3) Slowing down the growth rate of lithium dendrites. The conductivity of Li^+ is dependent on the motion of the PEO polymer segments in the SPEs, and mechanical strength shows a negative correlation with the ability of the PEO chain segments to move. To address this challenge, the interactions between polymers and other substances in PEO-based SPEs need to be enhanced, especially by introducing both organic molecules and inorganic particles, which can increase the dissociation of Li^+, inhibit the crystallinity of PEO polymers and form new ion transport channels at the electrolyte–electrode interface. Furthermore, the introduction of inorganic particles can also improve the mechanical strength and high-voltage compatibility of PEO-based SPEs. Notably, the IC of SPEs at RT can be increased to 10^{-4} S cm^{-1}, and the EW can be increased to 4.5–5.5 V to match the high-voltage cathode under this strategy. A large amount of inorganic fillers can improve the mechanical strength of PEO, and further inhibit the formation and growth of lithium dendrites.

The commercialization of PEO-based SPEs is just around the corner, but there is still a long way to go for the commercialization of room-temperature PEO solid polymer electrolytes for high-voltage LIBs, especially in solid-state batteries. There are certainly many challenges and opportunities to successfully utilize solid polymer-based electrolytes in the next generation of lithium batteries.

8.1 Studying Lithium-Ion Migration Mechanism in PEO

Lithium-ion migration mechanisms in a single PEO phase, a single filler phase, and a composite phase of the PEO and filler were explored. However, the ion migration mechanism of PEO-based SPEs should transfer from a single-phase polymer ionic conduction to a two-phase or a three-phase mechanism that includes phase-interface conduction to assist in the design and development of PEO-based SPEs verified by more theoretical calculation and in situ characterizations.

8.2 Developing High Ion Conductivity of PEO-Based SPEs

Although the ion conductivity at room temperature can reach about 10^{-4} S cm^{-1}, it is still much lower than that of liquid electrolytes (10^{-2} S cm^{-1}), which is unable to meet the practical application of ASSBs at room temperature. Therefore, this paper looks forward to developing a new type of composite polymer electrolytes that is applicable to the long-term cycling, such as in situ coupling reaction combining PEO and inorganic fillers, block copolymer engineering combining organics or the addition of ionic liquids.

8.3 Optimizing the Interface Between Electrodes and Electrolytes

In situ polymerization can reduce the interface resistance between SPEs and electrodes. Constructing a fast pathway for Li^+ transportation from the cathode to the PEO-based SPEs might also be a feasible way. Overall, there is still a long way to go for research and industrialization of PEO-based SPEs. Therefore, it is urgent to study the mechanisms on the degradation of PEO-based SPEs and the evolution of the electrode/electrolyte interface. The multiple improvements, such as building stable SEIs, changing the shape and size of anodes and improving the composition of SPEs, are expected. The interface can be improved by coating the cathode with inert materials and changing the composition of the solid phase inert polyethylene. A combination of strategies, such as simultaneously introducing multiple lithium salts and constructing multi-layer electrolytes, is expected and can greatly alleviate interface problems.

8.4 Advanced Characterization Techniques

A variety of in situ and ex situ testing methods (XPS, AFM, Raman, cryo-electron microscopy, etc.) are essential to understanding the chemical composition of the electrolyte–electrode interface in LIBs with PEO-based SPEs, study the interface reaction mechanism and better construct SEIs. However, the in-depth investigation of the mechanism on the ionic conductivity and the stabilization at the interface are necessary for the future study.

In general, there is still a long way to go for research and industrialization of PEO-based SPEs. There is a pressing need to study the intrinsic mechanisms of degradation and electrode/electrolyte interface evolution of PEO-based SPEs, which cannot be achieved without the help of comprehensive and novel characterization techniques. The multiple improvements summarized in detail in this review and the outlook for future research and development are expected to provide broad avenues for the current battery technology of PEO-based SPEs and to enhance the energy density of solid-state polymer batteries at RT and high voltage.

Acknowledgements X. S. would like to thank the support from the Young Taishan Scholars Program of Shandong Province and Natural Science Foundation of Shandong Province (2022HWYQ-074).

Conflict of interest The authors declare that they have no conflict of interest.

References

1. Guo, Y.P., Li, H.Q., Zhai, T.Y.: Reviving lithium-metal anodes for next-generation high-energy batteries. Adv. Mater. **29**, 1700007 (2017). https://doi.org/10.1002/adma.201700007
2. Liu, Y., Xu, B.Q., Zhang, W.Y., et al.: Composition modulation and structure design of inorganic-in-polymer composite solid electrolytes for advanced lithium batteries. Small **16**, 1902813 (2020). https://doi.org/10.1002/smll.201902813
3. Wang, H.S., Liu, Y.Y., Li, Y.Z., et al.: Lithium metal anode materials design: interphase and host. Electrochem. Energy Rev. **2**, 509–517 (2019). https://doi.org/10.1007/s41918-019-00054-2
4. Gu, S., Sun, C.Z., Xu, D., et al.: Recent progress in liquid electrolyte-based Li-S batteries: shuttle problem and solutions. Electrochem. Energy Rev. **1**, 599–624 (2018). https://doi.org/10.1007/s41918-018-0021-0
5. Yao, W.T., Zou, P.C., Wang, M., et al.: Design principle, optimization strategies, and future perspectives of anode-free configurations for high-energy rechargeable metal batteries. Electrochem. Energy Rev. **4**, 601–631 (2021). https://doi.org/10.1007/s41918-021-00106-6
6. Ding, Y.L., Cano, Z., Yu, A., et al.: Automotive Li-ion batteries: current status and future perspectives. Electrochem. Energy Rev. **2**, 1–28 (2019). https://doi.org/10.1007/s41918-018-0022-z
7. Chu, Y.L., Shen, Y.B., Guo, F., et al.: Advanced characterizations of solid electrolyte interphases in lithium-ion batteries. Electrochem. Energy Rev. **3**, 187–219 (2020). https://doi.org/10.1007/s41918-019-00058-y
8. Weiss, M., Simon, F.J., Busche, M.R., et al.: From liquid- to solid-state batteries: ion transfer kinetics of heteroionic interfaces. Electrochem. Energy Rev. **3**, 221–238 (2020). https://doi.org/10.1007/s41918-020-00062-7
9. Gür, T.M.: Review of electrical energy storage technologies, materials and systems: challenges and prospects for large-scale grid storage. Energy Environ. Sci. **11**, 3055–3055 (2018). https://doi.org/10.1039/c8ee01419a
10. Ding, P.P., Lin, Z.Y., Guo, X.W., et al.: Polymer electrolytes and interfaces in solid-state lithium metal batteries. Mater. Today **51**, 449–474 (2021). https://doi.org/10.1016/j.mattod.2021.08.005

11. Cheng, X.B., Zhang, R., Zhao, C.Z., et al.: Solid electrolyte interphases: a review of solid electrolyte interphases on lithium metal anode (adv. Sci. 3/2016). Adv. Sci. **3**, 1500213 (2016). https://doi.org/10.1002/advs.201500213
12. Janek, J., Zeier, W.G.: A solid future for battery development. Nat. Energy **1**, 16141 (2016). https://doi.org/10.1038/nenergy.2016.141
13. Xing, J.L., Bliznakov, S., Bonville, L., et al.: A review of nonaqueous electrolytes, binders, and separators for lithium-ion batteries. Electrochem. Energy Rev. **5**, 14 (2022). https://doi.org/10.1007/s41918-022-00131-z
14. Kong, L.C., Li, Y., Feng, W.: Strategies to solve lithium battery thermal runaway: from mechanism to modification. Electrochem. Energy Rev. **4**, 633–679 (2021). https://doi.org/10.1007/s41918-021-00109-3
15. Duan, J., Tang, X., Dai, H.F., et al.: Building safe lithium-ion batteries for electric vehicles: a review. Electrochem. Energy Rev. **3**, 1–42 (2019). https://doi.org/10.1007/s41918-019-00060-4
16. Goodenough, J.B., Kim, Y.: Challenges for rechargeable Li batteries. Chem. Mater. **22**, 587–603 (2010). https://doi.org/10.1021/cm901452z
17. Chen, S.M., Wen, K.H., Fan, J.T., et al.: Progress and future prospects of high-voltage and high-safety electrolytes in advanced lithium batteries: from liquid to solid electrolytes. J. Mater. Chem. A **6**, 11631–11663 (2018). https://doi.org/10.1039/c8ta03358g
18. Park, K.H., Bai, Q., Kim, D.H., et al.: Design strategies, practical considerations, and new solution processes of sulfide solid electrolytes for all-solid-state batteries. Adv. Energy Mater. **8**, 1800035 (2018). https://doi.org/10.1002/aenm.201800035
19. Pham, H., Nguyen, V., Ramiah, V., et al.: The effects of environmental regulation on the Singapore stock market. J. Risk Financial Manag. **12**, 175 (2019). https://doi.org/10.3390/jrfm12040175
20. Schnell, J., Günther, T., Knoche, T., et al.: All-solid-state lithium-ion and lithium metal batteries: paving the way to large-scale production. J. Power. Sources **382**, 160–175 (2018). https://doi.org/10.1016/j.jpowsour.2018.02.062
21. Cheng, X.B., Zhang, R., Zhao, C.Z., et al.: Toward safe lithium metal anode in rechargeable batteries: a review. Chem. Rev. **117**, 10403–10473 (2017). https://doi.org/10.1021/acs.chemrev.7b00115
22. Chen, J., Wu, J.W., Wang, X.D., et al.: Research progress and application prospect of solid-state electrolytes in commercial lithium-ion power batteries. Energy Storage Mater. **35**, 70–87 (2021). https://doi.org/10.1016/j.ensm.2020.11.017
23. Zhao, Y., Wang, L., Zhou, Y.N., et al.: Solid polymer electrolytes with high conductivity and transference number of Li ions for Li-based rechargeable batteries. Adv. Sci. **8**, 2003675 (2021). https://doi.org/10.1002/advs.202003675
24. Cheng, Z.W., Liu, T., Zhao, B., et al.: Recent advances in organic-inorganic composite solid electrolytes for all-solid-state lithium batteries. Energy Storage Mater. **34**, 388–416 (2021). https://doi.org/10.1016/j.ensm.2020.09.016
25. Wang, H.C., Sheng, L., Yasin, G., et al.: Reviewing the current status and development of polymer electrolytes for solid-state lithium batteries. Energy Storage Mater. **33**, 188–215 (2020). https://doi.org/10.1016/j.ensm.2020.08.014
26. Wu, J.H., Shen, L., Zhang, Z.H., et al.: All-solid-state lithium batteries with sulfide electrolytes and oxide cathodes. Electrochem. Energy Rev. **4**, 101–135 (2021). https://doi.org/10.1007/s41918-020-00081-4
27. Jia, M.Y., Zhao, N., Huo, H.Y., et al.: Comprehensive investigation into garnet electrolytes toward application-oriented solid lithium batteries. Electrochem. Energy Rev. **3**, 656–689 (2020). https://doi.org/10.1007/s41918-020-00076-1
28. Long, L.Z., Wang, S.J., Xiao, M., et al.: Polymer electrolytes for lithium polymer batteries. J. Mater. Chem. A. **4**, 10038–10069 (2016). https://doi.org/10.1039/c6ta02621d
29. Fenton, D.E., Parker, J.M., Wright, P.V.: Complexes of alkali metal ions with poly(ethylene oxide). Polymer **14**, 589–589 (1973). https://doi.org/10.1016/0032-3861(73)90146-8
30. Feng, J.N., Wang, L., Chen, Y.J., et al.: PEO based polymer-ceramic hybrid solid electrolytes: a review. Nano Convergence. **8**, 1–12 (2021). https://doi.org/10.1186/s40580-020-00252-5
31. Nair, J.R., Imholt, L., Brunklaus, G., et al.: Lithium metal polymer electrolyte batteries: opportunities and challenges. Electrochem. Soc. Inte. **28**, 55–61 (2019). https://doi.org/10.1149/2.f05192if
32. Dias, F.B., Plomp, L., Veldhuis, J.B.J.: Trends in polymer electrolytes for secondary lithium batteries. J. Power. Sources **88**, 169–191 (2000). https://doi.org/10.1016/S0378-7753(99)00529-7
33. Tan, S.J., Zeng, X.X., Ma, Q., et al.: Recent advancements in polymer-based composite electrolytes for rechargeable lithium batteries. Electrochem. Energy Rev. **1**, 113–138 (2018). https://doi.org/10.1007/s41918-018-0011-2
34. Zhang, H.R., Zhang, J.J., Ma, J., et al.: Polymer electrolytes for high energy density ternary cathode material-based lithium batteries. Electrochem. Energy Rev. **2**, 128–148 (2019). https://doi.org/10.1007/s41918-018-00027-x
35. Yu, Q.M., Luo, Y.T., Mahmood, A., et al.: Engineering two-dimensional materials and their heterostructures as high-performance electrocatalysts. Electrochem. Energy Rev. **2**, 373–394 (2019). https://doi.org/10.1007/s41918-019-00045-3
36. Zhao, W.J., Yi, J., He, P., et al.: Solid-state electrolytes for lithium-ion batteries: fundamentals, challenges and perspectives. Electrochem. Energy Rev. **2**, 574–605 (2019). https://doi.org/10.1007/s41918-019-00048-0
37. Pang, Y.P., Pan, J.Y., Yang, J.H., et al.: Electrolyte/electrode interfaces in all-solid-state lithium batteries: a review. Electrochem. Energy Rev. **4**, 169–193 (2021). https://doi.org/10.1007/s41918-020-00092-1
38. Xue, Z.G., He, D., Xie, X.L.: Poly(ethylene oxide)-based electrolytes for lithium-ion batteries. J. Mater. Chem. A. **3**, 19218–19253 (2015). https://doi.org/10.1039/c5ta03471j
39. An, Y., Han, X., Liu, Y.Y., et al.: Progress in solid polymer electrolytes for lithium-ion batteries and beyond. Small **18**, 2103617 (2022). https://doi.org/10.1002/smll.202103617
40. Zhou, Q., Ma, J., Dong, S.M., et al.: Intermolecular chemistry in solid polymer electrolytes for high-energy-density lithium batteries. Adv. Mater. **31**, 1902029 (2019). https://doi.org/10.1002/adma.201902029
41. Zhao, Y.B., Bai, Y., Li, W.D., et al.: Design strategies for polymer electrolytes with ether and carbonate groups for solid-state lithium metal batteries. Chem. Mater. **32**, 6811–6830 (2020). https://doi.org/10.1021/acs.chemmater.9b04521
42. Chen, L., Li, Y.T., Li, S.P., et al.: PEO/garnet composite electrolytes for solid-state lithium batteries: from "ceramic-in-polymer" to "polymer-in-ceramic." Nano Energy **46**, 176–184 (2018). https://doi.org/10.1016/j.nanoen.2017.12.037
43. Zhu, X.Q., Wang, K., Xu, Y.N., et al.: Strategies to boost ionic conductivity and interface compatibility of inorganic-organic solid composite electrolytes. Energy Storage Mater. **36**, 291–308 (2021). https://doi.org/10.1016/j.ensm.2021.01.002
44. Lightfoot, P., Mehta, M.A., Bruce, P.G.: Crystal structure of the polymer electrolyte poly(ethylene oxide)$_3$: $LiCF_3SO_3$. Science **262**, 883–885 (1993). https://doi.org/10.1126/science.262.5135.883
45. Munshi, M.Z.A., Owens, B.B.: Ionic transport in poly(ethylene oxide) (PEO)-LiX polymeric solid electrolyte. Polym. J. **20**, 577–586 (1988). https://doi.org/10.1295/polymj.20.577

46. Robitaille, C.D., Fauteux, D.: Phase diagrams and conductivity characterization of some PEO-LiX electrolytes. J. Electrochem. Soc. **133**, 315–325 (1986). https://doi.org/10.1149/1.2108569
47. Skaarup, S.: Mixed phase solid electrolytes. Solid State Ion. **28**(29/30), 975–978 (1988). https://doi.org/10.1016/0167-2738(88)90314-1
48. Li, J.N., Yang, J.Z., Ji, Z.Q., et al.: Prospective application, mechanism, and deficiency of lithium bis(oxalate)borate as the electrolyte additive for lithium-batteries. Adv. Energy Mater. **13**, 2301422 (2023). https://doi.org/10.1002/aenm.202301422
49. Labrèche, C., Lévesque, I., Prud'homme, J.: An appraisal of tetraethylsulfamide as plasticizer for poly(ethylene oxide)–$LiN(CF_3SO_2)_2$ rubbery electrolytes. Macromolecules **29**, 7795–7801 (1996). https://doi.org/10.1021/ma9609361
50. Manuel Stephan, A.: Review on gel polymer electrolytes for lithium batteries. Eur. Polym. J. **42**, 21–42 (2006). https://doi.org/10.1016/j.eurpolymj.2005.09.017
51. Judez, X., Zhang, H., Li, C.M., et al.: Lithium bis(fluorosulfonyl) imide/poly(ethylene oxide) polymer electrolyte for all solid-state Li–S cell. J. Phys. Chem. Lett. **8**, 1956–1960 (2017). https://doi.org/10.1021/acs.jpclett.7b00593
52. Marzantowicz, M., Dygas, J.R., Krok, F., et al.: Crystalline phases, morphology and conductivity of PEO: LiTFSI electrolytes in the eutectic region. J. Power. Sources **159**, 420–430 (2006). https://doi.org/10.1016/j.jpowsour.2006.02.044
53. Jing, B.B., Evans, M.: Catalyst-free dynamic networks for recyclable, self-healing solid polymer electrolytes. J. Am. Chem. Soc. **141**, 18932–18937 (2019). https://doi.org/10.1021/jacs.9b09811
54. Arya, A., Sharma, A.L.: Effect of salt concentration on dielectric properties of Li-ion conducting blend polymer electrolytes. J. Mater. Sci. Mater. Electron. **29**, 17903–17920 (2018). https://doi.org/10.1007/s10854-018-9905-3
55. Stolz, L., Homann, G., Winter, M., et al.: The Sand equation and its enormous practical relevance for solid-state lithium metal batteries. Mater. Today **44**, 9–14 (2021). https://doi.org/10.1016/j.mattod.2020.11.025
56. Zhao, E.Q., Guo, Y.D., Xin, Y., et al.: Enhanced electrochemical properties and interfacial stability of poly(ethylene oxide) solid electrolyte incorporating nanostructured $Li_{1.3}Al_{0.3}Ti_{1.7}(PO_4)_3$ fillers for all solid state lithium ion batteries. Int. J. Energy Res. **45**, 6876–6887 (2021). https://doi.org/10.1002/er.6278
57. Mindemark, J., Lacey, M.J., Bowden, T., et al.: Beyond PEO: alternative host materials for Li^+-conducting solid polymer electrolytes. Prog. Polym. Sci. **81**, 114–143 (2018). https://doi.org/10.1016/j.progpolymsci.2017.12.004
58. Homann, G., Stolz, L., Winter, M., et al.: Elimination of "voltage noise" of poly (ethylene oxide)-based solid electrolytes in high-voltage lithium batteries: Linear versus network polymers. iScience. **23**, 101225 (2020). https://doi.org/10.1016/j.isci.2020.101225
59. Wang, C., Yang, T.Q., Zhang, W.K., et al.: Hydrogen bonding enhanced SiO_2/PEO composite electrolytes for solid-state lithium batteries. J. Mater. Chem. A. **10**, 3400–3408 (2022). https://doi.org/10.1039/d1ta10607d
60. Homann, G., Stolz, L., Neuhaus, K., et al.: Effective optimization of high voltage solid-state lithium batteries by using poly(ethylene oxide)-based polymer electrolyte with semi-interpenetrating network. Adv. Funct. Mater. **30**, 2006289 (2020). https://doi.org/10.1002/adfm.202006289
61. Yang, T., Zheng, J., Cheng, Q., et al.: Composite polymer electrolytes with $Li_7La_3Zr_2O_{12}$ garnet-type nanowires as ceramic fillers: mechanism of conductivity enhancement and role of doping and morphology. ACS Appl. Mater. Interfaces **9**, 21773–21780 (2017). https://doi.org/10.1021/acsami.7b03806
62. Wu, H.P., Gao, P.Y., Jia, H., et al.: A polymer-in-salt electrolyte with enhanced oxidative stability for lithium metal polymer batteries. ACS Appl. Mater. Interfaces **13**, 31583–31593 (2021). https://doi.org/10.1021/acsami.1c04637
63. Zhao, Y.R., Wu, C., Peng, G., et al.: A new solid polymer electrolyte incorporating $Li_{10}GeP_2S_{12}$ into a polyethylene oxide matrix for all-solid-state lithium batteries. J. Power. Sources **301**, 47–53 (2016). https://doi.org/10.1016/j.jpowsour.2015.09.111
64. Xiong, H.M., Zhao, X., Chen, J.S.: New polymer-inorganic nanocomposites: PEO-ZnO and PEO-ZnO-$LiClO_4$ films. J. Phys. Chem. B **105**, 10169–10174 (2001). https://doi.org/10.1021/jp0103169
65. Samsinger, R.F., Schopf, S.O., Schuhmacher, J., et al.: Influence of the processing on the ionic conductivity of solid-state hybrid electrolytes based on glass-ceramic particles dispersed in PEO with LiTFSI. J. Electrochem. Soc. **167**, 120538 (2020). https://doi.org/10.1149/1945-7111/abb37f
66. Wang, C., Wang, T., Wang, L.L., et al.: Differentiated lithium salt design for multilayered PEO electrolyte enables a high-voltage solid-state lithium metal battery. Adv. Sci. **6**, 1901036 (2019). https://doi.org/10.1002/advs.201901036
67. Li, L.S., Wang, J., Zhang, L.T., et al.: Rational design of a heterogeneous double-layered composite solid electrolyte via synergistic strategies of asymmetric polymer matrices and functional additives to enable 4.5 V all-solid-state lithium batteries with superior performance. Energy Storage Mater. **45**, 1062–1073 (2022). https://doi.org/10.1016/j.ensm.2021.10.047
68. Li, L.S., Deng, Y.F., Duan, H.H., et al.: LiF and $LiNO_3$ as synergistic additives for PEO-PVDF/LLZTO-based composite electrolyte towards high-voltage lithium batteries with dual-interfaces stability. J. Energy Chem. **65**, 319–328 (2022). https://doi.org/10.1016/j.jechem.2021.05.055
69. Zhao, Q., Chen, P.Y., Li, S.K., et al.: Solid-state polymer electrolytes stabilized by task-specific salt additives. J. Mater. Chem. A. **7**, 7823–7830 (2019). https://doi.org/10.1039/c8ta12008k
70. Li, S., Chen, Y.M., Liang, W.F., et al.: A superionic conductive, electrochemically stable dual-salt polymer electrolyte. Joule. **2**, 1838–1856 (2018). https://doi.org/10.1016/j.joule.2018.06.008
71. Panday, A., Mullin, S., Gomez, E.D., et al.: Effect of molecular weight and salt concentration on conductivity of block copolymer electrolytes. Macromolecules **42**, 4632–4637 (2009). https://doi.org/10.1021/ma900451e
72. Rolland, J., Brassinne, J., Bourgeois, J.P., et al.: Chemically anchored liquid-PEO based block copolymer electrolytes for solid-state lithium-ion batteries. J. Mater. Chem. A. **2**, 11839–11846 (2014). https://doi.org/10.1039/c4ta02327g
73. Wang, Z., Ouyang, L., Li, H.L., et al.: Layer-by-layer assembly of strong thin films with high lithium ion conductance for batteries and beyond. Small **17**, 2100954 (2021). https://doi.org/10.1002/smll.202100954
74. Guo, Y., Qu, X.X., Hu, Z.Y., et al.: Highly elastic and mechanically robust polymer electrolytes with high ionic conductivity and adhesiveness for high-performance lithium metal batteries. J. Mater. Chem. A. **9**, 13597–13607 (2021). https://doi.org/10.1039/d1ta02579a
75. Gao, L., Li, J.X., Ju, J.G., et al.: Designing of root-soil-like polyethylene oxide-based composite electrolyte for dendrite-free and long-cycling all-solid-state lithium metal batteries. Chem. Eng. J. **389**, 124478 (2020). https://doi.org/10.1016/j.cej.2020.124478
76. Tian, L.Y., Liu, Y., Su, Z., et al.: A lithiated organic nanofiber-reinforced composite polymer electrolyte enabling Li-ion conduction highways for solid-state lithium metal batteries. J. Mater. Chem. A. **9**, 23882–23890 (2021). https://doi.org/10.1039/d1ta06269g
77. Zhang, D.C., Xu, X.J., Huang, X.Y., et al.: A flexible composite solid electrolyte with a highly stable interphase for dendrite-free and durable all-solid-state lithium metal batteries. J.

Mater. Chem. A. **8**, 18043–18054 (2020). https://doi.org/10.1039/d0ta06697d
78. Prasanth, R., Shubha, N., Hng, H.H., et al.: Effect of poly(ethylene oxide) on ionic conductivity and electrochemical properties of poly(vinylidenefluoride) based polymer gel electrolytes prepared by electrospinning for lithium ion batteries. J. Power. Sources **245**, 283–291 (2014). https://doi.org/10.1016/j.jpowsour.2013.05.178
79. Weston, J.E., Steele, B.C.H.: Effects of inert fillers on the mechanical and electrochemical properties of lithium salt-poly(ethylene oxide) polymer electrolytes. Solid State Ion. **7**, 75–79 (1982). https://doi.org/10.1016/0167-2738(82)90072-8
80. Croce, F., Appetecchi, G.B., Persi, L., et al.: Nanocomposite polymer electrolytes for lithium batteries. Nature **394**, 456–458 (1998). https://doi.org/10.1038/28818
81. Song, Y.L., Yang, L.Y., Li, J.W., et al.: Synergistic dissociation-and-trapping effect to promote Li-ion conduction in polymer electrolytes via oxygen vacancies. Small **17**, 2102039 (2021). https://doi.org/10.1002/smll.202102039
82. Dissanayake, M.A.K.L., Jayathilaka, P.A.R.D., Bokalawala, R.S.P., et al.: Effect of concentration and grain size of alumina filler on the ionic conductivity enhancement of the $(PEO)_9LiCF_3SO_3$: Al_2O_3 composite polymer electrolyte. J. Power. Sources **119**(120/121), 409–414 (2003). https://doi.org/10.1016/S0378-7753(03)00262-3
83. Croce, F., Sacchetti, S., Scrosati, B.: Advanced, lithium batteries based on high-performance composite polymer electrolytes. J. Power. Sources **162**, 685–689 (2006). https://doi.org/10.1016/j.jpowsour.2006.07.038
84. Reddy, M.J., Chu, P.P., Kumar, J.S., et al.: Inhibited crystallization and its effect on conductivity in a nano-sized Fe oxide composite PEO solid electrolyte. J. Power. Sources **161**, 535–540 (2006). https://doi.org/10.1016/j.jpowsour.2006.02.104
85. Johan, M.R., Fen, L.B.: Combined effect of CuO nanofillers and DBP plasticizer on ionic conductivity enhancement in the solid polymer electrolyte PEO–$LiCF_3SO_3$. Ionics **16**, 335–338 (2010). https://doi.org/10.1007/s11581-009-0406-5
86. Karmakar, A., Ghosh, A.: Poly ethylene oxide (PEO)-LiI polymer electrolytes embedded with CdO nanoparticles. J. Nanopart. Res. **13**, 2989–2996 (2011). https://doi.org/10.1007/s11051-010-0194-x
87. Mohamed Ali, T., Padmanathan, N., Selladurai, S.: Effect of nanofiller CeO_2 on structural, conductivity, and dielectric behaviors of plasticized blend nanocomposite polymer electrolyte. Ionics **21**, 829–840 (2015). https://doi.org/10.1007/s11581-014-1240-y
88. Chen, H., Adekoya, D., Hencz, L., et al.: Stable seamless interfaces and rapid ionic conductivity of Ca-CeO_2/LiTFSI/PEO composite electrolyte for high-rate and high-voltage all-solid-state battery. Adv. Energy Mater. **10**, 2000049 (2020). https://doi.org/10.1002/aenm.202000049
89. Xu, L.Q., Li, J.Y., Deng, W.T., et al.: Boosting the ionic conductivity of PEO electrolytes by waste eggshell-derived fillers for high-performance solid lithium/sodium batteries. Mater. Chem. Front. **5**, 1315–1323 (2021). https://doi.org/10.1039/d0qm00541j
90. Tan, J.W., Ao, X., Dai, A., et al.: Polycation ionic liquid tailored PEO-based solid polymer electrolytes for high temperature lithium metal batteries. Energy Storage Mater. **33**, 173–180 (2020). https://doi.org/10.1016/j.ensm.2020.08.009
91. Bao, W.D., Zhao, L.Q., Zhao, H.J., et al.: Vapor phase infiltration of ZnO quantum dots for all-solid-state PEO-based lithium batteries. Energy Storage Mater. **43**, 258–265 (2021). https://doi.org/10.1016/j.ensm.2021.09.010
92. Wieczorek, W., Raducha, D., Zalewska, A., et al.: Effect of salt concentration on the conductivity of PEO-based composite polymeric electrolytes. J. Phys. Chem. B **102**, 8725–8731 (1998). https://doi.org/10.1021/jp982403f
93. Wieczorek, W., Florjanczyk, Z., Stevens, J.R.: Composite polyether based solid electrolytes. Electrochim. Acta **40**, 2251–2258 (1995). https://doi.org/10.1016/0013-4686(95)00172-B
94. Croce, F., Persi, L., Scrosati, B., et al.: Role of the ceramic fillers in enhancing the transport properties of composite polymer electrolytes. Electrochim. Acta **46**, 2457–2461 (2001). https://doi.org/10.1016/S0013-4686(01)00458-3
95. Lin, D.C., Liu, W., Liu, Y.Y., et al.: High ionic conductivity of composite solid polymer electrolyte via in situ synthesis of monodispersed SiO_2 nanospheres in poly(ethylene oxide). Nano Lett. **16**, 459–465 (2016). https://doi.org/10.1021/acs.nanolett.5b04117
96. Pan, K.C., Zhang, L., Qian, W.W., et al.: A flexible ceramic/polymer hybrid solid electrolyte for solid-state lithium metal batteries. Adv. Mater. **32**, 2000399 (2020). https://doi.org/10.1002/adma.202000399
97. Zhang, Z., Zhang, G.Z., Chao, L.: Three-dimensional fiber network reinforced polymer electrolyte for dendrite-free all-solid-state lithium metal batteries. Energy Storage Mater. **41**, 631–641 (2021). https://doi.org/10.1016/j.ensm.2021.06.030
98. Peng, J., Wu, L.N., Lin, J.X., et al.: A solid-state dendrite-free lithium-metal battery with improved electrode interphase and ion conductivity enhanced by a bifunctional solid plasticizer. J. Mater. Chem. A. **7**, 19565–19572 (2019). https://doi.org/10.1039/c9ta07165b
99. Huang, J.X., Huang, Y., Zhang, Z., et al.: $Li_{6.7}La_3Zr_{1.7}Ta_{0.3}O_{12}$ reinforced PEO/PVDF-HFP based composite solid electrolyte for all solid-state lithium metal battery. Energy Fuels **34**, 15011–15018 (2020). https://doi.org/10.1021/acs.energyfuels.0c03124
100. Wen, J., Zhao, Q.N., Jiang, X.P., et al.: Graphene oxide enabled flexible PEO-based solid polymer electrolyte for all-solid-state lithium metal battery. ACS Appl. Energy Mater. **4**, 3660–3669 (2021). https://doi.org/10.1021/acsaem.1c00090
101. Wu, N., Chien, P.H., Qian, Y.M., et al.: Enhanced surface interactions enable fast Li^+ conduction in oxide/polymer composite electrolyte. Angew. Chem. Int. Ed. **59**, 4131–4137 (2020). https://doi.org/10.1002/anie.201914478
102. Wang, G.L., Zhu, X.Y., Rashid, A., et al.: Organic polymeric filler-amorphized poly(ethylene oxide) electrolyte enables all-solid-state lithium–metal batteries operating at 35 °C. J. Mater. Chem. A. **8**, 13351–13363 (2020). https://doi.org/10.1039/d0ta00335b
103. Zhu, P., Yan, C.Y., Dirican, M., et al.: $Li_{0.33}La_{0.557}TiO_3$ ceramic nanofiber-enhanced polyethylene oxide-based composite polymer electrolytes for all-solid-state lithium batteries. J. Mater. Chem. A. **6**, 4279–4285 (2018). https://doi.org/10.1039/c7ta10517g
104. Duan, H.H., Li, L.S., Zou, K.X., et al.: Cyclodextrin-integrated PEO-based composite solid electrolytes for high-rate and ultrastable all-solid-state lithium batteries. ACS Appl. Mater. Interfaces **13**, 57380–57391 (2021). https://doi.org/10.1021/acsami.1c18589
105. Li, W.W., Sun, C.Z., Jin, J., et al.: Realization of the Li^+ domain diffusion effect via constructing molecular brushes on the LLZTO surface and its application in all-solid-state lithium batteries. J. Mater. Chem. A. **7**, 27304–27312 (2019). https://doi.org/10.1039/c9ta10400c
106. Wang, X.Z., Zhang, Y.B., Zhang, X., et al.: Lithium-salt-rich PEO/$Li_{0.3}La_{0.557}TiO_3$ interpenetrating composite electrolyte with three-dimensional ceramic nano-backbone for all-solid-state lithium-ion batteries. ACS Appl. Mater. Interfaces **10**, 24791–24798 (2018). https://doi.org/10.1021/acsami.8b06658
107. Sun, Z.J., Li, Y.H., Zhang, S.Y., et al.: G-C_3N_4 nanosheets enhanced solid polymer electrolytes with excellent electrochemical performance, mechanical properties, and thermal stability.

J. Mater. Chem. A. **7**, 11069–11076 (2019). https://doi.org/10.1039/c9ta00634f
108. Zhai, P.F., Peng, N., Sun, Z.Y., et al.: Thin laminar composite solid electrolyte with high ionic conductivity and mechanical strength towards advanced all-solid-state lithium-sulfur battery. J. Mater. Chem. A. **8**, 23344–23353 (2020). https://doi.org/10.1039/d0ta07630a
109. Li, Y.H., Zhang, L.B., Sun, Z.J., et al.: Hexagonal boron nitride induces anion trapping in a polyethylene oxide based solid polymer electrolyte for lithium dendrite inhibition. J. Mater. Chem. A. **8**, 9579–9589 (2020). https://doi.org/10.1039/d0ta03677c
110. Xu, L.Q., Li, J.Y., Li, L., et al.: Carbon dots evoked Li ion dynamics for solid state battery. Small **17**, 2102978 (2021). https://doi.org/10.1002/smll.202102978
111. Xu, S.J., Sun, Z.H., Sun, C.G., et al.: Homogeneous and fast ion conduction of PEO-based solid-state electrolyte at low temperature. Adv. Funct. Mater. **30**, 2007172 (2020). https://doi.org/10.1002/adfm.202007172
112. Hu, J.L., Chen, K.Y., Yao, Z.G., et al.: Unlocking solid-state conversion batteries reinforced by hierarchical microsphere stacked polymer electrolyte. Sci. Bull. **66**, 694–707 (2021). https://doi.org/10.1016/j.scib.2020.11.017
113. Kim, J.W., Ji, K.S., Lee, J.P., et al.: Electrochemical characteristics of two types of PEO-based composite electrolyte with functional SiO_2. J. Power. Sources **119**(120/121), 415–421 (2003). https://doi.org/10.1016/S0378-7753(03)00263-5
114. Al-Harbi, L.M., Alsulami, Q.A., Farea, M.O., et al.: Tuning optical, dielectric, and electrical properties of Polyethylene oxide/Carboxymethyl cellulose doped with mixed metal oxide nanoparticles for flexible electronic devices. J. Mol. Struct. **1272**, 134244 (2023). https://doi.org/10.1016/j.molstruc.2022.134244
115. Al-Muntaser, A.A., Pashameah, R.A., Sharma, K., et al.: α-MoO_3 nanobelts/CMC-PVA nanocomposites: hybrid materials for optoelectronic and dielectric applications. J. Polym. Res. **29**, 1–11 (2022). https://doi.org/10.1007/s10965-022-03134-y
116. Atta, M.R., Algethami, N., Farea, M.O., et al.: Enhancing the structural, thermal, and dielectric properties of the polymer nanocomposites based on polymer blend and barium titanate nanoparticles for application in energy storage. Int. J. Energy Res. **46**, 8020–8029 (2022). https://doi.org/10.1002/er.7703
117. Farea, M.A., Bhanuse, G.B., Mohammed, H.Y., et al.: Ultrahigh sensitive and selective room-temperature carbon monoxide gas sensor based on polypyrrole/titanium dioxide nanocomposite. J. Alloys Compd. **917**, 165397 (2022). https://doi.org/10.1016/j.jallcom.2022.165397
118. Farea, M.O., Pashameah, R.A., Sharma, K., et al.: Gamma irradiation boosted the optical and electrical properties of PVP/NaAlg/Au ternary nanocomposite films for flexible optoelectronic devices. Polym. Bull. **80**, 9195–9215 (2023). https://doi.org/10.1007/s00289-022-04498-3
119. Angulakshmi, N., Nahm, K.S., Nair, J.R., et al.: Cycling profile of $MgAl_2O_4$-incorporated composite electrolytes composed of PEO and $LiPF_6$ for lithium polymer batteries. Electrochim. Acta **90**, 179–185 (2013). https://doi.org/10.1016/j.electacta.2012.12.003
120. Wu, J.F., Guo, X.: MOF-derived nanoporous multifunctional fillers enhancing the performances of polymer electrolytes for solid-state lithium batteries. J. Mater. Chem. A. **7**, 2653–2659 (2019). https://doi.org/10.1039/c8ta10124h
121. Tang, C.Y., Hackenberg, K., Fu, Q., et al.: High ion conducting polymer nanocomposite electrolytes using hybrid nanofillers. Nano Lett. **12**, 1152–1156 (2012). https://doi.org/10.1021/nl202692y
122. Gao, X., Dong, Y., Li, S.W., et al.: MOFs and COFs for batteries and supercapacitors. Electrochem. Energy Rev. **3**, 81–126 (2020). https://doi.org/10.1007/s41918-019-00055-1
123. Yuan, C.F., Li, J., Han, P.F., et al.: Enhanced electrochemical performance of poly(ethylene oxide) based composite polymer electrolyte by incorporation of nano-sized metal-organic framework. J. Power. Sources **240**, 653–658 (2013). https://doi.org/10.1016/j.jpowsour.2013.05.030
124. Zhu, K., Liu, Y.X., Liu, J.: A fast charging/discharging all-solid-state lithium ion battery based on PEO-MIL-53(Al)-LiTFSI thin film electrolyte. RSC Adv. **4**, 42278–42284 (2014). https://doi.org/10.1039/c4ra06208f
125. Senthil Kumar, R., Raja, M., Anbu Kulandainathan, M., et al.: Metal organic framework-laden composite polymer electrolytes for efficient and durable all-solid-state-lithium batteries. RSC Adv. **4**, 26171–26175 (2014). https://doi.org/10.1039/c4ra03147d
126. Mathew, D.E., Gopi, S., Kathiresan, M., et al.: Influence of MOF ligands on the electrochemical and interfacial properties of PEO-based electrolytes for all-solid- state lithium batteries. Electrochim. Acta **319**, 189–200 (2019). https://doi.org/10.1016/j.electacta.2019.06.157
127. Sun, C.C., Yusuf, A.M., Li, S.W., et al.: Metal organic frameworks enabled rational design of multifunctional PEO-based solid polymer electrolytes. Chem. Eng. J. **414**, 128702 (2021). https://doi.org/10.1016/j.cej.2021.128702
128. Cai, D., Wu, X.Z., Xiang, J.Y., et al.: Ionic-liquid-containing polymer interlayer modified PEO-based electrolyte for stable high-voltage solid-state lithium metal battery. Chem. Eng. J. **424**, 130522 (2021). https://doi.org/10.1016/j.cej.2021.130522
129. Wu, N., Chien, P.H., Li, Y.T., et al.: Fast Li^+ conduction mechanism and interfacial chemistry of a NASICON/polymer composite electrolyte. J. Am. Chem. Soc. **142**, 2497–2505 (2020). https://doi.org/10.1021/jacs.9b12233
130. Zheng, J., Tang, M.X., Hu, Y.Y.: Lithium ion pathway within $Li_7La_3Zr_2O_{12}$-polyethylene oxide composite electrolytes. Angew. Chem. Int. Ed. **55**, 12538–12542 (2016). https://doi.org/10.1002/anie.201607539
131. Jung, Y.C., Lee, S.M., Choi, J.H., et al.: All solid-state lithium batteries assembled with hybrid solid electrolytes. J. Electrochem. Soc. **162**, A704–A710 (2015). https://doi.org/10.1149/2.0731504jes
132. Kumar, B., Scanlon, L.G.: Polymer-ceramic composite electrolytes. J. Power. Sources **52**, 261–268 (1994). https://doi.org/10.1016/0378-7753(94)02147-3
133. Fu, C.K., Lou, S.F., Xu, X., et al.: Capacity degradation mechanism and improvement actions for 4 V-class all-solid-state lithium-metal polymer batteries. Chem. Eng. J. **392**, 123665 (2020). https://doi.org/10.1016/j.cej.2019.123665
134. Guo, Z.M., Pang, Y.P., Xia, S.X., et al.: Uniform and anisotropic solid electrolyte membrane enables superior solid-state Li metal batteries. Adv. Sci. **8**, 2100899 (2021). https://doi.org/10.1002/advs.202100899
135. Ranque, P., Zagórski, J., Devaraj, S., et al.: Characterization of the interfacial Li-ion exchange process in a ceramic-polymer composite by solid state NMR. J. Mater. Chem. A. **9**, 17812–17820 (2021). https://doi.org/10.1039/d1ta03720j
136. Yu, X.W., Manthiram, A.: A long cycle life, all-solid-state lithium battery with a ceramic-polymer composite electrolyte. ACS Appl. Energy Mater. **3**, 2916–2924 (2020). https://doi.org/10.1021/acsaem.9b02547
137. Lin, Y.K., Liu, K., Xiong, C., et al.: A composite solid electrolyte with an asymmetric ceramic framework for dendrite-free all-solid-state Li metal batteries. J. Mater. Chem. A. **9**, 9665–9674 (2021). https://doi.org/10.1039/d1ta00451d
138. Siyal, S.H., Li, M.J., Li, H., et al.: Ultraviolet irradiated PEO/LATP composite gel polymer electrolytes for lithium-metallic batteries (LMBs). Appl. Surf. Sci. **494**, 1119–1126 (2019). https://doi.org/10.1016/j.apsusc.2019.07.179

139. Zhai, H.W., Xu, P.Y., Ning, M.Q., et al.: A flexible solid composite electrolyte with vertically aligned and connected ion-conducting nanoparticles for lithium batteries. Nano Lett. **17**, 3182–3187 (2017). https://doi.org/10.1021/acs.nanolett.7b00715
140. Liu, C., Wang, J.X., Kou, W.J., et al.: A flexible, ion-conducting solid electrolyte with vertically bicontinuous transfer channels toward high performance all-solid-state lithium batteries. Chem. Eng. J. **404**, 126517 (2021). https://doi.org/10.1016/j.cej.2020.126517
141. Ye, Y., Deng, Z., Gao, L., et al.: Lithium-rich anti-perovskite Li_2OHBr-based polymer electrolytes enabling an improved interfacial stability with a three-dimensional-structured lithium metal anode in all-solid-state batteries. ACS Appl. Mater. Interfaces **13**, 28108–28117 (2021). https://doi.org/10.1021/acsami.1c04514
142. Cheng, J., Hou, G.M., Chen, Q., et al.: Sheet-like garnet structure design for upgrading PEO-based electrolyte. Chem. Eng. J. **429**, 132343 (2022). https://doi.org/10.1016/j.cej.2021.132343
143. Zhang, Z.Z., Shao, Y.J., Lotsch, B., et al.: New horizons for inorganic solid state ion conductors. Energy Environ. Sci. **11**, 1945–1976 (2018). https://doi.org/10.1039/c8ee01053f
144. Huo, H.Y., Chen, Y., Luo, J., et al.: Rational design of hierarchical "ceramic-in-polymer" and "polymer-in-ceramic" electrolytes for dendrite-free solid-state batteries. Adv. Energy Mater. **9**, 1804004 (2019). https://doi.org/10.1002/aenm.201804004
145. Wu, P.F., Zhou, W.W., Su, X., et al.: Recent advances in conduction mechanisms, synthesis methods, and improvement strategies for $Li_{1+x}Al_xTi_{2-x}(PO_4)_3$ solid electrolyte for all-solid-state lithium batteries. Adv. Energy Mater. **13**, 2203440 (2023). https://doi.org/10.1002/aenm.202203440
146. Rhim, J.W., Mohanty, A.K., Singh, S.P., et al.: Effect of the processing methods on the performance of polylactide films: thermocompression versus solvent casting. J. Appl. Polym. Sci. **101**, 3736–3742 (2006). https://doi.org/10.1002/app.23403
147. Bi, Z.J., Mu, S., Zhao, N., et al.: Cathode supported solid lithium batteries enabling high energy density and stable cyclability. Energy Storage Mater. **35**, 512–519 (2021). https://doi.org/10.1016/j.ensm.2020.11.038
148. Zhang, X., Liu, T., Zhang, S.F., et al.: Synergistic coupling between $Li_{6.75}La_3Zr_{1.75}Ta_{0.25}O_{12}$ and poly(vinylidene fluoride) induces high ionic conductivity, mechanical strength, and thermal stability of solid composite electrolytes. J. Am. Chem. Soc. **139**, 13779–13785 (2017). https://doi.org/10.1021/jacs.7b06364
149. Zhang, J.X., Zhao, N., Zhang, M., et al.: Flexible and ion-conducting membrane electrolytes for solid-state lithium batteries: dispersion of garnet nanoparticles in insulating polyethylene oxide. Nano Energy **28**, 447–454 (2016). https://doi.org/10.1016/j.nanoen.2016.09.002
150. Zhang, Z.H., Zhao, Y.R., Chen, S.J., et al.: An advanced construction strategy of all-solid-state lithium batteries with excellent interfacial compatibility and ultralong cycle life. J. Mater. Chem. A. **5**, 16984–16993 (2017). https://doi.org/10.1039/c7ta04320a
151. Huang, Z.Y., Pang, W.Y., Liang, P., et al.: A dopamine modified $Li_{6.4}La_3Zr_{1.4}Ta_{0.6}O_{12}$/PEO solid-state electrolyte: enhanced thermal and electrochemical properties. J. Mater. Chem. A. **7**, 16425–16436 (2019). https://doi.org/10.1039/c9ta03395e
152. Duan, H., Yin, Y.X., Zeng, X.X., et al.: In-situ plasticized polymer electrolyte with double-network for flexible solid-state lithium-metal batteries. Energy Storage Mater. **10**, 85–91 (2018). https://doi.org/10.1016/j.ensm.2017.06.017
153. Zuo, X.X., Wu, J.H., Ma, X.D., et al.: A poly(vinylidene fluoride)/ethyl cellulose and amino-functionalized nano-SiO_2 composite coated separator for 5 V high-voltage lithium-ion batteries with enhanced performance. J. Power. Sources **407**, 44–52 (2018). https://doi.org/10.1016/j.jpowsour.2018.10.056
154. Liang, J.N., Sun, Q., Zhao, Y., et al.: Stabilization of all-solid-state Li-S batteries with a polymer-ceramic sandwich electrolyte by atomic layer deposition. J. Mater. Chem. A. **6**, 23712–23719 (2018). https://doi.org/10.1039/c8ta09069f
155. Choudhury, S., Stalin, S., Deng, Y., et al.: Soft colloidal glasses as solid-state electrolytes. Chem. Mater. **30**, 5996–6004 (2018). https://doi.org/10.1021/acs.chemmater.8b02227
156. Wan, Z.P., Lei, D.N., Yang, W., et al.: All-solid-state batteries: low resistance-integrated all-solid-state battery achieved by $Li_7La_3Zr_2O_{12}$ nanowire upgrading polyethylene oxide (PEO) composite electrolyte and PEO cathode binder (adv. Funct. Mater. 1/2019). Adv. Funct. Mater. **29**, 1805301 (2019). https://doi.org/10.1002/adfm.201970006
157. Fu, K.K., Gong, Y., Dai, J., et al.: Flexible, solid-state, ion-conducting membrane with 3D garnet nanofiber networks for lithium batteries. Proc. Natl. Acad. Sci. U.S.A. **113**, 7094–7099 (2016). https://doi.org/10.1073/pnas.1600422113
158. Zhou, W.D., Wang, S.F., Li, Y.T., et al.: Plating a dendrite-free lithium anode with a polymer/ceramic/polymer sandwich electrolyte. J. Am. Chem. Soc. **138**, 9385–9388 (2016). https://doi.org/10.1021/jacs.6b05341
159. Wu, N., Li, Y.T., Dolocan, A., et al.: In situ formation of Li_3P layer enables fast Li^+ conduction across Li/solid polymer electrolyte interface. Adv. Funct. Mater. **30**, 2000831 (2020). https://doi.org/10.1002/adfm.202000831
160. Liu, W., Lee, S.W., Lin, D.C., et al.: Enhancing ionic conductivity in composite polymer electrolytes with well-aligned ceramic nanowires. Nat. Energy **2**, 17035 (2017). https://doi.org/10.1038/nenergy.2017.35
161. Tsuchida, E., Ohno, H., Tsunemi, K., et al.: Lithium ionic conduction in poly (methacrylic acid)-poly (ethylene oxide) complex containing lithium perchlorate. Solid State Ion. **11**, 227–233 (1983). https://doi.org/10.1016/0167-2738(83)90028-0
162. Jinisha, B., Anilkumar, K.M., Manoj, M., Pradeep, V.S., Jayalekshmi, S.: Development of a novel type of solid polymer electrolyte for solid state lithium battery applications based on lithium enriched poly (ethylene oxide) (PEO)/poly (vinyl pyrrolidone) (PVP) blend polymer. Electrochim. Acta **235**, 210–222 (2017). https://doi.org/10.1016/j.electacta.2017.03.118
163. Tanaka, R., Sakurai, M., Sekiguchi, H., et al.: Improvement of room-temperature conductivity and thermal stability of PEO-$LiClO_4$ systems by addition of a small proportion of polyethylenimine. Electrochim. Acta **48**, 2311–2316 (2003). https://doi.org/10.1016/s0013-4686(03)00220-2
164. Acosta, J.: Structural, morphological and electrical characterization of polymer electrolytes based on PEO/PPO blends. Solid State Ion. **85**, 85–90 (1996). https://doi.org/10.1016/0167-2738(96)00045-8
165. Bao, J.J., Qu, X.B., Qi, G.Q., et al.: Solid electrolyte based on waterborne polyurethane and poly(ethylene oxide) blend polymer for all-solid-state lithium ion batteries. Solid State Ion. **320**, 55–63 (2018). https://doi.org/10.1016/j.ssi.2018.02.030
166. Chen, B., Huang, Z., Chen, X.T., et al.: A new composite solid electrolyte PEO/$Li_{10}GeP_2S_{12}$/SN for all-solid-state lithium battery. Electrochim. Acta **210**, 905–914 (2016). https://doi.org/10.1016/j.electacta.2016.06.025
167. Ma, Y.X., Wan, J.Y., Yang, Y.F., et al.: Scalable, ultrathin, and high-temperature-resistant solid polymer electrolytes for energy-dense lithium metal batteries. Adv. Energy Mater. **12**, 2103720 (2022). https://doi.org/10.1002/aenm.202103720
168. Diddens, D., Heuer, A.: Simulation study of the lithium ion transport mechanism in ternary polymer electrolytes: the critical role of the segmental mobility. J. Phys. Chem. B **118**, 1113–1125 (2014). https://doi.org/10.1021/jp409800r
169. Ushakova, E.E., Sergeev, A.V., Morzhukhin, A., et al.: Free-standing Li^+-conductive films based on PEO-PVDF blends.

RSC Adv. **10**, 16118–16124 (2020). https://doi.org/10.1039/d0ra02325f
170. Klongkan, S., Pumchusak, J.: Effects of nano alumina and plasticizers on morphology, ionic conductivity, thermal and mechanical properties of PEO-$LiCF_3SO_3$ solid polymer electrolyte. Electrochim. Acta **161**, 171–176 (2015). https://doi.org/10.1016/j.electacta.2015.02.074
171. Wang, Y.J., Pan, Y., Wang, L., et al.: Conductivity studies of plasticized PEO-Lithium chlorate-FIC filler composite polymer electrolytes. Mater. Lett. **59**, 3021–3026 (2005). https://doi.org/10.1016/j.matlet.2005.05.011
172. Dong, D.R., Zhou, B., Sun, Y.F., et al.: Polymer electrolyte glue: a universal interfacial modification strategy for all-solid-state Li batteries. Nano Lett. **19**, 2343–2349 (2019). https://doi.org/10.1021/acs.nanolett.8b05019
173. Jung, Y.C., Park, M.S., Doh, C.H., et al.: Organic-inorganic hybrid solid electrolytes for solid-state lithium cells operating at room temperature. Electrochim. Acta **218**, 271–277 (2016). https://doi.org/10.1016/j.electacta.2016.09.141
174. Liu, Y.L., Zhao, Y., Lu, W., et al.: PEO based polymer in plastic crystal electrolytes for room temperature high-voltage lithium metal batteries. Nano Energy **88**, 106205 (2021). https://doi.org/10.1016/j.nanoen.2021.106205
175. Yang, L.Y., Wei, D.X., Xu, M., et al.: Transferring lithium ions in nanochannels: a PEO/Li^+ solid polymer electrolyte design. Angew. Chem. Int. Ed. **53**, 3631–3635 (2014). https://doi.org/10.1002/anie.201307423
176. Wan, J.Y., Xie, J., Kong, X., et al.: Ultrathin, flexible, solid polymer composite electrolyte enabled with aligned nanoporous host for lithium batteries. Nat. Nanotechnol. **14**, 705–711 (2019). https://doi.org/10.1038/s41565-019-0465-3
177. Li, C.H., Zhou, S., Dai, L.J., et al.: Porous polyamine/PEO composite solid electrolyte for high performance solid-state lithium metal batteries. J. Mater. Chem. A. **9**, 24661–24669 (2021). https://doi.org/10.1039/d1ta04599g
178. Asghar, A., Abdul Samad, Y., Singh Lalia, B., et al.: PEG based quasi-solid polymer electrolyte: mechanically supported by networked cellulose. J. Membr. Sci. **421**(422), 85–90 (2012). https://doi.org/10.1016/j.memsci.2012.06.037
179. Liu, L.H., Lyu, J., Mo, J.S., et al.: Comprehensively-upgraded polymer electrolytes by multifunctional aramid nanofibers for stable all-solid-state Li-ion batteries. Nano Energy **69**, 104398 (2020). https://doi.org/10.1016/j.nanoen.2019.104398
180. Shi, Z.Q., Guo, W.Y., Zhou, L.Z., et al.: A 3D fiber skeleton reinforced PEO-based polymer electrolyte for high rate and ultra-long cycle all-solid-state batteries. J. Mater. Chem. A. **9**, 21057–21070 (2021). https://doi.org/10.1039/d1ta04619e
181. Blensdorf, T., Joenathan, A., Hunt, M., et al.: Hybrid composite polymer electrolytes: ionic liquids as a magic bullet for the poly(ethylene glycol)-silica network. J. Mater. Chem. A. **5**, 3493–3502 (2017). https://doi.org/10.1039/c6ta09986f
182. Wang, X.F., Fu, C.K., Feng, Z.J., et al.: Flyash/polymer composite electrolyte with internal binding interaction enables highly-stable extrinsic-interfaces of all-solid-state lithium batteries. Chem. Eng. J. **428**, 131041 (2022). https://doi.org/10.1016/j.cej.2021.131041
183. Atik, J., Diddens, D., Thienenkamp, J., et al.: Cation-assisted lithium-ion transport for high-performance PEO-based ternary solid polymer electrolytes. Angew. Chem. Int. Ed. **60**, 11919–11927 (2021). https://doi.org/10.1002/anie.202016716
184. Li, Y.H., Sun, Z.J., Shi, L., et al.: Poly(ionic liquid)-polyethylene oxide semi-interpenetrating polymer network solid electrolyte for safe lithium metal batteries. Chem. Eng. J. **375**, 121925 (2019). https://doi.org/10.1016/j.cej.2019.121925
185. Falco, M., Simari, C., Ferrara, C., et al.: Understanding the effect of UV-induced cross-linking on the physicochemical properties of highly performing PEO/LiTFSI-based polymer electrolytes. Langmuir **35**, 8210–8219 (2019). https://doi.org/10.1021/acs.langmuir.9b00041
186. Ballard, D.G.H., Cheshire, P., Mann, T.S., et al.: Ionic conductivity in organic solids derived from amorphous macromolecules. Macromolecules **23**, 1256–1264 (1990). https://doi.org/10.1021/ma00207a006
187. Morita, M., Fukumasa, T., Motoda, M., et al.: Polarization behavior of lithium electrode in solid electrolytes consisting of a poly(ethylene oxide)-grafted polymer. J. Electrochem. Soc. **137**, 3401–3404 (1990). https://doi.org/10.1149/1.2086228
188. Xia, D.W., Soltz, D., Smid, J.: Conductivities of solid polymer electrolyte complexes of alkali salts with polymers of methoxy-polyethyleneglycol methacrylates. Solid State Ion. **14**, 221–224 (1984). https://doi.org/10.1016/0167-2738(84)90102-4
189. Kuo, P.L., Wu, C.A., Lu, C.Y., et al.: High performance of transferring lithium ion for polyacrylonitrile-interpenetrating crosslinked polyoxyethylene network as gel polymer electrolyte. ACS Appl. Mater. Interfaces **6**, 3156–3162 (2014). https://doi.org/10.1021/am404248b
190. Cho, K.Y., Lee, K.H., Park, J.K.: Preparation, characterization, and ion conductivities of the polymer electrolytes based on poly(ethylene oxide)-g-poly(ethylene glycol). Polym. J. **32**, 537–542 (2000). https://doi.org/10.1295/polymj.32.537
191. Ballal, D., Srivastava, R.: Modeling the interfacial properties of Poly(Ethylene oxide-*Co*-Propylene oxide) polymers at water-toluene interface. Fluid Phase Equilib. **427**, 209–218 (2016). https://doi.org/10.1016/j.fluid.2016.07.013
192. Kao, H.M., Chao, S.W., Chang, P.C.: Multinuclear solid-state NMR, self-diffusion coefficients, differential scanning calorimetry, and ionic conductivity of solid organic-inorganic hybrid electrolytes based on PPG–PEG–PPG diamine, siloxane, and lithium perchlorate. Macromolecules **39**, 1029–1040 (2006). https://doi.org/10.1021/ma051550q
193. Yang, G., Lehmann, M.L., Zhao, S., et al.: Anomalously high elastic modulus of a poly(ethylene oxide)-based composite electrolyte. Energy Storage Mater. **35**, 431–442 (2021). https://doi.org/10.1016/j.ensm.2020.11.031
194. Zhu, Y.S., Xiao, S.Y., Shi, Y., et al.: A composite gel polymer electrolyte with high performance based on poly(vinylidene fluoride) and polyborate for lithium ion batteries. Adv. Energy Mater. **4**, 1300647 (2014). https://doi.org/10.1002/aenm.201300647
195. Abbrent, S., Plestil, J., Hlavata, D., et al.: Crystallinity and morphology of PVdF-HFP-based gel electrolytes. Polymer **42**, 1407–1416 (2001). https://doi.org/10.1016/S0032-3861(00)00517-6
196. Gao, L., Luo, S.B., Li, J.X., et al.: Core-shell structure nanofibers-ceramic nanowires based composite electrolytes with high Li transference number for high-performance all-solid-state lithium metal batteries. Energy Storage Mater. **43**, 266–274 (2021). https://doi.org/10.1016/j.ensm.2021.09.013
197. Prabakaran, P., Manimuthu, R.P., Gurusamy, S., et al.: Plasticized polymer electrolyte membranes based on PEO/PVdF-HFP for use as an effective electrolyte in lithium-ion batteries. Chin. J. Polym. Sci. **35**, 407–421 (2017). https://doi.org/10.1007/s10118-017-1906-9
198. Tong, R.A., Chen, L.H., Fan, B.B., et al.: Solvent-free process for blended PVDF-HFP/PEO and LLZTO composite solid electrolytes with enhanced mechanical and electrochemical properties for lithium metal batteries. ACS Appl. Energy Mater. **4**, 11802–11812 (2021). https://doi.org/10.1021/acsaem.1c02566
199. Tan, J.W., Ao, X., Zhuo, H., et al.: Cryogenic engineering of solid polymer electrolytes for room temperature and 4V-class all-solid-state lithium batteries. Chem. Eng. J. **420**, 127623 (2021). https://doi.org/10.1016/j.cej.2020.127623
200. Fang, R.Y., Xu, B.Y., Grundish, N.S., et al.: Li_2S_6-integrated PEO-based polymer electrolytes for all-solid-state

lithium-metal batteries. Angew. Chem. Int. Ed. **60**, 17701–17706 (2021). https://doi.org/10.1002/anie.202106039
201. Zhang, Y.H., Lu, W., Cong, L.N., et al.: Cross-linking network based on Poly(ethylene oxide): solid polymer electrolyte for room temperature lithium battery. J. Power. Sources **420**, 63–72 (2019). https://doi.org/10.1016/j.jpowsour.2019.02.090
202. Liu, W., Liu, N., Sun, J., et al.: Ionic conductivity enhancement of polymer electrolytes with ceramic nanowire fillers. Nano Lett. **15**, 2740–2745 (2015). https://doi.org/10.1021/acs.nanolett.5b00600
203. Gomez, E.D., Panday, A., Feng, E.H., et al.: Effect of ion distribution on conductivity of block copolymer electrolytes. Nano Lett. **9**, 1212–1216 (2009). https://doi.org/10.1021/nl900091n
204. Zhang, W.J., Haman, K.J., Metzger, J.M., et al.: Quantifying binding of ethylene oxide-propylene oxide block copolymers with lipid bilayers. Langmuir **33**, 12624–12634 (2017). https://doi.org/10.1021/acs.langmuir.7b02279
205. Meabe, L., Huynh, T.V., Lago, N., et al.: Poly(ethylene oxide carbonates) solid polymer electrolytes for lithium batteries. Electrochim. Acta **264**, 367–375 (2018). https://doi.org/10.1016/j.electacta.2018.01.101
206. Zardalidis, G., Ioannou, E., Gatsouli, K., et al.: Ionic conductivity and self-assembly in poly(isoprene-b-ethylene oxide) electrolytes doped with LiTf and EMITf. Macromolecules **48**, 1473–1482 (2015). https://doi.org/10.1021/acs.macromol.5b00089
207. Zhang, X.Z., Chu, Y., Cui, X.M., et al.: An ultra-thin polymer electrolyte based on single-helical-structured agarose for high performance solid-state lithium batteries. J. Mater. Chem. A. **9**, 26939–26948 (2021). https://doi.org/10.1039/d1ta08195k
208. Zhu, Z.Q., Hong, M.L., Guo, D.S., et al.: All-solid-state lithium organic battery with composite polymer electrolyte and pillar[5]quinone cathode. J. Am. Chem. Soc. **136**, 16461–16464 (2014). https://doi.org/10.1021/ja507852t
209. Li, S., Zhang, S.Q., Shen, L., et al.: Progress and perspective of ceramic/polymer composite solid electrolytes for lithium batteries. Adv. Sci. **7**, 1903088 (2020). https://doi.org/10.1002/advs.201903088
210. Gao, S.L., Sun, F.Y., Liu, N., et al.: Ionic conductive polymers as artificial solid electrolyte interphase films in Li metal batteries: a review. Mater. Today **40**, 140–159 (2020). https://doi.org/10.1016/j.mattod.2020.06.011
211. Lin, D.C., Liu, Y.Y., Cui, Y.: Reviving the lithium metal anode for high-energy batteries. Nat. Nanotechnol. **12**, 194–206 (2017). https://doi.org/10.1038/nnano.2017.16
212. Yang, C.P., Zhang, L., Liu, B.Y., et al.: Continuous plating/stripping behavior of solid-state lithium metal anode in a 3D ion-conductive framework. Proc. Natl. Acad. Sci. U. S. A. **115**, 3770–3775 (2018). https://doi.org/10.1073/pnas.1719758115
213. Zhou, D., Liu, R.L., He, Y.B., et al.: SiO_2 hollow nanosphere-based composite solid electrolyte for lithium metal batteries to suppress lithium dendrite growth and enhance cycle life. Adv. Energy Mater. **6**, 1502214 (2016). https://doi.org/10.1002/aenm.201502214
214. Yun, Q.B., He, Y.B., Lv, W., et al.: Chemical dealloying derived 3D porous current collector for Li metal anodes. Adv. Mater. **28**, 6932–6939 (2016). https://doi.org/10.1002/adma.201601409
215. Zhao, H., Lei, D.N., He, Y.B., et al.: Compact 3D copper with uniform porous structure derived by electrochemical dealloying as dendrite-free lithium metal anode current collector. Adv. Energy Mater. **8**, 1800266 (2018). https://doi.org/10.1002/aenm.201800266
216. Keller, M., Appetecchi, G.B., Kim, G.T., et al.: Electrochemical performance of a solvent-free hybrid ceramic-polymer electrolyte based on $Li_7La_3Zr_2O_{12}$ in $P(EO)_{15}$LiTFSI. J. Power. Sources **353**, 287–297 (2017). https://doi.org/10.1016/j.jpowsour.2017.04.014
217. Wang, S., Sun, Q.F., Peng, W.X., et al.: Ameliorating the interfacial issues of all-solid-state lithium metal batteries by constructing polymer/inorganic composite electrolyte. J. Energy Chem. **58**, 85–93 (2021). https://doi.org/10.1016/j.jechem.2020.09.033
218. Zhang, Z., Huang, Y., Gao, H., et al.: An all-solid-state lithium battery using the $Li_7La_3Zr_2O_{12}$ and $Li_{6.7}La_3Zr_{1.7}Ta_{0.3}O_{12}$ ceramic enhanced polyethylene oxide electrolytes with superior electrochemical performance. Ceram. Int. **46**, 11397–11405 (2020). https://doi.org/10.1016/j.ceramint.2020.01.170
219. Peled, E., Golodnitsky, D., Ardel, G., et al.: The sei model: application to lithium-polymer electrolyte batteries. Electrochim. Acta **40**, 2197–2204 (1995). https://doi.org/10.1016/0013-4686(95)00163-9
220. Ismail, I., Noda, A., Nishimoto, A., et al.: XPS study of lithium surface after contact with lithium-salt doped polymer electrolytes. Electrochim. Acta **46**, 1595–1603 (2001). https://doi.org/10.1016/s0013-4686(00)00758-1
221. Liang, J.Y., Zeng, X.X., Zhang, X.D., et al.: Engineering Janus interfaces of ceramic electrolyte via distinct functional polymers for stable high-voltage Li-metal batteries. J. Am. Chem. Soc. **141**, 9165–9169 (2019). https://doi.org/10.1021/jacs.9b03517
222. Zhang, Z., Wang, J.L., Zhang, S.L., et al.: Stable all-solid-state lithium metal batteries with Li_3N-LiF-enriched interface induced by lithium nitrate addition. Energy Storage Mater. **43**, 229–237 (2021). https://doi.org/10.1016/j.ensm.2021.09.002
223. Wen, X., Zeng, Q.H., Guan, J.Z., et al.: 3D structural lithium alginate-based gel polymer electrolytes with superior high-rate long cycling performance for high-energy lithium metal batteries. J. Mater. Chem. A. **10**, 707–718 (2022). https://doi.org/10.1039/d1ta07252h
224. Sharafi, A., Kazyak, E., Davis, A.L., et al.: Surface chemistry mechanism of ultra-low interfacial resistance in the solid-state electrolyte $Li_7La_3Zr_2O_{12}$. Chem. Mater. **29**, 7961–7968 (2017). https://doi.org/10.1021/acs.chemmater.7b03002
225. O'Kane, S.E.J., Campbell, I.D., Marzook, M.W.J., et al.: Physical origin of the differential voltage minimum associated with lithium plating in Li-ion batteries. J. Electrochem. Soc. **167**, 090540 (2020). https://doi.org/10.1149/1945-7111/ab90ac
226. Xu, B.Y., Li, X.Y., Yang, C., et al.: Interfacial chemistry enables stable cycling of all-solid-state Li metal batteries at high current densities. J. Am. Chem. Soc. **143**, 6542–6550 (2021). https://doi.org/10.1021/jacs.1c00752
227. Kato, A., Suyama, M., Hotehama, C., et al.: High-temperature performance of all-solid-state lithium-metal batteries having Li/Li_3PS_4 Interfaces modified with Au thin films. J. Electrochem. Soc. **165**, A1950–A1954 (2018). https://doi.org/10.1149/2.1451809jes
228. Yang, X.F., Sun, Q., Zhao, C.T., et al.: Self-healing electrostatic shield enabling uniform lithium deposition in all-solid-state lithium batteries. Energy Storage Mater. **22**, 194–199 (2019). https://doi.org/10.1016/j.ensm.2019.07.015
229. Han, S.H., Li, Z.B., Zhang, Y.J., et al.: In-situ formation of a nanoscale lithium aluminum alloy in lithium metal for high-load battery anode. Energy Storage Mater. **48**, 384–392 (2022). https://doi.org/10.1016/j.ensm.2022.03.036
230. Yin, J.Y., Xu, X., Jiang, S., et al.: High ionic conductivity PEO-based electrolyte with 3D framework for dendrite-free solid-state lithium metal batteries at ambient temperature. Chem. Eng. J. **431**, 133352 (2022). https://doi.org/10.1016/j.cej.2021.133352
231. Yang, X.F., Gao, X.J., Zhao, C.T., et al.: Suppressed dendrite formation realized by selective Li deposition in all-solid-state lithium batteries. Energy Storage Mater. **27**, 198–204 (2020). https://doi.org/10.1016/j.ensm.2020.01.031
232. Galluzzo, M.D., Halat, D.M., Loo, W.S., et al.: Dissolution of lithium metal in poly(ethylene oxide). ACS Energy Lett. **4**, 903–907 (2019). https://doi.org/10.1021/acsenergylett.9b00459

233. Zhao, C.Z., Zhang, X.Q., Cheng, X.B., et al.: An anion-immobilized composite electrolyte for dendrite-free lithium metal anodes. Proc. Natl. Acad. Sci. U. S. A. **114**, 11069–11074 (2017). https://doi.org/10.1073/pnas.1708489114
234. Li, T.Y., Cui, Y., Fan, L.L., et al.: A self-healing liquid metal anode with PEO-Based polymer electrolytes for rechargeable lithium batteries. Appl. Mater. Today **21**, 100802 (2020). https://doi.org/10.1016/j.apmt.2020.100802
235. Nie, K.H., Wang, X.L., Qiu, J.L., et al.: Increasing poly(ethylene oxide) stability to 4.5 V by surface coating of the cathode. ACS Energy Lett. **5**, 826–832 (2020). https://doi.org/10.1021/acsenergylett.9b02739
236. Liang, J.N., Sun, Y.P., Zhao, Y., et al.: Engineering the conductive carbon/PEO interface to stabilize solid polymer electrolytes for all-solid-state high voltage $LiCoO_2$ batteries. J. Mater. Chem. A. **8**, 2769–2776 (2020). https://doi.org/10.1039/c9ta08607b
237. Liang, J.N., Hwang, S., Li, S., et al.: Stabilizing and understanding the interface between nickel-rich cathode and PEO-based electrolyte by lithium niobium oxide coating for high-performance all-solid-state batteries. Nano Energy **78**, 105107 (2020). https://doi.org/10.1016/j.nanoen.2020.105107
238. Ma, J.B., Zhong, G.M., Shi, P.R., et al.: Constructing a highly efficient "solid-polymer-solid" elastic ion transport network in cathodes activates the room temperature performance of all-solid-state lithium batteries. Energy Environ. Sci. **15**, 1503–1511 (2022). https://doi.org/10.1039/d1ee03345j
239. Sahore, R., Yang, G., Chen, X., et al.: A bilayer electrolyte design to enable high-areal-capacity composite cathodes in polymer electrolytes based solid-state lithium metal batteries. ACS Appl. Energy Mater. **5**, 1409–1413 (2022). https://doi.org/10.1021/acsaem.2c00050
240. Li, Z.Y., Li, A.J., Zhang, H.R., et al.: Interfacial engineering for stabilizing polymer electrolytes with 4V cathodes in lithium metal batteries at elevated temperature. Nano Energy **72**, 104655 (2020). https://doi.org/10.1016/j.nanoen.2020.104655
241. Miyashiro, H., Kobayashi, Y., Seki, S., et al.: Fabrication of all-solid-state lithium polymer secondary batteries using Al_2O_3-coated $LiCoO_2$. Chem. Mater. **17**, 5603–5605 (2005). https://doi.org/10.1021/cm0517115
242. Seki, S., Kobayashi, Y., Miyashiro, H., et al.: Fabrication of high-voltage, high-capacity all-solid-state lithium polymer secondary batteries by application of the polymer electrolyte/inorganic electrolyte composite concept. Chem. Mater. **17**, 2041–2045 (2005). https://doi.org/10.1021/cm047846c
243. Ma, J., Liu, Z.L., Chen, B.B., et al.: A strategy to make high voltage $LiCoO_2$ compatible with polyethylene oxide electrolyte in all-solid-state lithium ion batteries. J. Electrochem. Soc. **164**, A3454–A3461 (2017). https://doi.org/10.1149/2.0221714jes
244. Han, L.F., Liao, C., Mu, X.W., et al.: Flame-retardant ADP/PEO solid polymer electrolyte for dendrite-free and long-life lithium battery by generating Al. P-rich SEI layer. Nano Lett. **21**, 4447–4453 (2021). https://doi.org/10.1021/acs.nanolett.1c01137
245. Santiago, A., Judez, X., Castillo, J., et al.: Improvement of lithium metal polymer batteries through a small dose of fluorinated salt. J. Phys. Chem. Lett. **11**, 6133–6138 (2020). https://doi.org/10.1021/acs.jpclett.0c01883
246. Zheng, J.G., Sun, C.G., Wang, Z.X., et al.: Double ionic–electronic transfer interface layers for all-solid-state lithium batteries. Angew. Chem. Int. Ed. **60**, 18448–18453 (2021). https://doi.org/10.1002/anie.202104183
247. Li, C.Y., Xue, P., Chen, L.N., et al.: Reducing the crystallinity of PEO-based composite electrolyte for high performance lithium batteries. Compos. B Eng. **234**, 109729 (2022). https://doi.org/10.1016/j.compositesb.2022.109729

Xin Su is the director of the Advanced Battery Technology Center, Harbin Institute of Technology, Weihai, with more than 15 years of academic and industrial research and development (R&D) experience (from Brown University, Argonne National Lab, A123 Systems LLC to Harbin Institute of Technology) in the field of battery materials and the design of lithium batteries. His current focus is materials and design of lithium batteries for various applications, including fundamental research, applied R&D, and manufacturing.

Ji Wu received his Ph.D. degree in Chemistry from Texas Christian University in 2007. He then joined Dr. Bruce Hinds' laboratory at the University of Kentucky and worked on the synthesis, characterization, and applications of carbon nanotube membranes. He is now a tenured professor of analytical/materials chemistry at Georgia Southern University, whose research focuses on the synthesis of advanced nanomaterials for electrochemical energy storage and controllable drug delivery. He has so far contributed 65 peer-review journal articles, two book chapters, and one U.S. patent.

Li-Zhen Fan is the director of the Advanced Energy Materials Lab at the University of Science and Technology Beijing, China. She received her Ph.D. degree in Materials Science and Engineering from Tsinghua University in 2004. She worked as a postdoctoral research fellow at Kyushu University from 2004 to 2005, and then she worked as an Alexander von Humboldt fellow at the Max Planck Institute for Solid State Research from 2005 to 2007. She was a visiting scholar of Prof. John B. Goodenough's group at The University of Texas at Austin in 2014. Her research interest focuses on solid-state lithium batteries, and she has co-authored nearly 200 relevant peer-reviewed publications.